PHYSICAL REVIEW
LETTERS

VOLUME 2 FEBRUARY 15, 1959 NUMBER 4

MEASUREMENT OF THE TEMPERATURE VARIATION OF THE ENERGY GAP IN SUPERCONDUCTING ALUMINUM

Manfred A. Biondi and M. P. Garfunkel
Westinghouse Research Laboratories,
Pittsburgh, Pennsylvania
(Received January 23, 1959)

Direct evidence for the existence of a gap in the electron energy spectrum of superconductors[1] has been obtained from studies of the absorption of electromagnetic energy in the frequency range $h\nu \sim kT_c$ (the millimeter microwave and far infrared regions).[2-5] By the extension of the measurements[3] on superconducting aluminum (T_c =1.178°K) to lower temperatures (T = 0.38°K) and to shorter wavelengths (λ = 3.1 mm), we have been able to determine the value of the energy gap at absolute zero and to measure the variation of the gap with temperature.

The apparatus previously described[6] has been modified in that the inner liquid helium Dewar now is filled with He^3. Pumping on this bath reduces the temperature to T = 0.35°K. The present measurements were made on a sample in which spurious absorption has been reduced to <1% of the normal state value. Thus it is possible to determine unequivocally the photon energy which spans the gap at absolute zero (actually, at small reduced temperature values) by noting an abrupt rise in the absorption as a critical frequency is exceeded.

Examples of the absorption data, expressed as curves of surface resistance ratio $r \equiv R/R_n$ (R_n is the surface resistance in the normal state) versus reduced temperature $t \equiv T/T_c$ for several wavelengths, are shown in Fig. 1. It will be seen that for wavelengths longer than 3.96 mm ($h\nu < 3.08\ kT_c$) the low-temperature values of r are less than 1%, suggesting that the intrinsic absorptivity of the metal goes to zero at absolute zero. However, for wavelengths shorter than 3.36 mm ($h\nu > 3.63\ kT_c$) the absorption remains appreciable as the temperature approaches zero. This abrupt increase in the absorptivity at absolute zero implies the existence of a forbidden energy gap which has been spanned by photons of these energies.

The curve at $h\nu = 0.64kT_c$ exhibits the general features of absorption curves obtained at lower frequencies in that an abrupt decrease in absorption is noted as the temperature falls below T_c, and the curve tends to zero absorption at absolute zero. However, at higher frequencies, e.g., $h\nu = 3.08kT_c$, the absorption curves no longer decrease abruptly just below T_c. In a previous paper[3] this behavior was attributed to additional absorption, largely the result of induced transitions of electrons across the temperature-dependent energy gap, and a method was outlined for separating this effect from the

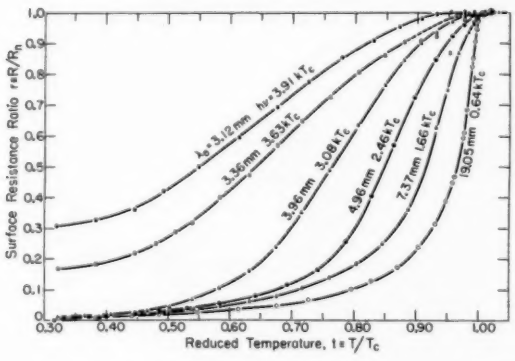

FIG. 1. Measured values of the surface resistance ratio, r, as a function of the reduced temperature, t, for superconducting aluminum. The wavelengths and corresponding photon energies are indicated on the curves.

normal electron absorption. In the present paper the larger temperature and frequency ranges covered permit us to determine directly the onset of additional absorption by examination of isotherms of surface resistance ratio versus photon energy.

Isotherms derived from our measured curves for a number of temperatures are given in Fig. 2. The curve labelled $t=0$ is determined by extrapolation of our r vs t curves to absolute zero. It will be seen that for temperatures substantially below the transition temperature the surface resistance ratio initially increases rather slowly with frequency. However, above a critical frequency (photon energy) the absorption rises much more rapidly. The effect becomes less pronounced on successive isotherms as $t\to 1$. To a first approximation we may take the energy at which the onset of this increased absorption occurs as the value of the energy gap for the particular temperature. This neglects the effect of the electromagnetic penetration depth, which is altered in the vicinity of an absorption edge.

The inferred values of the energy gap at each temperature are shown in Fig. 3. The error limits shown result from uncertainty in the choice of the onset, as indicated by the arrows on the $t=0.70$ curve of Fig. 2. At small values of the reduced temperature ($t<0.5$), where penetration effects are less important, uncertainty in the choice of gap values results from the rather long interpolation between our available photon energies. The values of the energy gap derived by this direct method are in essential agreement with the earlier results[3] which were obtained by calculations based on a two-fluid model.

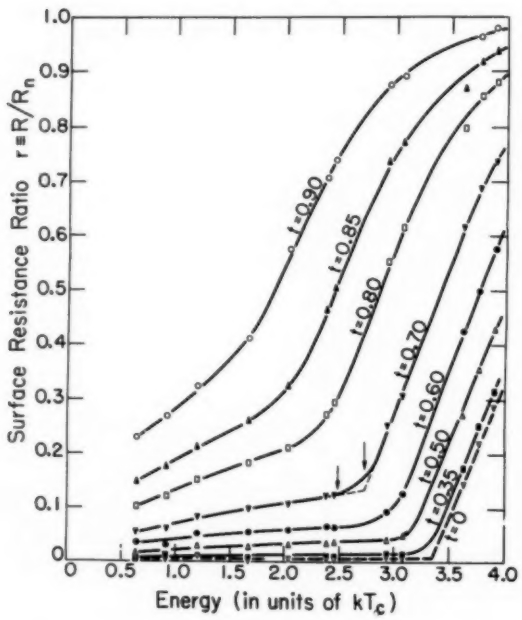

FIG. 2. Isotherms of surface resistance ratio versus photon energy. The experimental points are taken from the absorption curves at each of the measured frequencies. The arrows on the curve, $t=0.70$, indicate limits of uncertainty in determining the values of the energy gap.

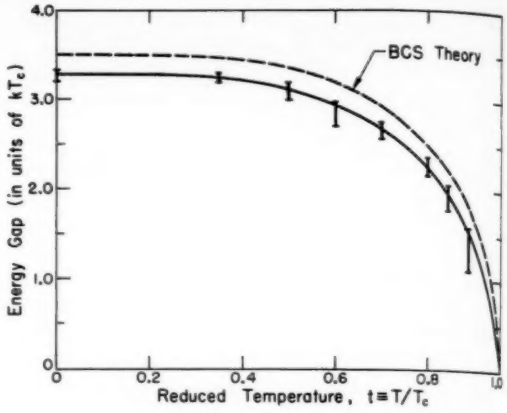

FIG. 3. Inferred energy gap variation with temperature. The solid line indicates the experimentally determined curve, the dashed line the theory of Bardeen, Cooper, and Schrieffer. The value of the gap at absolute zero is $\mathcal{E}_g(0)=(3.25\pm0.1)kT_c$.

A comparison of the results with the theory of Bardeen, Cooper, and Schrieffer[7] (the dashed curve of Fig. 3) shows that although there is good agreement concerning the shapes of the energy gap versus temperature curves, there is only fair agreement between the experimental value of the gap at absolute zero, $\mathcal{E}_g(0)=(3.25\pm0.10)kT_c$, and the theoretical value of $3.52kT_c$.

Richards and Tinkham[8] have obtained the values $\mathcal{E}_g(0)=(4.1\pm0.2)kT_c$ for lead and $(3.4\pm0.3)kT_c$ for tin. Our result on aluminum continues the pattern of a slow, monotonic variation of $\mathcal{E}_g(0)/kT_c$ with T_c/Θ suggested by Goodman[8]; Θ is the Debye temperature of the metal. However, these three metals equally well fit a slow, monotonic variation of $\mathcal{E}_g(0)/kT_c$ with either T_c or Θ alone, and therefore studies of other metals are needed.

The authors wish to thank Mark Heald for his

assistance and suggestions concerning the microwave components of the apparatus.

[1]A general review of both direct and indirect evidence for an energy gap is given in Biondi, Forrester, Garfunkel, and Satterthwaite, Revs. Modern Phys. 30, 1109 (1958).
[2]R. E. Glover and M. Tinkham, Phys. Rev. 108, 243 (1957).
[3]Biondi, Garfunkel, and McCoubrey, Phys. Rev. 108, 495 (1957).
[4]Biondi, Forrester, and Garfunkel, Phys. Rev. 108, 497 (1957).
[5]P. L. Richards and M. Tinkham, Phys. Rev. Lett. 1, 318 (1958).
[6]See reference 1, p. 1127.
[7]Bardeen, Cooper, and Schrieffer, Phys. Rev. 108, 1175 (1957).
[8]B. B. Goodman, Compt. rend. 246, 3031 (1958).

QUENCHED-IN LATTICE VACANCIES IN COPPER

G. Airoldi, G. L. Bacchella, and E. Germagnoli
Laboratori Centro Informazioni Studi Esperienze, Milano, Italy
(Received January 22, 1959)

Preliminary experiments on quenching and annealing of pure copper are reported. Thin copper wires, of 0.04- and 0.07-mm diameter,[1] were electrically heated in purified argon; the wires were 30 cm long in order to minimize the effects of nonuniform temperature at their ends. Quenchings were performed by natural cooling after disconnecting the power supply: the total cooling times were oscillographically measured and were about 0.45 sec for 0.04-mm wires and 1.2 sec for 0.07-mm wires. The initial cooling rate was estimated to be about 5×10^3 °C/sec for the thinner wires.

Up to twenty quenchings and annealings could be done with reproducible results using the same specimen: later on smaller changes of resistivity due to quenching were found, the results depending somewhat upon the history of the specimen.

The changes in resistivity $\Delta\rho$, measured at room temperature, are exponentially dependent on $1/T$ for both diameters of wires, provided the quenching temperature T is less than 1150°K. They tend to saturate at higher temperature and this fact indicates that cooling is not fast enough for retaining all defects within the quenched specimens at high temperature. Results which have been obtained at low quenching temperatures for both diameters of wires are given in Fig. 1. Extrapolation to the melting point of copper gives $\Delta\rho \simeq 2\times10^{-7}$ ohm cm, which, according to calculations by Jongenburger[2] and Abelès,[3] corresponds to a concentration of vacancies of about 1.5×10^{-3}. The formation energy of vacancies is equal to 1.0 ± 0.1 ev.

Isothermal annealing curves were obtained for temperatures ranging between 350°C and 470°C and with initial concentration of vacancies near to 10^{-3}; the recovery of quenched-in resistivity was almost complete in any case.

Results given in Fig. 2 refer to 0.04-mm wires and show an activation energy equal to about 1.3 ev. The number of jumps a defect makes before disappearing at sinks is 10^6-10^7.

On the other hand, annealing curves obtained with 0.07-mm wires suggest an activation energy for recovery near to 1.6 ev. This difference may be related to the slower cooling rate obtainable with these wires, the formation of complex defects due to clustering of vacancies being responsible for the higher activation energy. The effect is probably present to some extent even with the 0.04-mm wires, though it is presumable that 1.3 ev is nearer to the true value of the

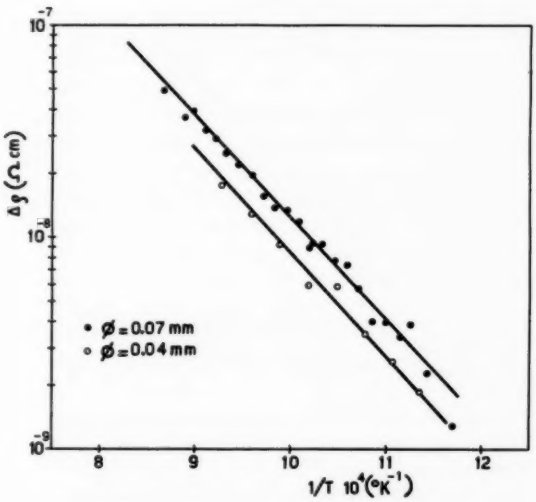

FIG. 1. Changes in resistivity due to quenching for 0.07- and 0.04-mm diameter copper wires.

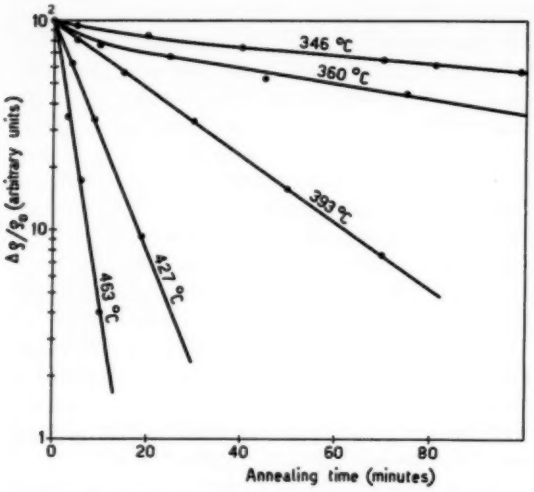

FIG. 2. Typical isothermal annealing curves. 0.04-mm wires quenched at about 930°K.

migration energy of vacancies. Recently Damask et al.[4] calculated the activation energy for migration of vacancies at 1.3 ev in copper.

The experimentally known value of the activation energy for self-diffusion in copper (2.05 ± 0.15 ev),[5] if combined with the above value of the energy for vacancy production, suggests that the migration energy of a vacancy must be somewhat larger than 1 ev, in agreement with the result by Granato et al.[6] This fact does not conflict with present annealing data.

A more accurate determination of the activation energy for migration of vacancies could have been obtained if faster quenchings were feasible: many attempts have been made to find out a suitable quenching agent, but they were unsuccessful, poor reproducibility having been achieved. Thinner copper wires might possibly be used with the purpose of getting shorter cooling times without loss of accuracy.

[1]99.999% pure, supplied by Johnson, Matthey, and Company, London.

[2]P. Jongenburger, Appl. Sci. Research B3, 237 (1953).

[3]F. Abelès, J. phys. radium 16, 345 (1955).

[4]Damask, Dienes, and Weizer, Phys. Rev. (to be published).

[5]Kuper, Letaw, Slifkin, Sonder, and Tomizuka, Phys. Rev. 96, 1224 (1954).

[6]Granato, Hikata, and Lücke, Phys. Rev. 108, 1344 (1957).

THERMAL AND RADIATION ANNEALING OF Ge*

J. W. MacKay, E. E. Klontz, and G. W. Gobeli
Purdue University, Lafayette, Indiana
(Received January 19, 1959)

It is found that about 50% of the defects produced by 1.10-Mev electron irradiation of Ge at temperatures near 10°K can be annealed either by heating to 80°K or by irradiating with electrons of energy less than the threshold for damage.

Nearly degenerate single crystals of n-type Ge ($n_0 = 7\times10^{17}/\text{cm}^3$) were used in this investigation. Samples, 60 to 80μ thick, were mounted in a cryostat which permitted measurement of Hall coefficient, R, and conductivity, σ, as a function of irradiation. The sample temperature was maintained by heat exchange through low pressure He gas to a liquid He reservoir. Temperature was measured by means of two calibrated carbon resistor thermometers, one soldered to each end of the sample. The resistors were shielded from the electron beam. The rise in sample temperature during irradiation was less than 6°. All measurements of R and σ were made at 4.2°K.

Both σ and carrier concentration, n, decreased almost linearly under 1.10-Mev irradiation. The change in mobility, $\Delta(R\sigma)$, accounted for about 60% of the change in σ. The rate of removal of carriers was 2 (carriers/cm³) per (electron/cm²). This is about twice the value obtained for nondegenerate samples at 78°K.

Figure 1 illustrates the thermal recovery of σ after 1.10-Mev irradiation. Each point represents the value at 4.2°K after 7.5 minutes at the temperature of anneal. Two recovery regions were observed. The first, near 30°K, was well defined on all anneals. The second was more or less distinct depending on the sample and its history. No further recovery was observed between 80° and 130°K. The recovery in Fig. 1 amounts to 50% of the change under irradiation. If a first-order recovery process is assumed, the 30°K recovery occurs with an activation energy of 0.04 ev. Values for the higher temperature recovery lie between 0.06 and 0.09 ev.

These results are in substantial agreement with those of Gobeli,[1] who observed thermal recovery in both n- and p-type Ge after irradiation near 4.2°K with 3.7-Mev α-particles. Cleland

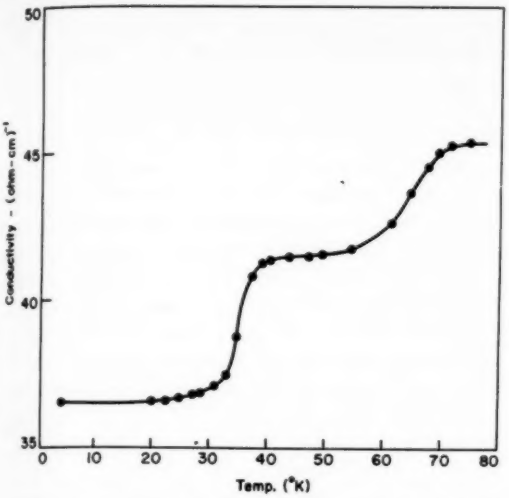

FIG. 1. Isochronal thermal recovery of conductivity in n-type Ge, after irradiation by 4×10^{16} electrons/cm^2, at 1.10 Mev.

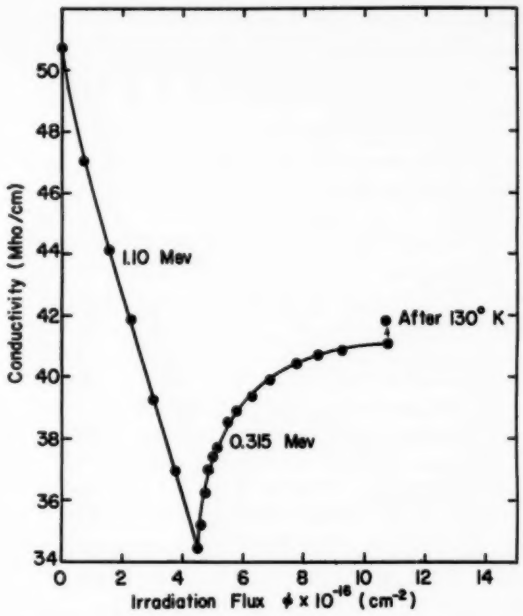

FIG. 2. Conductivity changes in n-type Ge with 1.10-Mev electron irradiation followed by 0.315-Mev irradiation.

and Crawford[2] report that they observed no recovery below 80°K for neutron-irradiated Ge. However, as they point out, their measurements were made in the presence of a strong γ-ray field. Either minority-carrier trapping or radiation-induced recovery of the defects, due to the γ-flux, may possibly account for the different results. In our experiments there was no evidence of minority-carrier trapping.

Figure 2 shows the effect of irradiation at 1.10 Mev followed by 0.315 Mev. The 1.10-Mev irradiation produced an almost linear decrease of σ, indicating little if any radiation-induced recovery. However, subsequent irradiation at 0.315 Mev, which is below the threshold for bulk damage in Ge, produced rapid recovery of σ. A similar recovery occurred for n and $R\sigma$. The recovery of n can be described by an equation of the form

$$dn/d\phi = S(n_a - n),$$

where n_a is the asymptotic carrier concentration and S is the cross section for the process. This fit yields a value of $S \approx 10^{-16}$ cm^2 for 0.315 Mev.

The slight curvature in 1.10-Mev irradiations and rapid recovery under 0.315-Mev irradiation suggests that S decreases with increasing energy. This was verified by using 0.60-Mev electrons to produce radiation annealing after a 1.10-Mev irradiation. Although 0.60 Mev is well above the threshold for damage, analysis indicates that S for this energy is about 5×10^{-17} cm^2.

Thermal recovery and radiation-induced recovery are equivalent in that each suppresses the other and each produces about the same amount of recovery after equal irradiation at 1.10 Mev. Thermal treatment after 0.315-Mev irradiation produced only the small additional recovery indicated in Fig. 2. Irradiation by 0.315-Mev electrons after a thermal anneal at 130°K produced no measurable changes in R or σ. We regard this behavior as strong evidence that the thermal anneal resulted in the disappearance of centers introduced by 1.10-Mev irradiation. If the recovery were due to release of carriers from traps, without destruction of the trapping centers, we would expect to observe a decrease in σ and n, due to retrapping of carriers on these centers, under subsequent 0.315-Mev irradiation.

We conclude that a significant fraction of the defects produced in Ge at temperatures below 10°K, are unstable. These defects are most probably close vacancy-interstitial pairs. The very large value and the inverted energy dependence of the cross section suggest that ionization

may play a role in the radiation-induced recovery.

*This research is supported by the U. S. Atomic Energy Commission.

[1]G. W. Gobeli, Phys. Rev. 112, 732 (1958).
[2]J. W. Cleland and J. H. Crawford, Jr., J. Appl. Phys. 29, 149 (1958).

X-RAY MEASUREMENT OF THE DISTRIBUTION OF ELECTRONS IN IRON AND COPPER

R. J. Weiss and J. J. De Marco
Materials Research Laboratory, Watertown, Massachusetts
(Received December 24, 1958; revised manuscript received January 8, 1959)

Batterman[1] has recently reported some x-ray measurements on powdered Fe and Cu in which he concludes that the number of $3d$ electrons in Fe is 6.2 ± 0.4 measured relative to copper (assumed to have ten $3d$ electrons) and is 6.9 ± 1.0 relative to a NaCl standard. Simultaneously with reporting this he has made available to us samples of Fe and Cu powder which he used in making these determinations and we are grateful for his consideration.

We have repeated his measurements and made several of our own and while we find no major differences in the raw data, our analysis of the data fixes the number of $3d$ electrons in Fe at approximately 2.5 ± 1.5. The differences in the analyses undoubtedly arise from factors such as absorption coefficients, Hönl corrections, Debye-Waller factors, extinction corrections, and packing effects which cannot all be evaluated until Batterman reports these in detail. However, some of these differences can be discussed.

Firstly, Batterman has used tabulated Hönl corrections whereas we have measured these and find them to be -1.9 for Fe and -1.84 for Cu (Fe $K\alpha$). These have been measured by comparing the intensity ratio of the Fe 211 and Cu 311 peaks to an Al 311 peak at both Mo $K\alpha$ and Fe $K\alpha$. In this comparison the Debye-Waller factors, preferred orientation, and any uncertainty in the scattering factors approximately cancel out and the only major difference in the ratios at the two wavelengths is the Hönl correction at Fe $K\alpha$ (the correction is small at Mo $K\alpha$). Secondly, we have found large packing density differences in the integrated intensities of Fe between compressed and loose-packed samples (~25%) and believe this to be the case for NaCl since its linear absorption coefficient is not much smaller than that of Fe. Unfortunately the onset of preferred orientation in compressed NaCl prevents a direct measurement, but an indication that such an effect is present can be obtained by comparing the total integrated intensities of all the peaks in a compressed and loose-packed sample. If only preferred orientation sets in on compression, then intensity lost from some peaks will be gained by others. We have done this and find a 45% increase in the compressed sample. While some peaks are unchanged on compression, this is no doubt due to preferred orientation and packing effects cancelling each other. The precise reason for this effect is not understood as we have also observed this effect with more penetrating radiation (Mo $K\alpha$) on samples of V, Fe, and α brass. We believe that this effect may be related to the packing density since it is independent of angle. Hence the use of loose-packed NaCl to standardize compressed Fe and Cu samples will be in error. Thirdly, we find at least 12% extinction in Batterman's Cu sample as determined from the 111/222 ratio (this is free of preferred orientation). Of course this depends on the Debye temperature used (we used $\theta = 320°$),[2] and on precisely how one draws the background since the 222 peak is broad. In order to circumvent these uncertainties, we have standardized his Cu 111 peak against the 311 peak of compressed 325-mesh Al filings which were free of extinction on compression and exhibited little preferred orientation. We found his Cu 111 peak to be $(12 \pm 4)\%$ low which we believe supports our contention of extinction.

If we combine the 12% extinction correction with our measured Hönl correction, then Batterman's measured Fe 110 scattering factor is reduced from 18.9 (relative to copper) to 17.1 or, in terms of $3d$ electrons, from 6.2 to 2.8. (As a result of the changed $3d$ electron configuration a correction of ~0.5 $3d$ electron has been made due to the argon core contraction.[3])

As an independent check, we have measured the Fe 110 peak relative to the above-mentioned Al standard and obtained $f = 17.0 \pm 0.9$ with Fe $K\alpha$ and 17.0 ± 0.9 with Mo $K\alpha$. These measurements correspond to 2.5 ± 1.5 $3d$ electrons.

While the numbers we quote result from a straightforward analysis of the data, we believe that powder measurements can be taken seriously

only when all possible sources of error are understood, and to date we do not believe this to be the case.

We wish to acknowledge the help and advice of Dr. D. Chipman, Dr. K. Tauer, and Dr. A. Paskin.

[1]B. W. Batterman, Phys. Rev. Lett. 2, 47 (1959).
[2]D. Chipman (private communication).
[3]D. R. Hartree (private communication).

INVERSION OF PARAMAGNETIC RESONANCE LINES IN IRRADIATED CALCITE*

J. L. Burkhardt
Hycon Eastern, Incorporated,
Cambridge, Massachusetts
(Received January 19, 1959)

Spin-lattice relaxation times as long as three minutes have been observed for radiation-induced paramagnetic resonance lines in calcite at 1.6°K. At 77°K the corresponding time is 5 milliseconds.

Resonance was observed with a conventional superheterodyne bridge spectrometer operating at 9 kMc/sec.[1] Samples were cut from reasonably clear natural calcite crystals and ground to fit rectangular X-band waveguide. Their lengths were adjusted to be resonant at the desired frequency; no iris was used.

Irradiations were performed with 3-Mev electrons. Measurements on one crystal indicated that a dose of 60 microcoulombs/cm^2, administered in two separated 30-second periods, produced ~10^{17} paramagnetic centers/cm^3 of the type which contributed to the strongest line. This spin density was measured by comparison with a crystal of copper-doped zinc Tutton's salt of known copper concentration. The above dosage rate caused the crystal to heat appreciably, and lower rates were found to be more efficient in producing centers. The centers fade in a few hours at room temperature and in a few days at liquid nitrogen temperature.

Several of the crystals, both before and after irradiation, exhibited a number of relatively weak lines which were identified as the spectrum of Mn^{++}, present as an impurity in the calcite. The positions and intensities of these lines agreed exactly with the work of Hurd et al.,[2] and served as a convenient calibration for the radiation-induced lines.

At least seven additional lines appeared as a result of irradiation. These are listed in Table I for a typical run on a crystal cut so that its optic axis is parallel to the static magnetic field ($\theta = 0°$). All Mn^{++} lines would be classified as "weak" or "very weak" on the scale of relative intensities used in the table. The strongest line (3271 gauss) exhibits a g value of 2.00, constant with changing radio-frequency and nearly constant with changing θ. The other lines change considerably with both frequency and θ.

Inversion of the various lines has been accomplished by adiabatic fast passage, using both field and frequency sweeps. Spin-lattice relaxation times (T_1) were measured by observing the rate of decay of the inverted absorption signal back toward its equilibrium value. Measured T_1 values at 1.6°K for five of the irradiation-induced lines are listed in Table I. Inversion of the other lines in the table was not attempted. An effort to invert a few of the larger Mn^{++} lines was unsuccessful, indicated $T_1 < 1$ second for these lines.

The relaxation times shown in Table I are probably somewhat smaller than the true values, for two reasons. First, the strength of the lines is so large that it is extremely difficult to avoid saturating the lines with the microwave power ($< 10^{-12}$ watt) used for observation. Further reduction of this power was impossible because of system noise, originating principally in the detector. Second, the inverted spin system reduced the loaded Q of the cavity appreciably, causing regeneration and an artificially rapid decay. This effect was minimized for T_1 measurements by using low-Q cavity modes and by

Table I. Resonance lines caused by irradiation in $CaCO_3$. Radio-frequency 9155 Mc/sec, $\theta = 0°$.[a]

Relative intensity	Magnetic field (gauss)	T_1 at 1.6°K (min)
Strong	4620	3
Medium	3950	
Strong	3406	1
Weak	3288	
Very strong	3271	1
Weak	3245	2
Strong	2410	3

[a]The first, second, and last lines in the table were outside the range of the proton resonance magnetometer. Magnetic fields for these lines were estimated from the magnet current readings.

broadening the resonance line with a slightly inhomogeneous field.

Complete inversion of the irradiation-induced lines was possible at frequency sweep rates as low as 2×10^{10} cycles/sec^2 using 0.1 watt of rf power. Thus the transverse relaxation time (T_2) is greater than 10^{-4} sec for these lines. Observed line widths were about one gauss, corresponding to T_2^* of the order of 10^{-7} sec, so the lines have appreciable inhomogeneous broadening.

No evidence was found for a two-stage spin-lattice relaxation process, as proposed by Townes.[3] In every case, the inverted lines decayed through the zero signal (equal population) configuration without observable change of rate.

Crystals which received the same 60-μcoul/cm^2 dose distributed over a four-minute period exhibited only a single, very strong resonance line, three gauss wide, centered at $g=2.00$, and apparently made up of several nonresolved components. The value of T_1 for this line at 1.6°K was still several minutes, even though some spin-spin interaction was evidently involved. Relaxation-time measurements were also made on such a crystal at liquid nitrogen temperature, using a frequency-sweep system. The observed T_1 was 5 ± 1 milliseconds, and the limits on fast passage indicated that T_2 was greater than 10^{-6} sec.

The extremely long spin-lattice relaxation time found in these experiments makes irradiated calcite a desirable material for use in two-level solid state maser oscillators and amplifiers. Spontaneous oscillations were observed on several occasions during the measurements at 1.6°K described above. Controlled oscillations were later obtained with a maximum power output of the order of 10^{-8} watt. An amplifier was then constructed by incorporating a ferrite circulator into the spectrometer to separate the input and output signals. Gains of 20 db and greater were observed at liquid helium temperature, and by progressively increasing the magnetic field homogeneity after inversion, amplification could be maintained for several seconds. The (gain)$^{1/2}$-bandwith product was not measured directly, but a value of 6×10^7 sec^{-1} would be expected theoretically for 10^{17} spins/cm^3 with $T_2^*=10^{-7}$ sec. Although there were not enough spins in the crystal to produce oscillation or amplification at liquid nitrogen temperature, it seems quite possible that a sufficiently large spin density might be achievable without excessive shortening of the relaxation times.

The use of calcite in these experiments was suggested by J. W. Culvahouse. His assistance and that of M. S. Cohen, H. J. Okoomian, W. G. Perry, and A. Pytte are gratefully acknowledged.

*This work was supported by the Rome Air Development Center, Griffiss Air Force Base, New York.

[1]See, for example, G. Feher, Bell System Tech. J. 36, 449 (1957).

[2]Hurd, Sachs, and Hershberger, Phys. Rev. 93, 373 (1954).

[3]Giordmaine, Alsop, Nash, and Townes, Phys. Rev. 109, 302 (1958).

DIAMAGNETISM OF CONDUCTION ELECTRONS IN METALS

J. E. Hebborn
Department of Mathematics,
Queen Mary College, London, England

and

E. H. Sondheimer*
Department of Physics,
University of Illinois, Urbana, Illinois

(Received January 26, 1959)

The calculation of the diamagnetic susceptibility of the conduction electrons has long been one of the most troublesome problems in the one-electron theory of metals. When the electrons can be treated as free the calculation is relatively simple,[1] but when the periodic lattice potential is introduced it is found that virtual interband transitions make a non-negligible contribution to the total susceptibility, and this greatly complicates the analysis. The problem has been discussed a number of times[2-4] since the original work of Peierls on the subject,[5] but no complete and really satisfactory treatment seems to have been given so far.[6] In a re-examination of the problem we have found that the field-independent part of the susceptibility can, in fact, be calculated exactly and put into a reasonably simple form. The method of calculation follows established lines,[3] and amounts to the determination of the term proportional to H^2 in the expansion of $\mathrm{Tr}[\exp(-\mathcal{H}/kT)]$ in ascending powers of H, where $\mathcal{H}$ is the Hamiltonian of an electron in the periodic lattice potential and a constant external magnetic field H (assumed to be in the z direction). The trace is formed by using as basis the

Bloch functions $\psi_{n,\vec{k}}(\vec{r})=u_{n,\vec{k}}(\vec{r})\exp(i\vec{k}\cdot\vec{r})$ which are eigenfunctions of $\mathcal{H}$ when $H=0$; the corresponding eigenvalues are the energy bands $E_n(\vec{k})$, characterized by the reduced wave vector $\vec{k}$ (with components k_1, k_2, k_3) and a band index n. The functions $u_{n,\vec{k}}(\vec{r})$ possess the periodicity of the lattice, and, for fixed $\vec{k}$, they form a complete set in the unit cell of the crystal. By using this property, and various sum rules derived from it, it is possible to carry out most of the repeated summations over band indices that are needed to evaluate the trace. The complete calculation, which is very lengthy, leads eventually to a general formula for the volume susceptibility χ of a crystal of arbitrary symmetry, oriented arbitrarily with respect to the magnetic field. The final result simplifies somewhat if it is assumed (as can be done in most cases of interest) that the crystal possesses a center of symmetry. In this case, when the electron gas is highly degenerate, one has

$$\chi = \chi_1 + \chi_2 + \chi_3 + \chi_4, \tag{1}$$

where

$$\chi_1=\frac{e^2}{48\pi^3\hbar^2c^2}\sum_n\int\left\{\frac{\partial^2E_n}{\partial k_1^2}\frac{\partial^2E_n}{\partial k_2^2}-\left(\frac{\partial^2E_n}{\partial k_1\partial k_2}\right)^2\right\}\frac{\partial f_0(E_n)}{\partial E_n}d\vec{k}, \tag{2}$$

$$\chi_2=\frac{e^2}{4\pi^3\hbar^2c^2}\sum_n\int\left\{\frac{1}{8}\left(\frac{\partial E_n}{\partial k_1}\frac{\partial^3E_n}{\partial k_1\partial k_2^2}+\frac{\partial E_n}{\partial k_2}\frac{\partial^3E_n}{\partial k_1^2\partial k_2}\right)+\left(\frac{\partial E_n}{\partial k_2}\right)^2\int\left|\frac{\partial u_n}{\partial k_1}\right|^2 d\tau_0 - 2\frac{\hbar^2}{m}\frac{\partial E_n}{\partial k_2}\int\left(k_1\frac{\partial u_n^*}{\partial k_1}\frac{\partial u_n}{\partial k_2} - i\frac{\partial u_n^*}{\partial k_1}\frac{\partial^2 u_n}{\partial x\partial k_2}\right)d\tau_0\right\}\frac{\partial f_0(E_n)}{\partial E_n}d\vec{k}, \tag{3}$$

$$\chi_3=-\frac{e^2}{2\pi^3mc^2}\sum_n\int\frac{\partial E_n}{\partial k_2}\sum_{l\neq n}\frac{1}{E_l-E_n}\int u_l^*\frac{\partial u_n}{\partial k_1}d\tau_0 \times\left\{i\int\left(\frac{\partial u_l^*}{\partial x}\frac{\partial u_n}{\partial k_2}-\frac{\partial u_l^*}{\partial y}\frac{\partial u_n}{\partial k_1}\right)d\tau_0 + \int u_l^*\left(k_1\frac{\partial}{\partial k_2}-k_2\frac{\partial}{\partial k_1}\right)u_n\,d\tau_0 + \frac{m}{\hbar^2}\frac{\partial E_n}{\partial k_1}\int u_l^*\frac{\partial u_n}{\partial k_2}d\tau_0\right\}f_0(E_n)\,d\vec{k}, \tag{4}$$

$$\chi_4=-\frac{e^2}{4\pi^3mc^2}\sum_n\int\left\{\int\left|\frac{\partial u_n}{\partial k_2}\right|^2 d\tau_0 - 2\frac{\hbar^2}{m}\sum_{l\neq n}\frac{1}{E_l-E_n}\left|k_1\int u_l^*\frac{\partial u_n}{\partial k_2}d\tau_0 + i\int\frac{\partial u_l^*}{\partial x}\frac{\partial u_n}{\partial k_2}d\tau_0\right|^2\right\}f_0(E_n)\,d\vec{k}. \tag{5}$$

Here e is the charge and m the mass of a free electron, $f_0(E)$ is the Fermi function, $\int d\tau_0$ denotes an integration over the unit cell, and $\int d\vec{k}$ denotes integration over the fundamental Brillouin zone. χ_1 and χ_2 may be written as surface integrals over the Fermi surface (which need not lie in a single band), while χ_3 and χ_4 are volume integrals extending over the occupied regions in every band.

Many alternative versions of the result are possible. For example, in our calculation we have assumed the vector potential giving rise to the magnetic field H to have the form $(-Hy, 0, 0)$. We could equally well have chosen the form $(-\frac{1}{2}Hy, \frac{1}{2}Hx, 0)$ and would then have obtained a result explicitly symmetrical with respect to an interchange of the x and y axes. It can be shown (and this serves as a check on the calculation) that the unsymmetrical form given here can be transformed directly into an expression possessing the required symmetry. (The symmetrized form is considerably more complicated than that given here and is therefore less useful in practice.)

No attempt has been made so far to evaluate the result for particular substances, and only some general remarks will be made here. The term χ_1 is the well-known Landau-Peierls expression.[5] For perfectly free electrons this term alone survives and reduces to the free-electron diamagnetism.[1] In the opposite limit of infinite lattice constant χ_4 alone survives and reduces correctly to the ordinary atomic diamagnetism. χ_2 and χ_3, however, do not have any analogs in the free-electron or the atomic diamagnetism. We note only that χ_3 contains terms of similar structure to terms in χ_4, while χ_2 contains a term involving the third derivatives of E which is similar in structure to the Landau-Peierls term χ_1.[7] This term vanishes when E is a quadratic function of $\vec{k}$, but in general it is of the same order of magnitude as χ_1 (but may be of opposite sign). Little can be said, however,

about the relative importance of the different contributions to χ without a detailed investigation. In the light of present-day knowledge of the wave functions and energy levels of electrons in solids, quantitative evaluation of the formula for the diamagnetic susceptibility should not prove beyond the bounds of possibility, particularly for substances (such as the monovalent metals) possessing a relatively simple electronic structure.[8]

A more detailed account of this work will be published in due course.

---

*On leave from Queen Mary College, London, England.

[1]L. Landau, Z. Physik 64, 629 (1930).

[2]E. N. Adams, II, Phys. Rev. 89, 633 (1953).

[3]A. H. Wilson, Proc. Cambridge Phil. Soc. 49, 292 (1953).

[4]T. Kjeldaas, Jr., and W. Kohn, Phys. Rev. 105, 806 (1957).

[5]R. Peierls, Z. Physik 80, 763 (1933).

[6]Adams' result, derived by means of the Wannier formalism, is stated to be exact, but appears as a very complicated expression. Wilson's calculation is incomplete, while Kjeldaas and Kohn consider only the special case of a small number of electrons contained near the minimum of a simple energy band in a cubic crystal.

[7]A similar term has recently been derived by G. Wentzel in an unpublished version of Phys. Rev. 108, 1593 (1957).

[8]Kjeldaas and Kohn (reference 4) have already obtained quantitative estimates of χ for Li and Na.

DYNAMICAL FEYNMAN'S THEOREM†

Edward H. Kerner*
Cornell Aeronautical Laboratory Incorporated,
Buffalo, New York
(Received January 7, 1959)

Feynman[1] in 1939 proved the following result of basic interest in molecular mechanics and solid-state physics: For fixed nuclei and stationary quantum states of the surrounding electrons, the force on any nucleus is the classically computed electrostatic force due to all other nuclei and to the quantum mechanical charge densities of the electrons. We should like to point out that this theorem has a simple dynamical extension allowing a calculation of the forces on nuclei in motion.

The theorem of Feynman invites a description of molecular motion in general in which the nuclei move classically and the electrons quantum-mechanically. Suppose then, that the nuclei have some prescribed motion, X = a nuclear coordinate $= X(t)$, so that the Hamiltonian may be written

$$H = T_X + T_x + U(x) + V(x, X) + W(X),$$

where T_X = nuclear kinetic energy involving terms like $\frac{1}{2}M\dot{X}^2$; T_x = electronic kinetic energy operator; and U, V, W represent electron-electron, electron-nuclear, and nuclear-nuclear potential energies. We regard $X, \dot{X}$ as explicitly time-dependent quantities, and so $i\hbar\dot{\psi} = H(t)\psi$ has no stationary states at all. We know, however, that

$$\frac{d}{dt}\langle H\rangle = \langle \partial H/\partial t\rangle = \int \psi^* \frac{\partial H}{\partial t}\psi\, dx,$$

where $\int dx$ means integration over all electronic coordinates. For any H that is free of the time, this states that energy is conserved, $\langle H\rangle = \text{const}$, irrespective of whether ψ is stationary or nonstationary. Now if H, as above, contains the time through some posited classical nuclear motion, we can ask: How shall this motion be determined so that $\langle H\rangle$ still is conserved? Such a total-energy conserving motion is the one that alone must be of primary interest.

We have now (looking just at a generic X for simplicity)

$$0 = M\ddot{X}\dot{X} + \frac{\partial W}{\partial X}\dot{X} + \dot{X}\int \psi^* \frac{\partial V}{\partial X}\psi\, dx,$$

or

$$M\ddot{X} = -\frac{\partial W}{\partial X} - \int |\psi|^2 \frac{\partial V}{\partial X}\, dx. \qquad (1)$$

The right-hand side is nothing other than the force $F_X(t)$ which indeed guarantees energy conservation and defines the nuclear motions accordingly. How to interpret the last term, $\langle \partial V/\partial X\rangle$, is now clear from Feynman's discussion: The term is identical with Feynman's, and his proof serves equally here to show that it represents the classical (instantaneous) electrostatic force on a nucleus M due to the total electronic charge density $\sum e\rho_i(x, t)$, the proof being independent of the stationarity or nonstationarity of ψ; here each ρ_i is the integral of $|\psi|^2$ over all electronic coordinates but the ith.

The following self-consistent or iterative scheme presents itself for managing, in principle, the very difficult Eq. (1) which entrains $X(t)$ so intricately: (a) Let $X(t)$ be surmised, for example from the Born-Oppenheimer[2] approximate internuclear potential (for static nuclei).

(b) Supposing $i\hbar\dot{\psi}=H(t)\psi$ to be solved, let F_X be computed and compared with $M\ddot{X}$, an unsatisfactory comparison leading to the next approximation $M\ddot{X}_2=F_{X_1}$, etc. In the case that the nuclear motion corresponds to a collision, as in atom-atom collisions, the initial state $\psi(x,-\infty)$ for step (b) is well defined; for bound nuclear motions it is not clear how to specify an initial state in general, though in special cases the periodicity and turning points of the classical motion may serve to fix $\psi(x,t)$ uniquely. As for the nonstationary states themselves, one can appeal to an expansion of $\psi(x,t)$ in instantaneous eigenfunctions, $\psi=\sum f_n(t)\phi_n(x,t)$ with $H(t)\phi_n(x,t)=E_n(t)\phi_n$. The $\phi_n(x,t)$ are of course closely related to the starting functions $\omega_n(x,X)$ of the Born-Oppenheimer approximation method, $H'\omega_n=\epsilon_n(X)\omega_n$, $(H'\equiv H-T_X)$ in which at first the nuclear kinetic energy is disregarded and X is a numerical parameter. It is interesting to see, however, that in the present scheme, in contrast to the Born-Oppenheimer scheme, the nuclear kinetic energy is at the outset taken into consideration, and that the expansion in time-frozen eigenfunctions is fundamentally simpler than the Born-Oppenheimer expansion $\sum U_n(X)\omega_n(x,X)$ in space-frozen eigenfunctions [first-order ordinary differential equations for $f_n(t)$, second-order partial differential equations for $U_n(X)$].

What has been done in the formulation of Eq. (1) is to break up the conservative motion of the whole molecular system into two individually nonconservative parts. This is but an essential cost of attempting to survey one of the parts, the nuclear motion, in abstraction from the rest, and emphasizes that no conservative view of the nuclear motion can wholly suffice for its description. The view supplied by the dynamical Feynman theorem should be capable in relatively simple fashion of accounting accurately, if only classically, for the "kinetic energy corrections" as a whole that arise from the billowing tides of electrons that are themselves induced by the rushing nuclei. The next step of quantization of the classical motion can be considered only after this motion is more fully understood. In a later report it is hoped to elaborate some of the points made here through a discussion of H_2^+.

†This research was supported by the Air Force Office of Scientific Research of the Air Research and Development Command.

*Consultant, Aerodynamics Research Department. Permanent address, Physics Department, University of Buffalo, Buffalo, New York.

[1]R. P. Feynman, Phys. Rev. 56, 340 (1939).

[2]M. Born and R. Oppenheimer, Ann. Physik 84, 457 (1927).

FINE STRUCTURE, HYPERFINE STRUCTURE, AND RELAXATION TIMES OF Cr^{3+} IN TiO_2 (RUTILE)*

H. J. Gerritsen, S. E. Harrison, H. R. Lewis, and J. P. Wittke

RCA Laboratories, Princeton, New Jersey

(Received January 20, 1959)

We have studied the paramagnetic spectrum of a single crystal of TiO_2 (rutile) in which 0.12% of the Ti ions were replaced by Cr ions. The resonances observed at 23 800 Mc/sec and 9520 Mc/sec are shown as a function of field and crystal orientation in Figs. 1 and 2. All of these points, with the exception of those which are denoted by cross marks, are attributed to Cr^{3+} ions which have replaced titanium ions in the crystal. The resonances not believed due to Cr have an intensity of about 1% of that of the Cr lines and are thought to be due to another paramagnetic impurity. Chemical analysis showed that Fe and Cu are indeed present in concentrations of 3-30 parts per million.

The rutile form of TiO_2 is a tetragonal crystal belonging to the class D_{4h}.[1] There are two Ti^{4+} ions in a unit cell and each of these has six

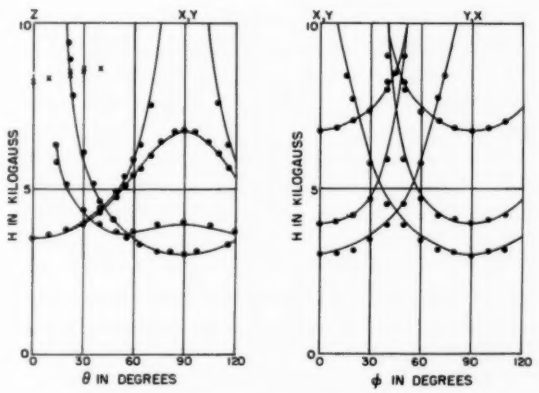

FIG. 1. The points shown in the figures are the observed resonances at 23 800 Mc/sec. The solid lines give the theoretical resonance fields for the parameters stated in the text.

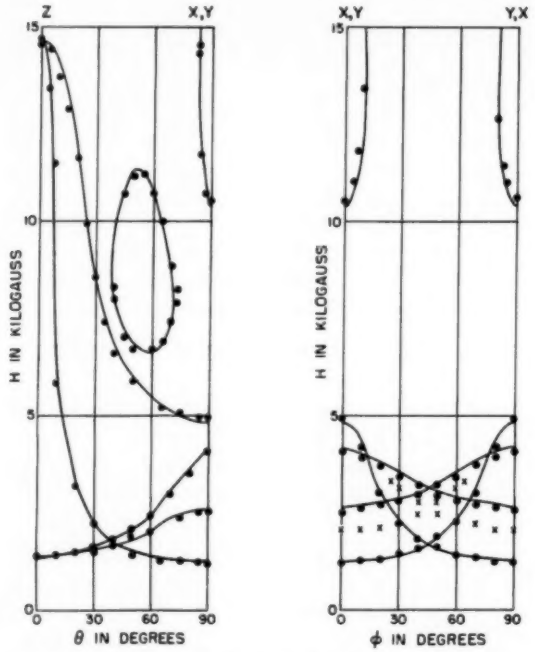

FIG. 2. The points shown in the figures are the observed resonances at 9520 Mc/sec. The solid lines give the theoretical resonance fields for the parameters stated in the text.

neighboring oxygen atoms which produce an orthorhombic field at the position of the titanium ion. The symmetry of the Ti^{4+} ion and the ligating oxygens is D_{2h}. The z axis is parallel to the c axis, while the magnetic x and y axes are parallel to the 110 and $1\bar{1}0$ directions. The positions of the oxygen ions around two nonequivalent titanium ions differ from one another by a rotation through 90° around the c axis. (See Fig. 3.) As a result the paramagnetic spectrum has a period of 90° when rotated around the tetragonal crystal axis.

The four lowest electronic levels of a Cr^{3+} ion which has replaced a Ti^{4+} ion in rutile are described by a spin-Hamiltonian[3] of the form

$$H=\beta g\vec{\mathbf{H}}\cdot\vec{\mathbf{S}}+D\left[S_z^2-\tfrac{1}{3}S(S+1)\right]+E(S_x^2-S_y^2). \quad (1)$$

We are able to fit the observed resonances in the zx, zy, and xy planes to those predicted by Eq. (1) if we assume

$$g=1.97,\ D=0.55\ \text{cm}^{-1},\ E=0.27\ \text{cm}^{-1}.$$

The calculation of the energy levels was done by machine computation for which purpose the secular determinant was developed in the form

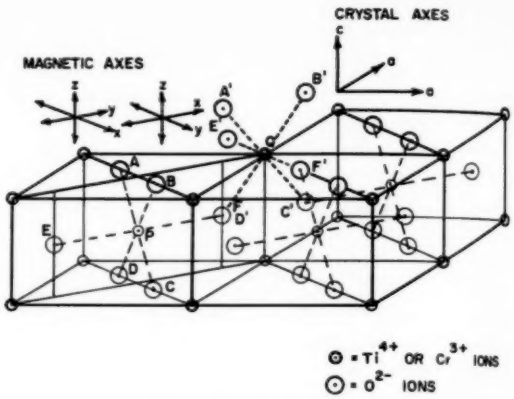

FIG. 3. Crystal structure of TiO_2 and magnetic axes. $\angle APE=\angle BPE=90°=\angle A'QE'=\angle B'QE'$. $\angle APB=\angle A'QB'=78°$. $EP=E'Q=1.99$A. $AP=BP=1.89$A$=A'Q=B'Q$.

$$0=W^4-W^2\left(\tfrac{5}{2}h^2+2D^2+6E^2\right)$$
$$+Wh^2\left(2D-6D\cos^2\theta-6E\sin^2\theta\cos2\phi\right)$$
$$+\tfrac{9}{16}h^4+\tfrac{1}{2}h^2\left(D^2-6D^2\cos^2\theta+9E^2\cos2\theta\right.$$
$$\left.+12DE\sin^2\theta\cos2\phi\right)+\left(D^2+3E^2\right)^2.$$

The symbols are: W = energy, $h=g\beta H$, θ = angle between z axis and magnetic field, and ϕ = angle between x axis and projection of magnetic field in the xy plane.

Values of observed line widths and resonant fields along the symmetry axes are given in Table I. These measurements were made at room temperature. A rough check at 78° and 4.2°K indicates that any shift in resonant fields with reduced temperature is not greater than 1%.

Relaxation times measured using conventional

Table I. Resonant fields and line widths of Cr in TiO_2.

Transition		Axis	Frequency (kMc/sec)	Resonant field	Line width (gauss)
1/2	3/2	z	9.520	1390	12
1/2	3/2	z	23.79	3505	9
-3/2	-1/2	z	9.520	14 800	
-3/2	-1/2	y	9.520	1200	21
-3/2	-1/2	y	23.79	3010	7
-1/2	3/2	y	23.79	3960	35
3/2	1/2	y	9.520	4065	21
3/2	1/2	y	9.520	10 600	
1/2	3/2	x	9.520	2560	17
1/2	3/2	x	23.79	6750	23
-3/2	-1/2	x	9.520	4940	29

Table II. Relaxation times of Cr in TiO_2.[a]

Transition		Axis	Frequency (kMc/sec)	Resonant field (gauss)	Temp. (°K)	T_2(sec)	T_1(sec)
1/2	3/2	z	23.79	3505	78	5.3×10^{-9}	4×10^{-4}
1/2	3/2	z	23.79	3505	4.2	5.3×10^{-9}	4×10^{-2}
1/2	3/2	x	23.79	6750	4.2	4.9×10^{-9}	5×10^{-2}

[a]The conversion factor needed to go from linewidth to T_2 is obtained by using the slope of the calculated curves for energy level vs magnetic field.

c.w. methods[3] are given in Table II. These are order-of-magnitude estimates; the large possible error arises almost entirely from uncertainty about the radio-frequency field distribution within the cavity. The dielectric constant of TiO_2 is very large, anisotropic, and temperature-dependent. Thus, mode distortion in the cavity due to the sample is difficult to estimate and further study will be required to fix more accurately the values of T_1.

Because some of the resonance lines are very narrow, the four-line hyperfine structure due to Cr^{53} (9.55% of natural Cr) is easily observed. The hyperfine splitting is described by adding to the spin-Hamiltonian terms of the form $A_zI_zS_z + A_xI_xS_x + A_yI_yS_y$.

A splitting of 50 gauss between the outer of the four hyperfine lines was observed along all three axes and at both frequencies used. One can show theoretically that the over-all splitting measured in this way is equal to $3A/g\beta$ independent of D, E or H, as long as these are large compared to A. The observed splittings of 50 gauss show that $A_x = A_y = A_z = 0.0015$ cm^{-1}. This is in good agreement with measurements on other Cr-doped crystals[4] and a further support of the theory of configurational interaction. Because the inner hyperfine lines were not completely separated from the strong resonance due to the Cr^{52}, it was not possible to detect quadrupole effects. The distances between the four hyperfine lines were equal to within 10%.

The narrow lines and long relaxation times of Cr^{3+} in TiO_2, together with the high dielectric constant and good mechanical properties of the crystal, indicate that it may be a very effective material for use in a solid-state maser. With 1 mw of power incident on a cavity with a Q of approximately 1000, we observed saturation parameters of about one at 78°K and 100 at 4.2°K. The voltage reflection coefficient was about 0.5.

Thanks are due to H. Whittaker for the chemical analysis and to M. Heller and F. Zonis for assistance in making measurements. The x-ray orientation of the crystal was done by G. Neighbor. The crystal was obtained from Linde Air Products.

*Work partially supported by the U. S. Army (Signal Corps).

[1]R. W. C. Wyckoff, Crystal Structures Handbook (Interscience Publishers, Inc., New York, 1958).

[2]B. Bleaney and K. W. H. Stevens, Reports on Progress in Physics (The Physical Society, London, 1953), Vol. 16, p. 107.

[3]Bloembergen, Pound, and Purcell, Phys. Rev. 73, 679 (1948).

[4]K. D. Bowers and J. Owen, Reports on Progress in Physics (The Physical Society, London, 1955), Vol. 18, p. 304.

POLARIZATION OF FLUORESCENCE IN ZnS AND CdS SINGLE CRYSTALS

A. Lempicki
Research Laboratories,
Sylvania Electric Products Incorporated,
Bayside, New York
(Received January 23, 1959)

The polarization of impurity fluorescence has been observed in both ZnS and CdS crystals. The specimens were obtained by vapor phase growth and in the case of ZnS have been deliberately doped with Cu and Mn. Plate-like crystals with the c axis in the plane were used for the measurements.

The fluorescence was excited by filtered 3650A radiation incident perpendicularly to the plate surface. Natural or plane polarized radiation

Table I. Data on the polarization of fluorescence.

	Type	Impurity in mole %	Fluorescence emission peak (A)	Structure	$p(0°)$	$p(90°)$	$p_n(0)$
1	ZnS:Cu	0.02	4500	hex	-0.03	0.20	-0.12
2	ZnS:Cu	0.02	4500	hex	-0.10	0.20	-0.16
3	ZnS:Mn	1.0	5800	cub	-0.03	0.07	-0.05
4	ZnS:Mn	0.1	5800	cub	-0.03	0.02	-0.03
5	CdS:(?)		~6200	hex	-0.52	0.51	-0.50

could be used. The measurement of fluorescence was made along the exciting beam direction by means of a photomultiplier and an analyzer. Filters were used to prevent the exciting radiation from reaching the photomultiplier.

The amount of polarization is defined by $p(\theta) = [(I_{\parallel} - I_{\perp})/(I_{\parallel}+I_{\perp})]_{\theta}$, where $I_{\parallel}$ is the intensity measured with the analyzer parallel to the polarizer and $I_{\perp}$ with the analyzer perpendicular to the polarizer. θ is the angle between the exciting electric vector $\vec{E}$ and the c axis of the crystal. For unipolarized excitation [amount of polarization denoted by $p_n(\theta)$], θ is the angle between the principal direction of the analyzer and the c axis.

Table I summarizes the results of the measurements for several crystals and Fig. 1 gives the full p vs θ curves for crystals 2 and 5. The CdS crystal was not grown in our laboratory and the nature and content of its impurity was not known. The accuracy of the polarization measurements is ± 0.02.

The following features are to be noted:

(a) For $\theta = 0$ the values of p and p_n are negative and for $\theta = 90°$ they are positive. This means that the fluorescence is polarized preferentially in the direction perpendicular to the c axis under any conditions of excitation.

(b) The largest value of p is obtained for crystal 5 which has hexagonal structure and a high degree of perfection. The ZnS:Cu crystals are also hexagonal but exhibit a certain amount of stacking disorder.

(c) For the CdS crystal, the amount of polarization p is nearly independent upon the nature of excitation (polarized or unpolarized). For ZnS we have, in general, $|p(0)| < |p_n(0)|$.

(d) The values of p for ZnS:Mn are significantly smaller than for ZnS:Cu. Since these crystals are predominantly cubic (with disorder) we cannot say whether this is a characteristic of the Mn center or of the structure.

Observations along the c axis were made on several ZnS:Cu and ZnS:Mn specimens grown with the c axis perpendicular to the plane of the plate. Invariably p and p_n were found to be zero.

The observed polarization cannot be due to the dichroism of the lattice since in both ZnS and CdS the absorption coefficients are larger for the direction perpendicular to c. This would make c the direction of preferential polarization. This point was checked directly by observing the degree of polarization of transmitted unpolarized light of about the same wavelength as the fluorescence. p was found to be very small (of the

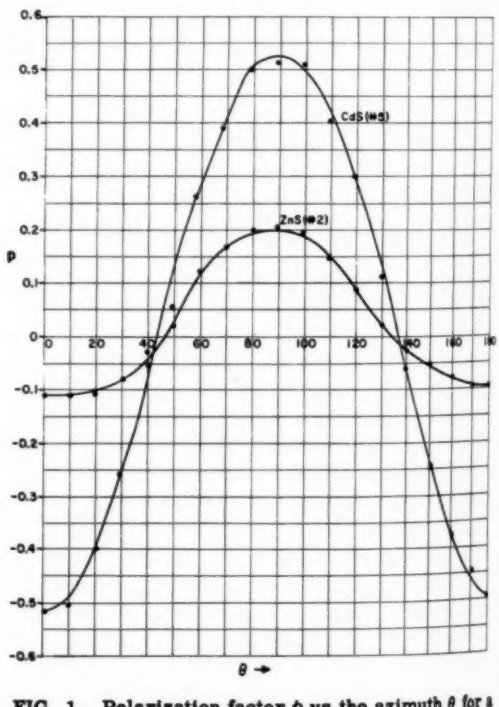

FIG. 1. Polarization factor p vs the azimuth θ for a ZnS:Cu and a CdS crystal. For $\theta = 0$ the exciting electric vector is parallel to the "c" axis.

order of experimental error) and of opposite sign to that observed in fluorescence. The phenomenon must thus be due to the centers themselves.

The fact that natural light produces polarized emission shows that the elementary oscillators cannot be randomly oriented.[1] Following the dipole theory as applied to the fluorescence in alkali halides[2-4] and diamond,[5] we can try to represent the centers as an array of oscillators all aligned along some direction in the crystal. The polarization depends then upon the elements of a polarizability tensor. It can be shown quite generally that such a model cannot account for the observed results.

We can also discard the possibility of the dipoles being oriented along the 12 equivalent directions in the wurtzite lattice. Such an array of dipoles would give rise to a nonvanishing mean square dipole moment only along the c axis and hence would lead to preferential polarization along c. A similar result is obtained in case of centers having the c axis as one of the principal axes of their polarizability tensor (common α_{zz} components) but randomly oriented principal axes in the x-y plane. None of these models can be salvaged by assuming that the exciting radiation is subject to a dichroic absorption by the lattice.

It is possible that experimental results can be accounted for by the introduction of separate absorption and emission oscillators, such as have been postulated by Feofilov[2] and others,[1-6] in order to explain the dispersion of p. Nevertheless, for a fixed excitation wavelength anisotropic (in particular linear) oscillators are sufficient to explain the results in the halides. The centers in ZnS and CdS must therefore have essentially different features. Our results are qualitatively very similar to those obtained by Dutton[7] on the polarization of edge luminescence in CdS. We have also observed that the green electroluminescence (involving band to band recombination[8]) of CdS crystals is polarized preferentially perpendicular to c. Values of p up to -0.3 have been measured although the instability of emission makes it very difficult. As shown by Birman in the accompanying Letter,[9] the polarization in all these cases is consistent with the Lambe-Klick model of luminescence.

More detailed work on the effect of crystal structure, crystal disorder, and type and level of doping on the polarization of fluorescence is under way. It is becoming evident that it may provide fundamental information on the nature of luminescent centers and processes.

The author wants to thank Dr. H. Samelson for supplying the ZnS crystals, Dr. I. Broser for the CdS crystal, Mr. V. A. Brophy and Mr. S. Kellner for x-ray analysis, and Dr. J. Birman and Dr. G. Neumark for many discussions.

[1] P. Pringsheim, Fluorescence and Phosphorescence (Interscience Publishers Inc., New York, 1949).
[2] P. P. Feofilov, J. phys. radium 17, 646 (1956).
[3] J. Lambe and W. D. Compton, Phys. Rev. 106, 684 (1957).
[4] E. J. West and W. D. Compton, Phys. Rev. 108, 576 (1957).
[5] Elliott, Matthews, and Mitchell, Phil. Mag. 3, 360 (1958).
[6] A. Jablonski, Z. Physik 96, 236 (1935).
[7] D. Dutton, J. Phys. Chem. Solids 6, 101 (1958).
[8] R. W. Smith, Phys. Rev. 105, 900 (1957).
[9] J. L. Birman, following Letter [Phys. Rev. Lett. 2, 157 (1959)].

POLARIZATION OF FLUORESCENCE IN CdS AND ZnS SINGLE CRYSTALS

Joseph L. Birman
Research Laboratories,
Sylvania Electric Products Incorporated,
Bayside, New York
(Received January 23, 1959)

The polarization of the fluorescence at 6200A in CdS and at 4500A and 5800A in ZnS is reported in the accompanying Letter,[1] along with the failure of various simple dipole theories to account for these results. Since a dipole-type model was able to account for color centers in the halides, and the localized centers in diamond, it was indicated that the CdS and ZnS centers in question may be of an essentially different type.[1] We shall suggest that the 6200A emission in CdS, and probably the 4500A in ZnS, be interpreted on the basis of the Lambe-Klick model[2] and shall make certain predictions based on this explanation which, if verified, will substantiate the interpretation. The 5800A Mn emission in ZnS apparently requires a more complex interpretation, which is not surprising in view of the complexity of the ground and excited states of Mn^{++}.

In Fig. 1 we show valence and conduction bands for zinc blende (ZB) and wurtzite (W) structures

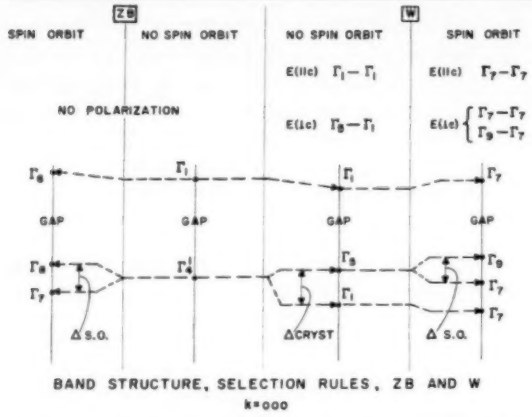

FIG. 1. Band structure and selection rules for *ZB* and *W* structures. Crystal splittings and spin-orbit splittings are indicated schematically. Transitions which are allowed for various polarizations of photon electric vector with respect to crystal "*c*" axis are indicated.

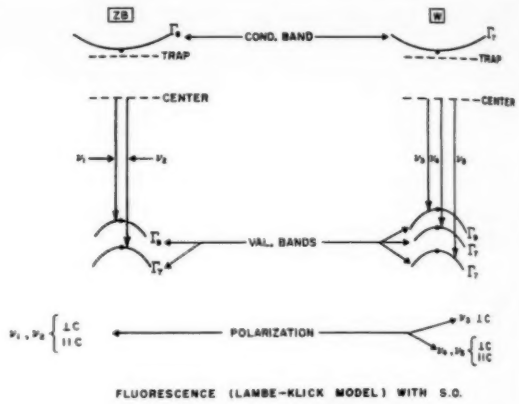

FIG. 2. Lambe-Klick model of fluorescence in *ZB* and *W* structures (schematic). The bands are labelled including spin-orbit and, in *W*, crystal splittings. Polarization rules follow assuming the "center" state has essentially the conduction band symmetry (edge emission is assumed to involve transitions from the shallow "trap" state to the valence band). Valence band maxima are probably not exactly at $\vec{k}=(000)$ since both structures do not have inversion symmetry, but are so indicated for purposes of simplicity.

at $\vec{k}=(000)$. We have indicated "crystal" and spin-orbit splittings, and the parentage of various states in terms of the familiar *ZB* levels.[3] Bands are shown in a normal order, and various "electric dipole" selection rules are indicated.[4] The relative magnitudes of crystal and spin-orbit splittings are unknown for ZnS and CdS but one expects $\Delta_C > \Delta_{S.O.}$. In general, the more ideal is the *W* structure the smaller we expect Δ_C to be[5] (hence smaller in ZnS than in CdS), while the $\Delta_{S.O.}$ should depend primarily on the anion and hence be about the same for ZnS and CdS. In Fig. 2 we show the Lambe-Klick model of fluorescence in the sulfides, indicating the appropriate complexity of valence band structure. We shall assume that $\Delta_C > \Delta_{S.O.}$ in *W* and shall neglect the lower Γ_7 band. Hence to account for the 6200Å CdS emission we assume that (a) the incident radiation creates electrons and holes, (b) the latter reach equilibrium between bands Γ_9 and Γ_7, (c) then the bound electron at the center and free hole recombine, and (d) radiation $\nu_3 + \nu_4$ is emitted. It is assumed that the bound electron is in a state whose wave function has symmetry Γ_7 (or close enough to it) so that selection rules for edge emission and luminescence are the same. The fluorescence is polarized, and the degree of its polarization is temperature dependent, as was already shown by Hopfield[6] for the edge emission, following the law

$$I_\perp / I_\parallel = a \exp(\Delta_{S.O.}/kT) + b, \qquad (1)$$

where a and b are ratios involving matrix elements and effective masses. The explanation of edge emission in CdS is substantially the same as the preceding, although the initial state is, in this case, a shallow trap rather than a deep center.[6] Hence the model leads us to make the following predictions:

(1) Polarization of both edge emission and 6200A fluorescence in CdS should obey Eq. (1). (2) Excitation spectrum of 6200A emission in CdS using polarized light should be identical to that of edge emission.[7] (3) The 6200A emission, like edge emission, should be polarized independently of polarization of exciting radiation (this is observed[1]). (4) The 6200A emission can be resolved into two bands, one totally polarized (ν_3) and the other not polarized.

We believe that (1) and (2) above are true tests of the model.

The 4500A ZnS emission might be accounted for on substantially the same (Lambe-Klick) model but with additional complexity due to crystal disorder (faulting) and mixed (*ZB*+*W*) crystals. The admixture of cubic (*ZB*) with hexagonal (*W*) regions in the "single" crystals would result in regions in which the emission was governed by selection rules appropriate to *ZB* (Fig. 2, left-hand side), i.e., was unpolarized, as well as regions where the emission was polarized (Fig. 2, right-hand side). The depolarization of 4500A emission in ZnS would be a sensitive func-

tion of crystal disorder and it would be necessary to obtain a homogeneous hexagonal (*W*) single crystal of ZnS to test whether the Lambe-Klick model is appropriate for ZnS edge and 4500A luminescence.

The interpretation of the 5800A Mn emission in ZnS is probably of a different nature. We expect the analysis to require an understanding of the effect of uniaxial field (caused by both pure *W* and [111] faulted *W* or *ZB*) upon the ground and excited states of the Mn^{++} center, which is commonly believed to be a tightly bound center,[8] not involving conduction or valence band transitions in emission. Such a model is beyond the scope of this note.

This work is continuing.

It is a pleasure to thank Mr. A. Lempicki for discussion of his work, as well as my colleagues, particularly E. Conwell and G. Neumark, for discussions.

[1]A. Lempicki, preceding Letter [Phys. Rev. Lett. 2, 155 (1959)].

[2]J. Lambe and C. C. Klick, Phys. Rev. 98, 909 (1955).

[3]R. H. Parmenter, Phys. Rev. 100, 573 (1955).

[4]G. Dresselhaus, Phys. Rev. 100, 580 (1955); Phys. Rev. 105, 135 (1957). The latter paper contains a number of errors which have been corrected in Figs. 1 and 2.

[5]J. L. Birman (to be published).

[6]Lambe, Klick, and Dexter, Phys. Rev. 103, 1715 (1956); J. Hopfield, Bull. Am. Phys. Soc. Ser. II, 3, 409 (1958) and J. Phys. Chem. Solids (to be published).

[7]D. Dutton, J. Phys. Chem. Solids 6, 101 (1958).

[8]C. C. Klick and J. H. Schulman, J. Opt. Soc. Am. 42, 910 (1952); F. E. Williams, Brit. J. Appl. Phys. Suppl. 4, S97 (1955).

COLLECTIVE DESCRIPTION OF ELECTRON INTERACTIONS WITHOUT SUBSIDIARY CONDITIONS

Harry J. Lipkin*
Department of Physics,
University of Illinois, Urbana, Illinois
(Received January 26, 1959)

The Bohm-Pines collective description[1] uses an extended Hamiltonian involving extra degrees of freedom and associated subsidiary conditions which are not easily satisfied in practical calculations. In this Letter a different approach[2] is used to obtain (1) similar results without introducing additional degrees of freedom, and (2) the Bohm-Pines extended Hamiltonian with additional degrees of freedom but without requiring subsidiary conditions.

The basic Hamiltonian for a system of electrons in a uniform background of positive charge is[1]

$$H=\sum_i (p_i^2/2m)+\tfrac{1}{2}\sum_{\vec{k}\neq 0}(\rho_{\vec{k}}\rho_{\vec{k}}^{*}-n)v_{\vec{k}}, \tag{1}$$

where $\rho_{\vec{k}}=\Sigma_i \exp(-i\vec{k}\cdot\vec{r}_i)$, n is the number of electrons in the system, taken to be of unit volume, and $v_k=4\pi^2/k^2$.

We now define

$$\sigma_{\vec{k}}=i\sum_i (e^{i\vec{k}\cdot\vec{r}_i/2}\,\vec{k}\cdot\vec{p}_i e^{i\vec{k}\cdot\vec{r}_i/2})/nk^2, \tag{2}$$

and assume the validity of the following approximate relations:

$$[\rho_{\vec{k}},\sigma_{\vec{k}'}]\approx i\hbar\delta_{kk'}, \quad k<k_c \tag{3a}$$

$$[\textstyle\sum_i p_i^2,\sigma_{\vec{k}}]\approx 0, \quad k<k_c \tag{3b}$$

where k_c is an arbitrary cutoff parameter. Equation (3a) is valid in the random phase approximation; Eq. (3b) is valid to the lowest order in the electron-plasmon coupling constant. These assumptions simplify the presentation of our general method, but are not essential.

From the relations (3) we obtain the equations of motion for the plasmon creation and annihilation operators:

$$[H,(\rho_{\vec{k}}+i\omega_p\sigma_{\vec{k}}^{*}/v_k)]=\hbar\omega_p(\rho_{\vec{k}}+i\omega_p\sigma_{\vec{k}}^{*}/v_k), \tag{4a}$$

$$[H,(\rho_{\vec{k}}^{*}-i\omega_p\sigma_{\vec{k}}/v_k)]=-\hbar\omega_p(\rho_{\vec{k}}^{*}-i\omega_p\sigma_{\vec{k}}/v_k), \tag{4b}$$

where the zero-order plasmon frequency $\omega_p=(nk^2v_k/m)^{1/2}$. We now define the "intrinsic" Hamiltonian

$$H_{\text{int}}=H-\tfrac{1}{2}\sum_{0\neq k<k_c} v_k(\rho_{\vec{k}}+i\omega_p\sigma_{\vec{k}}^{*}/v_k)\times(\rho_{\vec{k}}^{*}-i\omega_p\sigma_{\vec{k}}/v_k). \tag{5}$$

Let ψ_{on} be any eigenfunction of H describing a state with no plasmons present; that is, $(\rho_{\vec{k}}^{*}-i\omega_p\sigma_{\vec{k}}/v_k)\psi_{on}=0$ for all $k<k_c$. Then

$$H_{\text{int}}\psi_{on}=H\psi_{on}=E_n\psi_{on}. \tag{6}$$

From Eqs. (4) and (5), H_{int} commutes with all the $\rho_{\vec{k}}$'s and $\sigma_{\vec{k}}$'s for $k<k_c$. Thus if $F(\rho_{\vec{k}},\sigma_{\vec{k}})$ is an arbitrary function of these variables, then

$$H_{\text{int}}F(\rho_{\vec{k}}, \sigma_{\vec{k}})\psi_{on} = F(\rho_{\vec{k}}, \sigma_{\vec{k}})H_{\text{int}}\psi_{on}$$
$$= E_n F(\rho_{\vec{k}}, \sigma_{\vec{k}})\psi_{on}. \quad (7)$$

All the eigenfunctions of H can be constructed from the no-plasmon states ψ_{on} by operating on them with the plasmon creation operators which are functions of the $\rho_{\vec{k}}$ and $\sigma_{\vec{k}}$. Equation (7) shows that these are also eigenfunctions of H_{int}, but with the eigenvalue E_n of the no-plasmon state.

The eigenvalues of the "intrinsic" Hamiltonian H_{int} are therefore all the eigenvalues of the no-plasmon states of H, each with an infinite degeneracy. H_{int} may therefore be used instead of H to calculate the energy of the ground state or any other no-plasmon state. Trial wave functions should give better (i.e., lower) energy values in variational calculations with H_{int} than with H. H_{int} offers a better point of departure for a perturbation calculation than H because the troublesome long-range terms in the Coulomb interaction are absent in H_{int}.

We now compare H_{int} with the Hamiltonian obtained by BHP after a series of transformations. To the order in which our assumptions (3) are valid, H_{int} is identical to the part of the BHP Hamiltonian depending upon the electron variables. However, BHP require that their wave functions satisfy a subsidiary condition, and we do not.

A clearer picture of the relation of the H_{int} formalism to that of BHP is obtained by introducting a set of auxiliary variables $q_{\vec{k}}$ and their canonically conjugate momenta $\pi_{\vec{k}}$, which commute with all the particle variables. Wave functions $\psi(x_i, q_{\vec{k}})$ in the extended system depend upon both the real particle variables x_i and the nonphysical $q_{\vec{k}}$. However, in contrast to BHP, we do not add terms to the Hamiltonian. Rather, we follow LST and note that the Hamiltonian (1) is a "physical operator in the extended system" depending only upon the real particle variables and not upon the extra variables. LST have shown that the eigenvalue problem for such operators can be solved in the extended system without requiring the wave functions to satisfy subsidiary conditions; this procedure simply introduces an infinite spurious degeneracy for each eigenvalue.

We now define

$$S_1 = \sum_{0\neq k<k_c} \sigma_{\vec{k}}\pi_{\vec{k}}/v_k^{1/2}, \quad (8a)$$

$$S_2 = \sum_{0\neq k<k_c} \rho_{\vec{k}}^{*} q_{\vec{k}} v_k^{1/2}. \quad (8b)$$

Using Eq. (5) and noting that H_{int} and $\sigma_{\vec{k}}$ commute with S_1, while $\exp(+iS_1/\hbar)\rho_{\vec{k}}\exp(-S_1/\hbar) = \rho_{\vec{k}} - \pi_{\vec{k}}/v_k^{1/2}$, we make the canonical transformation

$$e^{+iS_1/\hbar} H e^{-iS_1/\hbar}$$
$$= H + \tfrac{1}{2}\sum_{0\neq k<k_c} (\pi_{\vec{k}}^{*}\pi_{\vec{k}} - 2\pi_{\vec{k}}^{*}\rho_{\vec{k}}v_k^{1/2}). \quad (9)$$

This is just the BHP extended Hamiltonian, obtained within a formulation which does not require subsidiary conditions.

We now follow the BHP treatment in making two canonical transformations on the BHP Hamiltonian (9). To the order of the assumptions (3) their first transformation is just that defined by our S_2 [Eq. (8b)], and their second transformation[3] is identical with our first [Eq. (9)]. We therefore obtain the BHP final Hamiltonian

$$H_{\text{BHP}} = e^{+iS_1/\hbar} e^{-iS_2/\hbar} e^{+iS_1/\hbar} H e^{-iS_1/\hbar} \times e^{+iS_2/\hbar} e^{-iS_1/\hbar}, \quad (10)$$

by making a total of three successive transformations on our original Hamiltonian H. Again using Eq. (5), we find the result of these transformations:

$$H_{\text{BHP}} = H_{\text{int}} + \tfrac{1}{2}\sum_{0\neq k<k_c} (\pi_{\vec{k}} + i\omega_p q_{\vec{k}}^{*}) \times (\pi_{\vec{k}}^{*} - i\omega_p q_{\vec{k}}). \quad (11)$$

The solution of the BHP problem thus is equivalent to the solution of the highly degenerate eigenvalue problem defined by H_{int} without requring subsidiary conditions.

The same approach can be used to calculate H_{int} to higher order. With a more accurate definition of the plasmon creation and annihilation operators,[4] the Hamiltonian (10) can be obtained in closed form with a complete separation of the electron and plasmon variables exact to all orders in the electron-plasmon coupling constant and assuming only the random phase approximation.

The author wishes to express his appreciation to J. Bardeen and G. Rickayzen for stimulating discussions.

---

*On leave from the Weizmann Institute of Science, Rehovoth, Israel.

[1]Bohm, Huang, and Pines, Phys. Rev. 107, 71 (1957). See also P. Nozieres and D. Pines, Phys.

Rev. 111, 442 (1958), hereafter referred to as BHP.
[1]Lipkin, de-Shalit, and Talmi, Nuovo cimento 2, 773 (1955), hereafter referred to as LST. See also H. J. Lipkin, Notes of Lectures at Ecole d'Ete de Physique Theorique, Les Houches, 1958 (unpublished).
[3]D. Pines and J. R. Schrieffer, Nuovo cimento 10, 496 (1958).
[4]R. Brout, Phys. Rev. 108, 515 (1957) defines these operators.

FINE STRUCTURE IN THE ZEEMAN EFFECT OF EXCITONS IN GERMANIUM*

Kenneth J. Button, Laura M. Roth,
W. H. Kleiner, Solomon Zwerdling,
and Benjamin Lax
Lincoln Laboratory,
Massachusetts Institute of Technology,
Lexington, Massachusetts
(Received January 21, 1959)

Exciton formation observed in the experimental study[1] of the indirect transitions in Ge produced two strong absorption edges at zero magnetic field which were identified with the split ground level. The original data were obtained by observing the transmission of linearly polarized infrared radiation through a 6-mm sample at 1.5°K using fields up to 38 9000 oersteds and a spectral slit width of 7×10^{-5} ev. With increasing magnetic field, the two absorption edges move to higher energy and a large number of smaller edges appear superimposed upon them as the Zeeman fine structure develops. These smaller edges also move to higher energy with increasing field, and this motion is best illustrated when the edges are transformed to maxima by taking the derivative of the transmission traces as shown in Fig. 1. Figure 2 shows a diagram of energy levels as a function of magnetic field intensity where the bars show the positions of the maxima, including those of Fig. 1, and the lines represent theoretical results.

The theory was based on the spin Hamiltonian derived by considering the symmetry properties of the exciton band edge. In Ge, the band edge for this exciton is at four equivalent [111] points on the reduced zone boundary,[2] which are assumed to contribute independently to the spectrum. States at each of these points are characterized by their symmetry with respect to the point group D_{3d}. The Hamiltonian is a linear combination of D_{3d} invariants constructed from

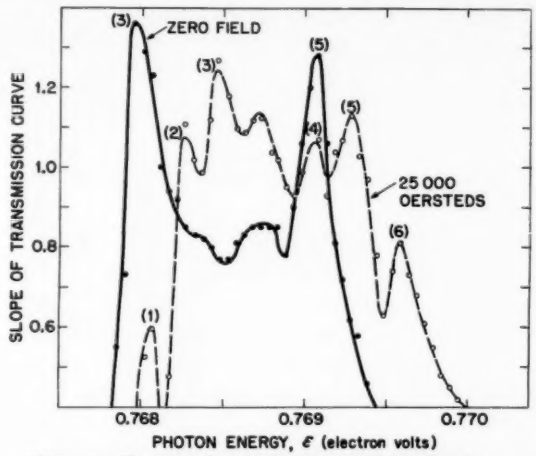

FIG. 1. Zeeman fine structure in the indirect exciton in Ge for $\vec{H}\parallel[100]$, $\vec{E}\parallel\vec{H}$ at 1.5°K. The two prominent maxima at zero field move to higher energy with increasing field and develop satellites which also move to higher energy.

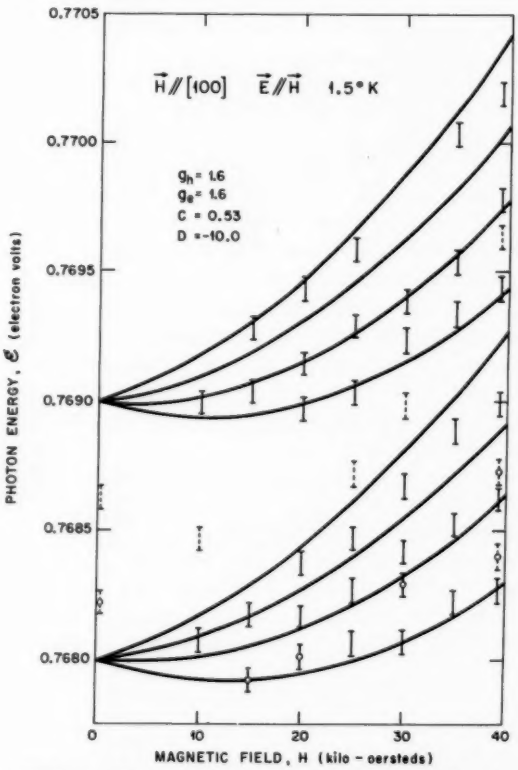

FIG. 2. Diagram of energy levels of the indirect exciton vs magnetic field intensity. The bars represent experimental maxima such as those of Fig. 1; those containing circles represent inflections and the dashed bars are not accounted for by the theoretical lines. The lines represent solutions of Eq. (1).

the angular momentum J of the hole ($\vec{J}=3/2$), the spin $\vec{S}$ of the electron ($S=\frac{1}{2}$), and the magnetic field $\vec{H}$. A simple combination which was found to fit the experimental energy spectrum is

$$\mathcal{H}=D(J_z^2-\vec{J}^2/3)-g_h\beta\vec{J}\cdot\vec{H}+g_e\beta\vec{S}\cdot\vec{H}+CH^2, \quad (1)$$

where β is the Bohr magneton. The first term represents the zero-field splitting, the z axis lying along a trigonal direction, the second and third terms represent Zeeman energies of the hole and electron, and the fourth represents an isotropic diamagnetic contribution which becomes significant above 10 000 oersteds.

The first two terms of Eq. (1) yield a 4×4 matrix. The effect of the magnetic field is to split the two zero-field levels into four. Addition of electron Zeeman splitting results in eight levels for each exciton valley. The experimental results for $\vec{H}\parallel[100]$, for which all valleys give the same spectrum in Ge, are compared with the theoretical spectrum in Fig. 2. The values of the coefficients obtained by fitting the experimental data for this orientation are $2D=(-10.2\pm5\%)\times10^{-4}$ ev, $g_h=1.6\pm10\%$, $g_e=1.6\pm15\%$, and $C=(0.53\pm5\%)\times10^{-12}$ ev/oe^2. Actually, any value within the range of uncertainty fits reasonably well.

Experimental results were also obtained for the magnetic field in the [111] direction. For $\vec{E}\parallel\vec{H}$, a reasonable fit was achieved by using the above parameter values and considering only the three valleys oriented equivalently with respect to $\vec{H}$. For $\vec{E}\perp\vec{H}$, more structure appeared, which is consistent with the appearance of a contribution from the fourth valley.

A detailed interpretation of the coefficients of the spin Hamiltonian can be considered with the effective-mass approximation. A theoretical estimate[3] of D agrees with the experimental value. The magnitude of D depends both on the electron anisotropy and the difference in mass of the heavy and light holes. The value of g_h obtained is only a quarter of the value 6.4 for the "free" hole estimated by Luttinger.[4,5] Thus, binding effects must be important. A theoretical estimate indicates that the electron g-factor should be less than two and highly anisotropic.[3] The spectra observed are not inconsistent with this. It may be possible to determine this anisotropy by performing a more accurate experiment, but in that case it may also be necessary to include other anisotropic terms in the spin Hamiltonian.

The indirect exciton data can be improved by using higher fields, circularly polarized radiation and an electronic method to differentiate the transmission signal continuously. The use of a sample at least one centimeter thick will improve the definition by appropriately matching the absorption coefficient. Alternatively, the emission technique[6] at liquid He temperature should produce discrete lines from the annihilation of the indirect exciton. The use of a Weierstrass sphere with larger-volume magnetic fields would focus the emergent radiation.

A similar analysis of the direct exciton[7] has been undertaken using a Hamiltonian analogous to Eq. (2) with $D=0$. Transitions to six levels are expected in the region below about 15 000 oersteds where the spin Hamiltonian should be valid. The six allowed transitions have not been properly resolved, although the fine structure has definitely been indicated by the three- to four-fold increase in line width at 38 900 oersteds. The electron spin g-factor[5] ($g=-2.6$) implies a Zeeman splitting of about 5×10^{-4} ev at maximum field. To resolve this structure, either higher fields will be required or the present line width of $\sim10^{-3}$ ev will have to be reduced by the use of thinner, strain-free samples.

We are indebted to Irwin B. Lurie for his assistance in analyzing the data.

---

*The work reported here was performed at Lincoln Laboratory, a technical center operated by Massachusetts Institute of Technology with the joint support of the Army, Navy and Air Force, under contract.

[1]Zwerdling, Lax, Roth, and Button, Phys. Rev. (to be published).

[2]G. Dresselhaus, J. Phys. Chem. Solids 1, 14 (1956).

[3]L. M. Roth and W. H. Kleiner, Bull. Am. Phys. Soc. Ser. II (to be published). See also L. M. Roth, Quarterly Progress Report on Solid-State Research, Lincoln Laboratory, Massachusetts Institute of Technology, February, 1959 (unpublished), Sec. IV.

[4]J. M. Luttinger, Phys. Rev. 102, 1030 (1956).

[5]Roth, Lax, and Zwerdling, Phys. Rev. (to be published).

[6]Haynes, Lax, and Flood, 1958 International Conference on Semiconductors, Rochester, New York, August 18-22, 1958, J. Phys. Chem. Solids (to be published).

[7]Zwerdling, Roth, and Lax, Phys. Rev. 109, 2207 (1958).

DIRECT OBSERVATION OF THE hfs OF A PARAMAGNETIC ION IN AN ANTIFERROMAGNET. NUCLEAR MAGNETIC RESONANCE OF Co^{59} IN CoF_2

V. Jaccarino
Bell Telephone Laboratories,
Murray Hill, New Jersey
(Received December 29, 1958)

Indirect experimental evidence[1] for the existence of a Co^{59} ($I=7/2$) hyperfine interaction in antiferromagnetic CoF_2 was found in the course of measuring the relaxation times of the F^{19} high-frequency nuclear magnetic resonance (NMR). The indirect observations consisted of two separate measurements: (1) measuring the frequency dependence of T_1^{19} and (2) measuring the degree of the "off-resonance" saturation of the μ^{19}.

We have now observed directly the high-frequency NMR of Co^{59} in a single crystal of CoF_2 in the range of frequencies of 160–190 Mc/sec in external fields extending to 10 kilo-oersteds and at temperatures of 1.3° to 4.2°K. The resonances occur at these high frequencies because of the intra-atomic hyperfine interaction of the Co^{59} magnetic moment with the huge fields of the unbalanced d electrons on the Co^{++} ion, and the spatial polarization of the Co^{++} spin moment in the ordered state.[2] Because of the nuclear electric quadrupole interaction, seven approximately equally spaced lines were seen, each of which is split in two by the external magnetic field. The latter effect results from the removal of the spatial degeneracy associated with the antiferromagnetic ordering.

With the external magnetic field parallel to the unique axis, [001], the Hamiltonian may be written as[2]

$$\mathcal{H}_0 = (A_z^{59}\langle S_z\rangle - \gamma^{59}\hbar H_z)I_z + \sum_{i=1}^{3} P_i I_i^2, \qquad (1)$$

where $\langle S_z\rangle$ is the time-average spin polarization per Co^{++} ion, A^{59} the magnetic hyperfine interaction constant, and

$$P_i = -\frac{eQ^{59}}{2I(2I-1)}\frac{\partial E_i}{\partial x_i};$$

Q^{59} is the Co^{59} nuclear quadrupole moment, $\partial E_i/\partial x_i$ is the x_ith electric field gradient component, and the directions x_i are the principal axes of the quadrupole interaction tensor, one of which coincides with [001]. If the quadrupole interaction be regarded as a perturbation, the eigenvalues of (1) correct to second order are given by

$$E_m = (A_z^{59}\langle S_z\rangle - \gamma^{59}\hbar H_z)m + \tfrac{1}{2}P_z m^2 + \frac{[(P_x - P_y)/2]^2}{A_z^{59}\langle S_z\rangle - \gamma^{59}\hbar H_z}\left[-m^3 + \frac{31}{2}m\right]. \qquad (2)$$

In Fig. 1 the field dependence of the 14 lines as a function of frequency is shown along with the experimental observations. The extrapolated zero-field splittings are given in Table I. The parameters determined from (2) with $H_{ext} = 0$

Table I. The experimentally determined parameters in the high-frequency NMR of $Co^{59}F_2$ at 1.3°K with H_{ext} parallel to [001].[a] The line widths, δH, represent the field separation of the extrema in the derivative of the line shape. Measurements of γ^{59} in diamagnetic cobalt compounds[b] have yielded $\gamma^{59}/2\pi = 1.01$ (kc/sec)/oe.

Line	$m \longleftrightarrow m-1$	$\nu(H_{ext}=0)$ (Mc/sec)	δH (oe)	$\gamma^{59}/2\pi$ (kc/sec)/oe
a_0	$\pm 7/2 \longleftrightarrow \pm 5/2$	165.030±0.025	165±10	1.23 ±0.02
b_0	$\pm 5/2 \longleftrightarrow \pm 3/2$	170.120±0.030	222±12	1.25 ±0.01
c_0	$\pm 3/2 \longleftrightarrow \pm 1/2$	175.275±0.030	263±15	1.248±0.010
d_0	$\pm 1/2 \longleftrightarrow \mp 1/2$	180.378±0.030	268±15	1.24 ±0.01
e_0	$\mp 1/2 \longleftrightarrow \mp 3/2$	185.383±0.040	242±15	
f_0	$\mp 3/2 \longleftrightarrow \mp 5/2$	190.530±0.100		
g_0	$\mp 5/2 \longleftrightarrow \mp 7/2$	195.800±0.200		

[a] In column 2, one must use either all the upper signs or all the lower signs.
[b] See reference 6.

are given in Table II. Since neither the sign nor the absolute magnitude of Q^{59} (or the gradient of the electric field) is known, only the quadrupole interaction energy is given and an uncertainty in the signs of the magnetic quantum numbers is necessarily present.

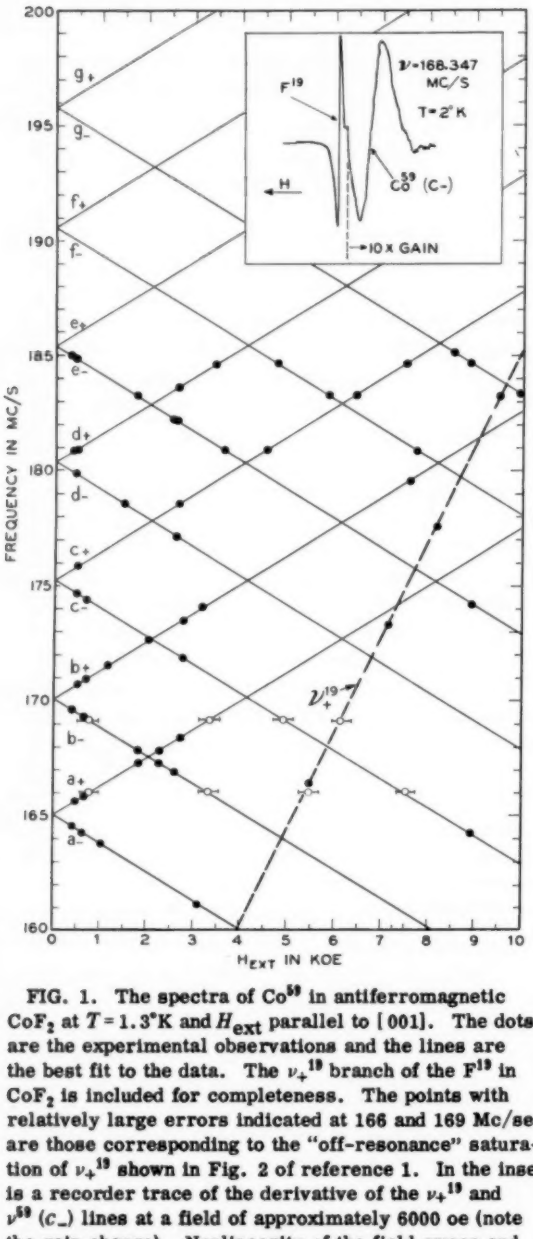

FIG. 1. The spectra of Co^{59} in antiferromagnetic CoF_2 at $T = 1.3°K$ and H_{ext} parallel to [001]. The dots are the experimental observations and the lines are the best fit to the data. The ν_+^{19} branch of the F^{19} in CoF_2 is included for completeness. The points with relatively large errors indicated at 166 and 169 Mc/sec are those corresponding to the "off-resonance" saturation of ν_+^{19} shown in Fig. 2 of reference 1. In the inset is a recorder trace of the derivative of the ν_+^{19} and ν^{59} (c_-) lines at a field of approximately 6000 oe (note the gain change). Nonlinearity of the field sweep and partial saturation contribute to the distortion of the two line shapes.

Moriya[3] has calculated A^{59} in the true $S = 3/2$ manifold using Stout's[4] value of A^{59} derived from electron paramagnetic resonance measurements of $Co{:}ZnF_2$ in which the latter author, following Tinkham,[5] employed the fictitious effective spin $S' = 1/2$. In this way an approximate mean value of $\langle S_z \rangle$ was determined.

Since the observed gyromagnetic ratios deviate by approximately 23% from the known[6] γ^{59}, and exhibit a negligible m dependence, the inadequacy of (1) in completely describing the observations is apparent. Phenomenologically we may add to (1) a term which allows for a field dependence of $\langle S_z \rangle$ in keeping with the known large parallel susceptibility of CoF_2 at 0°K.

$$A^{59}\langle S_z \rangle I_z \rightarrow [A_0^{59}\langle S_z \rangle_0 + A_H^{59}\langle S_z \rangle_H] I_z. \qquad (3)$$

However, γ^{19} in CoF_2 at the same temperature deviates only by 3.2% from the known γ^{19} and, considering the ratio of $H_{hf}^{59}/H_{hf}^{19} = 3.3$, it would follow that $\Delta\gamma^{59}/\gamma^{59}$ should be 10%. Thus a discrepancy still remains unless one assumes A_H^{59} to be quite different from A_0^{59}.

Table II. The derived values of the interaction constants using the data in Table I. Stout's value[a] for Co^{59}: ZnF_2 with $H_0 \| [001]$ is 225 Mc/sec ($S' = 1/2$). Moriya's derived value[b] for $S = 3/2$ is 132 Mc/sec.

$A^{59}\langle S_z \rangle = 180.4$ Mc/sec;	$\langle S_z \rangle_0 = 1.3$
$\lvert P_z \rvert = 1.70$ Mc/sec;	$\lvert P_x - P_y \rvert = 0 \pm 2$ Mc/sec

[a]See reference 4.
[b]See reference 3.

The measured line shapes (see inset of Fig. 1) are more nearly Gaussian than Lorentzian. This fact combined with the large values of the line widths generally confirms the T_2 mechanisms proposed by Suhl[7] and Nakamura.[8] More precise measurements including relaxation time studies are in progress and will be reported shortly.

We believe these experiments to be the first direct observation of the NMR of a paramagnetic ion nucleus.

The author is indebted to J. L. Davis for experimental assistance, to Professor J. W. Stout of the University of Chicago for the CoF_2 crystals and to Dr. T. Moriya and Dr. H. Suhl for many stimulating discussions.

[1]V. Jaccarino (to be published elsewhere).
[2]T. Moriya, Progr. Theoret. Phys. (Japan) 16, 641 (1956). Though many, including the author, have inde-

pendently considered the possibility of observing such resonances it was Moriya who first showed the theoretical feasibility of such studies.

[3]T. Moriya (private communication).

[4]J. W. Stout (private communication).

[5]M. Tinkham, Proc. Roy. Soc. (London) A236, 535, 549 (1956).

[6]W. C. Proctor and F. C. Yu, Phys. Rev. 81, 20 (1951).

[7]H. Suhl, Phys. Rev. 109, 606 (1958).

[8]T. Nakamura (private communication).

PHOTODETACHMENT CROSS SECTION OF THE NEGATIVE HYDROGEN ION

Stephen J. Smith and David S. Burch*
Atomic Physics Section,
National Bureau of Standards,
Washington, D. C.
(Received January 21, 1959)

This Letter reports the results of the first precise measurement of the wavelength dependence of the photodetachment cross section of the negative atomic hydrogen ion in the range from 0.4 to 1.3μ.

The importance of absorption by H^- in determining the opacity of the solar atmosphere,[1] and general interest in the theory of two-electron systems[2] have stimulated considerable effort in the calculation of the continuous absorption coefficient, or photodetachment cross section, of H^-. In particular, Chandrasekhar and co-workers[3] have conducted a series of calculations of the cross section using various refinements of the wave functions of the bound and free states and considering the differences in results obtained using dipole-length, velocity, and acceleration matrix elements. Calculations of this cross section also have been carried out recently by Geltman.[4]

Experimental results bearing on this subject have been meager. The H^- emission continuum has been studied[5] in arc and shock tube spectra. Branscomb and co-workers[6] have developed a method for observing photodetachment by collecting free electrons produced at the intersection of crossed ion and photon beams in a high-vacuum apparatus. Branscomb and Smith[7] measured an absolute integrated H^- photodetachment cross section and obtained a check on the shape of the cross section in the visible spectrum using the continuous emission from a tungsten lamp modified by a set of absorption filters. More recently they have developed a set of band-pass filters utilizing interference reflection filters to make relative point-by-point measurements of slowly varying cross sections.[8]

The present authors have undertaken to refine the negative-ion beam apparatus to obtain an accurate relative H^- photodetachment cross section for comparison with and evaluation of theoretical calculations. This has been accomplished by improving signal-to-noise in the experiment through improvement of preamplifier detection sensitivity and elimination of background signals (such as photoelectric signals); and by developing a direct, reliable method for relative determination of light intensity in the photon beam. These problems will be discussed in a future publication.

The results of our measurement of the photodetachment cross section of H^- are given in Fig. 1. We used band-pass filter combinations with widths ranging from 250 to 500A. It should be noted that this is then a low-resolution measurement, because of the necessity for transmitting as much as a half-watt of radiation to the ion beam. Each point in Fig. 1 is the average value of from six to twelve measurements with a single filter combination, with rms errors indicated by the bars. The value for the cross section at each band pass filter was obtained relative to the value at one reference filter at 5280A for which no error bar is shown. The shape of the cross section is determined relative to the value at 5280A to an accuracy of about 2%.

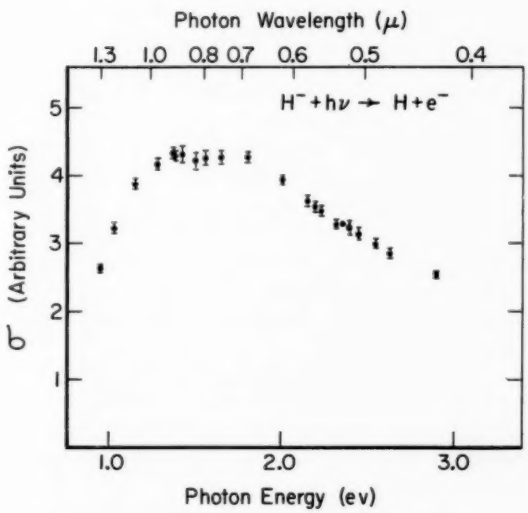

FIG. 1. Measured relative values of the photodetachment cross section for H^-.

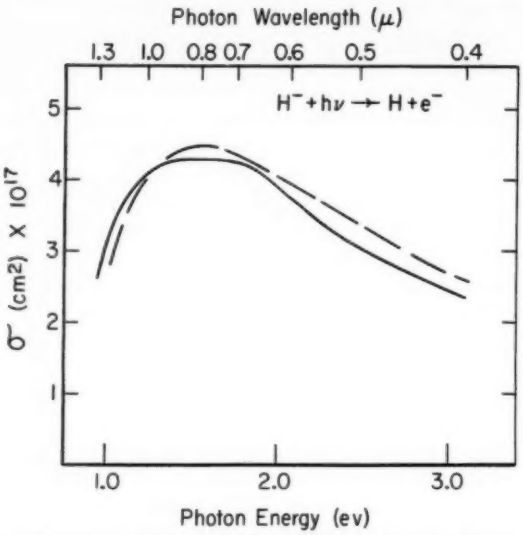

FIG. 2. Experimental cross section for photodetachment (solid curve) on an absolute scale (see text), compared with the theoretical curve of Chandrasekhar and Elbert (dashed curve).

We have used a smooth curve to represent our experimentally determined cross section. This curve, shown in Fig. 2, was put on an absolute scale through use of the Branscomb and Smith absolute measurement[7] of the integrated cross section. While the accuracy in the shape is about 2%, the absolute values are accurate only to 10%.

The present measurement of the shape of the cross section allows a critical comparison of theory with experiment. Included in Fig. 2, for comparison, is a curve drawn through values of the cross section very recently calculated by Chandrasekhar and Elbert[3] using dipole velocity matrix elements, Hart and Herzberg's 20-parameter ground-state wave function,[9] and a Hartree approximation for the free-state wave function. This theoretical curve is in significant disagreement with the energy dependence determined in the present measurement, although it is in fair agreement with the Branscomb and Smith absolute measurement of the cross section.

In addition, Chandrasekhar and Elbert[3] have calculated the cross section at $\lambda = 2985$A (4.15 ev) using the recently available free-state wave functions of Bransden et al.,[10] which include polarization and exchange effects. They obtain a value about 20% lower than the theoretical value based on the Hartree approximation, and point out that there should be smaller differences at lower energies. If so, this fragmentary result is more nearly in agreement with our measured energy dependence, and also appears to be still within the allowable error in our absolute scale. This supports the implication in the work of Bransden et al., that polarization and exchange effects in the free-state wave functions should be considered in the calculation of the absorption coefficient in the visible spectrum. Especially in view of the high degree of refinement already achieved in the development of H^- ground-state wave functions, further progress in obtaining agreement between this experiment and theory seems to depend on the development of free-state wave functions which accurately take account of polarization and exchange.

---

*Present address: Department of Physics, Oregon State College, Corvallis, Oregon.

[1]A. Unsöld, Physik der Sternatmosphären (Springer-Verlag, Berlin, 1955).

[2]H. A. Bethe and E. E. Salpeter, Quantum Mechanics of One- and Two- Electron Atoms (Academic Press, New York, 1957).

[3]S. Chandrasekhar and D. D. Elbert, Astrophys. J. 128, 633 (1958); S. Chandrasekhar, Astrophys. J. 128, 114 (1958), and references contained therein.

[4]S. Geltman, Phys. Rev. 104, 346 (1956).

[5]W. Lochte-Holtgreven, Naturwissenschaften 38, 258 (1951); O. Weber, Z. Physik 152, 281 (1958).

[6]L. M. Branscomb and W. L. Fite, Phys. Rev. 93, 651(A) (1954); S. J. Smith and L. M. Branscomb, J. Research Natl. Bur. Standards 55, 165 (1955).

[7]L. M. Branscomb and S. J. Smith, Phys. Rev. 98, 1028 (1955).

[8]Branscomb, Burch, Smith, and Geltman, Phys. Rev. 111, 504 (1958).

[9]J. F. Hart and G. Herzberg, Phys. Rev. 106, 79 (1957).

[10]Bransden, Dalgarno, John, and Seaton, Proc. Phys. Soc. (London) 71, 877 (1958).

PRESSURE-INDUCED INFRARED ABSORPTION OF MIXTURES OF RARE GASES*

Z. J. Kiss† and H. L. Welsh
McLennan Laboratory,
University of Toronto,
Toronto, Canada
(Received January 26, 1959)

A continuous absorption in the region 300 to 750 cm^{-1} has been observed in compressed helium-neon, helium-argon, and neon-argon gas

mixtures. A description and a qualitative interpretation of this new type of pressure-induced absorption will be given here.

The experiments were carried out with an absorption path length of 245 cm and total gas pressures in the range 50 to 180 atm, using a Globar source and a Perkin-Elmer Model 112 spectrometer with a CsBr prism. When the absorption cell was filled with a pure rare gas at the maximum pressure no change in transmission was observed. When a 1:1 mixture of two rare gases was introduced into the cell an absorption was recorded which decreased rapidly in intensity from ~350 cm^{-1}, the low-frequency limit of CsBr transmission, towards higher frequencies. For each pair of gases the intensity profile of the absorption was determined for a series of total gas pressures. The highest absorptions measured were of the order of 50%.

It was established that the absorption at a given frequency is proportional to the product of the partial densities, $\rho_X\rho_Y$, of the two component gases, X and Y, of the mixture. This is illustrated in Fig. 1 (a) where values of $(2.3/\rho_{He}\rho_A) \times \log_{10}(I_0/I)$ are plotted against the frequency for a He-A mixture; for three different total densities the reduced profile is the same within the experimental error. From the form of the density dependence it can be concluded that the absorption has its origin in binary collisions of the type XY. In such collisions the distortion of the charge distribution of the atoms by intermolecular forces gives rise to a dipole moment which is responsible for the absorption. On the other hand, the distortion of the charge distribution in binary collisions of like atoms has a center of symmetry and no dipole moment is produced; thus, the pure rare gases show no absorption.

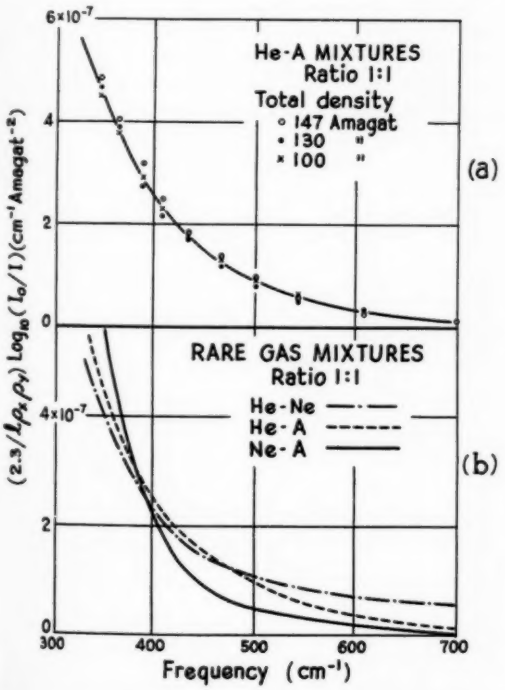

FIG. 1. Infrared absorption of binary mixtures of rare gases: (a) He-A at three different densities, (b) He-Ne, He-A, and Ne-A.

In binary collisions of rare gas atoms the distortion of the charge distribution must be due to overlap forces. Van Kranendonk[1] has shown that in hydrogen-hydrogen and hydrogen-helium collisions the magnitude of the electric dipole induced by the overlap forces falls of exponentially with the intermolecular distance, and one can assume the same type of variation in collisions of unlike rare gas atoms. Since the induced moment thus varies very rapidly with internuclear distance, transitions in the relative kinetic energy can take place under absorption of light. The effect might therefore be called collision-induced translational absorption.

If the translational motion of the molecules is treated classically the absorption arising from a head-on collision is entirely due to the variation of the magnitude of the induced dipole moment with internuclear separation, whereas in a collision with an impact parameter of the order of the atomic diameters the absorption should resemble the rotational absorption of a diatomic molecule. The observed spectrum is a superposition of spectra varying continuously from the rotational type to the pure translational type. The intensity distribution in the rotational-type spectrum should have, like a diatomic molecule, a maximum at a frequency depending on the temperature and the effective rotational constant, B_{eff}, of the combination; beyond the maximum the intensity should decrease gradually towards higher frequencies. There should, however, be no discrete rotational lines since B_{eff} is not sharply defined. In the present experiments only the high-frequency tail of the absorption is observed. To record the rest of the spectrum, in particular the maximum, would require pressure windows which are transparent in the far infrared.

The shape of the absorption depends on the particular pair of rare gas atoms producing it.

In Fig. 1 (b) reduced profiles for He-Ne, He-A, and Ne-A are compared. When the average atomic weight of the collision partners is high, the absorption is higher at 350 cm^{-1} and falls off more rapidly towards higher frequencies. It is evident that not much can be said about the integrated intensity of the absorption until the experiments are extended to the further infrared.

Participation of the relative kinetic energy of the colliding molecules in induced absorption processes has been observed in the pressure-induced vibrational absorption of hydrogen.[2] According to the theory of Van Kranendonk[1] the Q branch of this absorption owes most of its intensity to interaction in the region of the short-range overlap forces, whereas the rotational lines of the vibrational band are due mainly to the longer range quadrupole interaction. Experimentally, the Q branch shows two components, Q_P and Q_R, which have been interpreted as difference and summation tones, respectively, of the vibrational frequency of the hydrogen molecule with a continuum of frequencies associated with the relative kinetic energy. The magnitude of the changes in the translational energy is of the same order as that observed in the collision-induced translational spectra of the rare gases.

Pressure-induced translational continua have also been observed recently in another connection. The pressure-induced rotational spectrum of hydrogen was studied with CsBr optics and compared with intensity calculations based on pure quadrupole interaction.[3] It was found that, particularly in the case of the collisions of light atoms such as H_2-H_2, H_2-He, the observed intensity of the rotational absorption of hydrogen was considerably higher than that calculated, and the profile of the absorption different from that expected. The observations could be explained by assuming that the rotational spectrum was superimposed on a continuum decreasing in intensity towards higher frequencies, and a tentative interpretation of the continuum in terms of translational absorption was given. The present experiments with mixtures of the rare gases confirm that interpretation.

*This research was supported by a grant from the National Research Council of Canada.

†Holder of a scholarship from the National Research Council of Canada, 1957-58, and of a Canadian Kodak Fellowship, 1958-59.

[1]J. Van Kranendonk, Physica 23, 825 (1957); 24, 347 (1958).

[2]D. A. Chisholm and H. L. Welsh, Can. J. Phys. 32, 291 (1954).

[3]Kiss, Gush, and Welsh, Can. J. Phys. (to be published).

NEUTRON CROSS-SECTION MEASUREMENTS AT 4.5 Bev*

John H. Atkinson, Wilmot N. Hess, Victor Perez-Mendez, and Roger W. Wallace
Lawrence Radiation Laboratory, University of California, Berkeley, California

(Received January 26, 1959)

In this Letter we report the results of a series of measurements on the total and reaction cross sections for 4.5-Bev neutrons on carbon, copper, and lead.

The experimental arrangement is shown in Fig. 1. The neutron flux is taken at 0° relative to the proton beam incident on an internal target in the Bevatron. The beam-defining collimator is 5 ft long and is located 50 ft from the target; the aperture in the collimator is 2×2 in., and hence the emerging neutron beam has an angular spread of less than 0.1 degree. Two lead filters placed in the collimator serve to eliminate photons present in the neutral beam.

The energy distribution of the neutrons is known[1] to be peaked at about 4 Bev and to extend up to the beam energy of 6.2 Bev. The neutron detector described below has a threshold detection efficiency for neutrons starting at 3.5 Bev, hence the mean energy of the detected neutrons is ~4.5 Bev with an energy spread of $^{+1.5}_{-1.0}$ Bev.

Figure 1 shows the neutron detector schematically. It is a counter telescope with three scintillators and a gas Čerenkov counter.[2] First in the beam line is a scintillator connected in anti-

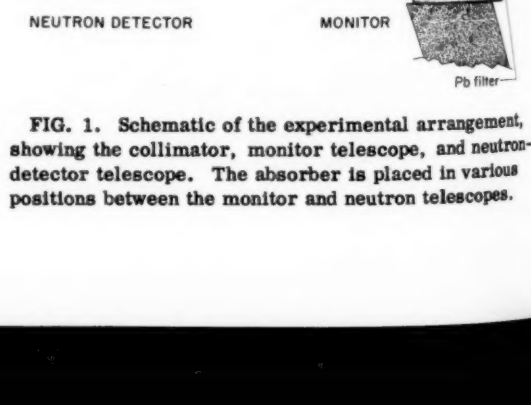

FIG. 1. Schematic of the experimental arrangement, showing the collimator, monitor telescope, and neutron-detector telescope. The absorber is placed in various positions between the monitor and neutron telescopes.

coincidence to the remaining three counters. This is followed by a 12-in. long Be converter, a scintillator, a Pb electron filter, a sweeping magnet, the gas Čerenkov counter, and a final scintillator. Neutrons are detected by the charged pions produced in the beryllium converter and recorded by the triple coincidence of the two scintillators and Čerenkov counter. The threshold energy of 3 Bev for detecting pions is set by the gas pressure in the Cerenkov counter. The Pb electron filter and the sweeping magnet serve to deflect out of the telescope the conversion electrons, originating from decaying π^0 mesons of all energies produced in the beryllium converter. Protons made in the converter have too low a β to count in the Čerenkov counter.

The neutron-counter telescope is placed at a fixed distance of 30 feet from the collimator. A similar telescope at the rear of the collimator monitors the neutron flux by detecting charged pions produced in the lead filter. Absorption measurements in "good" and "poor" geometry were done by placing the sample at various distances from the neutron detector. Figure 2 shows the results of such a series of measurements on Pb. Similar measurements have been performed on carbon and copper. The limiting values of the cross section for "good" and for "poor" geometry yield the total and reaction cross sections listed in Table I. The most interesting feature of the data is that the elastic cross sections, especially for the heavy elements, are considerably smaller than at lower energies, whereas the absorption cross sections

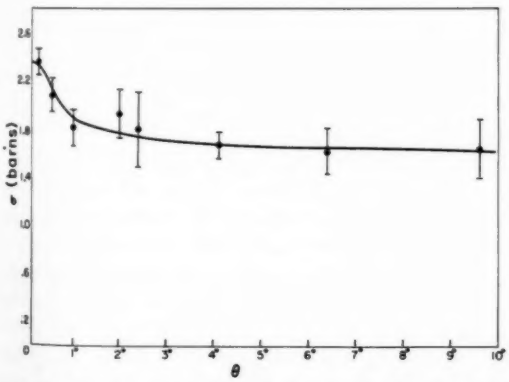

FIG. 2. Cross section of neutrons in lead as a function of the half angle subtended by the neutron detector. The solid curve is a least-squares fit to the data according to an opaque-nucleus calculation for a mean neutron energy of 4.5 Bev.

Table I. Neutron total and reaction cross sections.

	σ_t (in mb)	σ_r (in mb)
Pb	2320±130	1660±90
Cu	1088±22	638±24
C	354±11	218±8

remain essentially constant from 300 Mev up to our energy.

The following Letter discusses the interpretation that can be placed on these values, in relation to the Brookhaven measurements performed at a mean energy of 1.4 Bev, and lower-energy data.[3]

We should like to acknowledge the support of Professors A. Carl Helmholz and Burton J. Moyer for this experiment. We should also like to thank Dr. Edward J. Lofgren and the Bevatron crew for their help and unfailing courtesy in the performance of this experiment.

---

*Work done under the auspices of the U. S. Atomic Energy Commission.

[1]Fred N. Holmquist, University of California Radiation Laboratory Report UCRL-8559, December, 1958 (unpublished).

[2]V. Perez-Mendez and J. H. Atkinson, University of California Radiation Laboratory Report UCRL-8570, December, 1958 (unpublished).

[3]Coor, Hill, Hornyak, Smith, and Snow, Phys. Rev. 98, 1369 (1955).

GENERALIZED DIFFRACTION THEORY FOR VERY-HIGH-ENERGY COLLISIONS*

A. E. Glassgold and Kenneth R. Greider
Lawrence Radiation Laboratory,
University of California,
Berkeley, California
(Received January 26, 1959)

It has become customary to interpret nuclear scattering experiments in terms of the optical model in which one introduces a general single-particle operator (optical potential) for the incident projectile and attempts to determine its properties from experiment. Although this procedure has yielded many useful results it has a number of drawbacks, particularly for very high energies. On the other hand, there are a number of simplifications which obtain at very high energies which permit a more satisfactory treatment to be given.

To be specific, we consider the scattering of a neutral spinless particle by a spherical symmetric object. The scattering amplitude $f(\theta)$ in the usual notation is

$$k f(\theta) = \frac{1}{2i} \sum_{l=0}^{\infty} (2l+1)(\eta_l - 1) P_l(\cos\theta).$$

The amplitude η_l of the lth outgoing wave is related to the phase shift δ_l by the equation $\eta_l = \exp(2i\,\delta_l)$. We propose to treat the scattering in terms of these coefficients rather than with a potential model. In doing so we shall make the quasi-classical approximation in which η is a continuous function of l. In addition we emphasize the role of strong absorption at high energies by writing the scattering amplitude as a sum,

$$f(\theta) = f_0(\theta) + f_1(\theta).$$

The amplitude $f_0(\theta)$ corresponds to the complete absorption of L partial waves: $\eta_l = 0$ for $l \leq L$ and $\eta_l = 1$ otherwise. Thus $f(\theta)$ is the amplitude for the "black-sphere" model,[1,2] for which exact solutions exist.

We now generalize the simple diffraction theory by writing

$$\eta(l) = |\eta(l)| e^{i\alpha(l)},$$

and by assuming that (a) the opacity function, $1 - |\eta|^2$, decreases monotonically with l from an essentially constant value β for small l to zero for large l, (b) this transition occurs mainly within an interval of width 2Δ centered about a large value of the angular momentum L, and (c) the phase function α is continuous and vanishes for sufficiently large l. By expressing these assumptions in terms of certain definite analytic functions for $1 - |\eta|^2$ and α, one can find closed expressions for $f(\theta)$, $\sigma^{(T)}$, and $\sigma^{(t)}$. We have chosen various functional forms to represent the transition region, assuming constant phase, but find the results to be independent of the details in this region.

The significant feature of this result is that a scattering formalism of sufficient generality for high-energy collisions has been obtained which eliminates the need for any lengthy calculations. Closed-form expressions are thus available to discuss a large number of measurements in terms of a few physically significant parameters. Assuming constant phase, these parameters are: L, the number of partial waves strongly absorbed; 2Δ, the range over which the opacity function decreases from β to 0; β, the opacity for small l; and α, the phase.

As an example of this method we consider neutron total and reaction cross sections in the energy range from 0.3 to 4.5 Bev for C, Cu, and Pb. The measurements at the highest energy are reported in the preceding Letter.[3] The following reasonable assumptions are made about the dependence of L and Δ on k and A (atomic mass):

$$L \propto k A^{1/3}, \quad \Delta \propto k.$$

Good agreement can be obtained only if the phase is close to zero. In other words the scattering amplitude is practically pure imaginary. The results are plotted in Fig. 1, and the values deduced for β are:

	Energy (Bev)		
	0.3	1.0	4.5
Pb	0.97	1.00	0.94
Cu	0.94	0.99	0.92
C	0.80	0.93	0.90

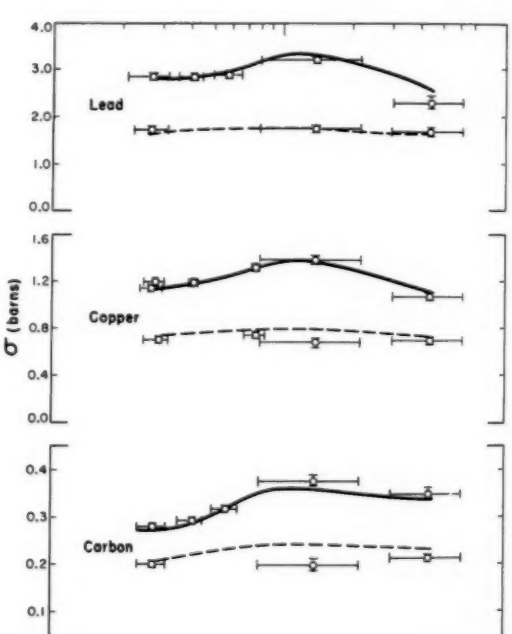

FIG. 1. Neutron total and reaction cross sections. The solid curves are the theoretical total cross sections and the dash curves are the theoretical reaction cross sections. The circles are the experimental measurements. The following values were used in the analysis: $L = (1.26 \times 10^{-13}\ \text{cm}) k A^{1/3}$ and $\Delta = (0.672 \times 10^{-13}\ \text{cm}) k$.

The dependence of β on k and A can be interpreted in terms of a classical picture of exponential absorption with distance, the absorption coefficient being related to the observed nucleon-nucleon total cross sections. The energy variations of the cross sections are best understood in terms of the basic formulas for the partial reaction and total cross sections:

$$\sigma_l^{(r)} = (1 - |\eta_l|^2)(2l+1)\pi\lambda^2,$$

$$\sigma_l^{(t)} = (1 - \mathrm{Re}\eta_l)\,2(2l+1)\pi\lambda^2.$$

For small real η, $\sigma_l^{(r)}$ is less sensitive to changes in η than $\sigma_l^{(t)}$, since the former is a quadratic function of η whereas the latter is linear. In addition, the reaction cross section does not depend on the phase of η, whereas the total cross section does. The observed large energy variation in the total cross section can only be obtained by choosing the phase for η close to zero.

---

*Work performed under the auspices of the U. S. Atomic Energy Commission.

[1]H. A. Bethe and G. Placzek, Phys. Rev. 57, 1075(A) (1940).

[2]A. Akhieser and I. Pomeranchuk, J. Phys. 9, 471 (1945).

[3]Atkinson, Hess, Perez-Mendez, and Wallace, preceding Letter [Phys. Rev. Lett. 2, 168 (1959)]. The writers would like to thank these authors for early communication of their results.

SECOND RESONANCE IN PION PHOTOPRODUCTION *

Michael J. Moravcsik
Lawrence Radiation Laboratory,
University of California,
Livermore, California

(Received January 15, 1959)

Recently several authors have made attempts[1-3] to determine the angular momentum and multipole state in which the alleged second resonance in pion photoproduction takes place. Qualitative arguments have been advanced concerning the features of the angular distribution[2] and the recoil nucleon polarization[3] in case of unpolarized incident photons. The present note discusses another type of experiment which might help to determine the resonating state. It is the measurement of the differential cross section for polarized photons. In particular, it is proposed that $(d\sigma/d\Omega)_\perp$, the differential cross section for photons polarized perpendicular to the production plane, be measured. This quantity has the great advantage that even in the case of charged pions the meson current (or photoelectric term) does not contribute to it. It has been shown[4] that due to the change in sign of its interference terms, the meson current term becomes very important for charged pions in the region between the first resonance and 500-Mev photon laboratory energy. No investigations have been made above 500 Mev, but there is no reason to believe that at high energies we would again encounter the somewhat fortuitous situation that prevails below the first resonance, where the interference terms of the meson current contribution cancel to a great extent its own square contribution. On the other hand, it is not simple to include the effect of the meson current term in qualitative considerations, and in fact for instance reference 2 omits it. Whether this omission alters the qualitative conclusions is not known at the present. It is an advantage, therefore, to be able to say that the considerations in this note, like those in reference 3, are completely independent of the meson current term.

In the absence of the meson current term the important contribution, at the second resonance, will come from the S-wave term and the resonance state. In making this statement we assume that the various nonresonating P states (including the state which gives the first resonance) contribute relatively little, compared to the two states mentioned above. The goodness of this assumption is open to question until a quantitative study is made of the entire problem of high-energy photoproduction. Assumptions of similar nature, however, are also made in the arguments of references 2 and 3.

With the above assumptions it can be shown that if and only if the second resonance is in the $D_{\frac{3}{2}}$, $E1$ state as Peierls[2] suggests, will $(d\sigma/d\Omega)_\perp$ be isotropic. This conclusion can be arrived at from the equations

$$|M|_\perp^2 = \sum_{i=0}^{5} A_i x^i, \qquad (1)$$

where

$$A_i = \sum_{j+k=i} U_j^{(k)}, \quad j = 0, \ldots 4; \; k = 0,1 \qquad (2)$$

and

$$U_j^{(\alpha)} = \sum_{\alpha+\beta=j} (H_{1\alpha}{}^* H_{1\beta} + H_{2\alpha}{}^* H_{2\beta}), \quad \alpha,\beta = 0,1,2 \qquad (3)$$

$$U_j^{(1)} = -2 \sum_{\alpha+\beta=j} \mathrm{Re}(H_{1\alpha}^{*} H_{2\beta}). \quad (4)$$

We denoted here the matrix element by M, and $x \equiv \cos\theta$, where θ is the production angle in the center-of-mass system. In the above equations

$$H_{\mu\nu} = \sum_n c_{\mu\nu,n} B_n, \quad \mu = 1,2; \ \nu = 0,1,2 \quad (5)$$

where B_n is the amplitude of a certain angular momentum and multipole state, described by the index n, and $c_{\mu\nu,n}$ is a 6 by n matrix. For the first ten angular momentum states this matrix is

μ	ν	$S_{\frac{1}{2}}$ $E1$	$P_{\frac{1}{2}}$ $M1$	$P_{\frac{3}{2}}$ $M1$	$P_{\frac{3}{2}}$ $E2$	$D_{\frac{3}{2}}$ $E1$	$D_{\frac{5}{2}}$ $E3$	$D_{\frac{3}{2}}$ $M2$	$D_{\frac{5}{2}}$ $M2$	$F_{\frac{5}{2}}$ $E2$	$F_{\frac{5}{2}}$ $M3$
1	0	1	0	0	0	1	-3/2	3	-3	0	0
1	1	0	0	3	3	0	0	0	0	3	12
1	2	0	0	0	0	0	15/2	0	15	0	0
2	0	0	1	2	0	0	0	0	0	0	-9/2
2	1	0	0	0	0	0	0	6	9	0	0
2	2	0	0	0	0	0	0	0	0	0	45/2

.(6)

The derivation of these results will be given later in connection with a quantitative study of high-energy photoproduction. We note here only that the above notation in motivated by the form in which Chew et al.[5] expressed the contributions of the various angular momentum states to the photoproduction amplitude. In our notation the $H_{\mu\nu}$'s depend only on the $\mathfrak{F}_\mu$'s ($\mu = 1, \ldots, 4$) of reference 5, and ν gives the power of x arising from the Legendre polynomials in $\mathfrak{F}_\mu$. On the other hand, the particular bilinear combinations of $H_{\mu\nu}^{*}$ and $H_{\mu\nu}$ which constitute the $U_j^{(k)}$'s depend only on the way the four vectorial expressions of reference 5 enter the formula for the cross section. Thus j gives the power of x contributed by the $\mathfrak{F}_\mu$'s, and k the power of x contributed by the vectorial forms.

One can see from the above equations that the angular distribution is isotropic if and only if

$$U_j^{(1)} = 0 \quad \text{for all } j, \quad (7)$$

and

$$U_j^{(0)} = 0 \quad \text{for all } j \neq 0. \quad (8)$$

The matrix (6) shows that, barring extremely fortuitous cancelations, these conditions are satisfied if and only if we have a linear combination of the $S_{\frac{1}{2}}$, $E1$ and $D_{\frac{3}{2}}$, $E1$ states.

It should be noted that the precise form of Eqs. (1) through (6) will be altered if angular momentum states even higher than those listed in Eq. (6) are considered but the final conclusion remains unchanged.

The experiment proposed here is a more difficult one than the measurement of the nucleon polarization suggested by reference 3. Production of pions by polarized photons, however, has been observed at Stanford[6] and thus the experiment is not unfeasible. Thus the present scheme might become a third, independent way of determining the state involved in the second resonance.

*Work performed under the auspices of the U.S. Atomic Energy Commission.

[1]R. R. Wilson, Phys. Rev. 110, 1212 (1958).
[2]R. F. Peierls, Phys. Rev. Lett. 1, 174 (1958).
[3]J. J. Sakurai, Phys. Rev. Lett. 1, 258 (1958).
[4]A. Lazarus, High-Energy Laboratory, Stanford University (private communication).
[5]Chew, Goldberger, Low, and Nambu, Phys. Rev. 106, 1345 (1957), Eq. (7.2).
[6]R. F. Mozley, High-Energy Laboratory, Stanford University (private communication).

POLARIZATION OF NUCLEONS IN INELASTIC SCATTERING FROM NUCLEI*

A. K. Kerman, H. McManus,† and R. M. Thaler‡
Laboratory for Nuclear Science,
Massachusetts Institute of Technology,
Cambridge, Massachusetts
(Received January 26, 1959)

Elastic scattering of nucleons by nuclei at high energies has been treated by several authors,[1] following the methods introduced by Watson and collaborators.[2] From a knowledge of the nucleon-nucleon scattering amplitude as given by a potential model or a phase-shift analysis[3] the high-energy elastic scattering of nucleons from nuclei, especially in the forward direction, can be calculated; for an even-even

nucleus like C^{12} with spin and isotopic spin zero, the calculation requires only a knowledge of the nucleon distribution in the nucleus. The good agreement with experiment obtained[1] suggests an extension of the method to inelastic scattering, which differs only in that nuclear matrix elements now appear as parameters. A special case has already been treated by Squires.[4]

Following the notation adopted by Bethe,[1] we write the two-nucleon scattering operator as

$$M_i(q) = A_i(q) + C_i(\sigma_{1n} + \sigma_{2n}) + B_i\sigma_{1n}\sigma_{2n} + E_i\sigma_{1q}\sigma_{2q} + F_i\sigma_{1p}\sigma_{2p}, \quad (1)$$

where the subscripts i refer to $T=1, 0$, and $\vec{n}$, $\vec{p}$, $\vec{q}$ are three mutually perpendicular unit vectors, chosen so that $\vec{n}$ is normal to the scattering plane.

In the impulse approximation, for scattering of a nucleon involving a nuclear transition from a state n to a state n' the spin, isotopic spin average of this operator is given by

$$\mathfrak{M}(q) = \langle n'|M(q)e^{i\vec{q}\cdot\vec{r}}|n\rangle, \quad (2)$$

and the nuclear scattering operator is given by[5]

$$T_{n'n} = -\frac{1}{2\pi}\frac{\hbar^2}{m}N\mathfrak{M}, \quad (3)$$

where N is the number of nucleons in the target nucleus. From Eq. (2), $\mathfrak{M}$ is easily calculated in terms of reduced nuclear matrix elements. After a straightforward calculation one arrives at the result that the angular distribution is given by

$$I_0 = \tfrac{1}{4}\,\mathrm{Tr}(\mathfrak{M}\mathfrak{M}^*) = (|\bar{A}|^2 + |\bar{C}|^2)L_1 + \tfrac{1}{2}(|\tilde{F}|^2 + |\tilde{B}|^2 + |\tilde{C}|^2)L_2 + \tfrac{1}{2}(2|E'|^2 - |F'|^2 - |B'|^2 - |C'|^2)L_3, \quad (4)$$

where

$$L_1 = \sum_l [1/(2l+1)]\,|N_l|^2, \quad (5)$$

$$L_2 = \sum_{l,k} [1/(2l+1)]\,|Q_k(ls)|^2, \quad (6)$$

$$L_3 = \sum_{l'l;k} [1/(2k+1)](1l00|k0)(1l'00|k0) \times Q_k(ls)Q_k^*(l's). \quad (7)$$

The symbols $Q_k(ls)$ and N_l represent the reduced nuclear matrix elements for transitions with and without spin flip, respectively, and the symbols $\bar{M}$, $\tilde{M}$, M' stand for suitable averages over isotopic spin of the target nucleons of any of the quantities A, F, etc. There is more than one such average because the isotopic spin averages are not independent of the spin averages.

In many cases only one value of l is important and then $M' = \tilde{M}$. The polarization then becomes

$$P = \mathrm{Tr}(\mathfrak{M}\vec{\sigma}\cdot\vec{n}\,\mathfrak{M}^*)/\mathrm{Tr}(\mathfrak{M}\mathfrak{M}^*) = \frac{2\,\mathrm{Re}(\bar{A}\bar{C}^*) + 2\lambda\,\mathrm{Re}(\tilde{B}\tilde{C}^*)}{|\bar{A}|^2 + |\bar{C}|^2 + \lambda(|\tilde{F}|^2 + |\tilde{B}|^2 + |\tilde{C}|^2) + 2\mu|\tilde{E}|^2}, \quad (8)$$

where $\lambda = (L_2 - L_3)/2L_1$, $\mu = L_3/2L_1$.

The polarization in scattering from a nucleus of spin and isotopic spin zero is especially simple: it depends primarily on whether the final state corresponds to "normal," i.e. $\Delta\pi = (-1)^J$, or "abnormal" parity change, and whether it has isotopic spin change 0 ($\Delta T = 0$) or 1 ($\Delta T = 1$). For a $T=0$ to $T=0$ transition $\bar{M}_{00} = \tilde{M}_{00} = \frac{3}{4}M_1 + \frac{1}{4}M_0$, whereas for a $T=0$ to $T=1$ transition $\bar{M}_{01} = \tilde{M}_{01} = \frac{1}{4}(M_1 - M_0)$. The angular distribution of polarization in these four cases is given in Fig. 1 for 156 Mev.

For "normal" parity change one has $\mu = 0$, and the polarization depends on a single nuclear parameter λ, which is a measure of the spin-flip matrix element to the non-spin-flip matrix element. Elastic scattering corresponds to this case with $\lambda = 0$ and $\Delta T = 0$, so that polarization in inelastic scattering with normal parity change and $\Delta T = 0$ should resemble that for elastic scattering if λ is small. The angular distribution of

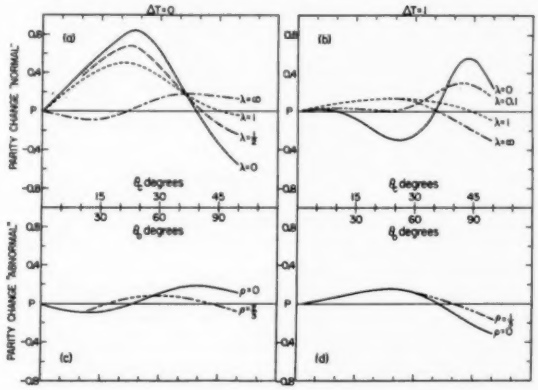

FIG. 1. Polarization in inelastic scattering for an even-even nucleus with spin and isotopic spin zero. The polarization (P) versus the two-nuclear center-of-mass angle θ_c for the four cases discussed in the text. Also shown is θ_C, the center-of-mass angle in scattering from a mass-12 target, $\theta_C \approx \theta_{\mathrm{lab}}$. λ and ρ are parameters involving nuclear matrix elements. The case $\lambda = 0$ in panel (a) corresponds to elastic scattering.

polarization for several values of λ for this case is given in Fig. 1 (a). Values of λ as large as unity do not give polarizations very different from that of elastic scattering. This case covers most of the low-lying states whose polarizations have been measured by the Uppsala group[6] at ~156 Mev, viz., the 4.4- and 9.6-Mev levels in C^{12} and the 6.1-Mev group in O^{16}. Experimentally the polarizations from these levels resemble each other and are much the same as for elastic polarization, indicating small values of λ, which is not inconsistent with shell model calculations.[7]

For normal parity change but with $\Delta T = 1$, the resulting angular distributions are shown in Fig. 1 (b) for several values of λ. The very great difference between $\bar{M}_{00}$ and $\bar{M}_{01}$ is reflected in these curves; a marked dependence on λ is seen even for fairly small values of λ and no relation to elastic scattering is found. This case corresponds to the polarization from the group of levels in the 19-21 Mev region in C^{12} and O^{16}, which from photonuclear data consists mainly of levels with $J = 1^-$ and $T = 1$. The polarization in this case is observed to be small.[6]

For "abnormal" parity change, $\Delta\pi = (-1)^{J+1}$, the non-spin-flip matrix element vanishes and the polarization becomes

$$P = 2(1-\rho)\mathrm{Re}(\bar{B}\bar{C}^*)/\{(1-\rho)(|\bar{F}|^2 + |\bar{B}|^2 + |\bar{C}|^2) + 2\rho|\bar{E}|^2\}, \quad (9)$$

and so depends on a single nuclear parameter $\rho = L_3/L_2$ whose values are restricted to lie between 0 and 1. The angular distribution in this case is shown for several values of ρ, for $\Delta T = 0$ in Fig. 1 (c) and for $\Delta T = 1$ in Fig. 1 (d). In both cases the polarization in the forward direction is small. Most of the levels in the 12.5-Mev O^{16} and ~15-Mev C^{12} region, whose polarization has been measured by the Uppsala group[6] and shown to be small, correspond to "abnormal" parity change.

Elastic polarization and polarization from the 2.43-Mev level of Be^9 have been measured by Hafner[8] for 220-Mev protons. This case is of much greater complexity than those discussed above, since the ground state[9] has $J = \frac{3}{2}^-$, $T = \frac{1}{2}$, and the excited state has $J = \frac{5}{2}^-$, $T = \frac{1}{2}$. Explicit calculations can, however, be made on the basis of shell model states. For example, in the case of L-S coupling, for elastic scattering, $\bar{M} = (13/18)M_1 + (5/18)M_0$ and $\tilde{M} = \frac{1}{2}(M_1 + M_0)$, with $\lambda \cong 0.025$ and $\mu \cong 0.003$; for inelastic scattering from the 2.43-Mev level $\bar{M} = (11/15)M_1 + (4/15)M_0$ while $\lambda \cong 0.005$, $\mu \cong 0.002$. As for elastic scattering from C^{12}, $\bar{M} = \frac{3}{4}M_1 + \frac{1}{4}M_0$ and $\lambda = \mu = 0$, the polarization both in the inelastic and elastic scattering from Be^9 should strongly resemble the elastic scattering from C^{12}, as is in fact observed.

High-energy nucleon scattering with very good energy resolution represents another tool for the possible determination of certain nuclear matrix elements. To determine nuclear matrix elements from inelastic nucleon angular distribution data, especially in the forward direction, requires a somewhat more certain determination of the two-nucleon scattering amplitude. Two-nucleon experiments now in progress[10] should provide much of this information.

*Work performed under the auspices of the U. S. Atomic Energy Commission.

†On leave from and now at Chalk River Laboratory, Chalk River, Ontario.

‡On leave from and now at Los Alamos Scientific Laboratory, Los Alamos, New Mexico.

[1]H. Bethe, Ann. Phys. 3, 190 (1958); H. McManus and R. M. Thaler, Phys. Rev. 110, 590 (1958); S. Ohnuma, Phys. Rev. 111, 1172 (1958); A. H. Cromer (to be published).

[2]W. Riesenfeld and K. M. Watson, Phys. Rev. 102, 1157 (1956).

[3]J. L. Gammel and R. M. Thaler, Phys. Rev. 107, 291, 1337 (1957); P. S. Signell and R. E. Marshak, Phys. Rev. 109, 1229 (1958); Stapp, Ypsilantis, and Metropolis, Phys. Rev. 105, 302 (1957).

[4]E. L. Squires, Nuclear Phys. 6, 504 (1958).

[5]The effect of distorted waves has been neglected. Its effect is expected to be small for light nuclei in the interesting angular region.

[6]P. Hillman et al., Nuclear Phys. 4, 648 (1957); R. Alphonse et al., Nuclear Phys. 4, 672 (1957); H. Tyren et al., Nuclear Phys. 3, 336 (1957).

[7]J. P. Elliott and B. H. Flowers, Proc. Roy. Soc. (London) A242, 57 (1957).

[8]E. M. Hafner, Phys. Rev. 111, 297 (1958).

[9]F. Ajzenberg-Selove and T. Lauritsen, Revs. Modern Phys. 27, 77 (1955).

[10]Private communications from Richard Wilson, A. Ashmore, and others.

Λ INTERACTIONS IN HYDROGEN*

Frank S. Crawford, Jr., Marcello Cresti, Myron L. Good, Frank T. Solmitz, M. Lynn Stevenson, and Harold K. Ticho
Lawrence Radiation Laboratory, University of California, Berkeley, California
(Received January 23, 1959)

While studying the associated-production pro-

cesses, we have encountered six cases in which the Λ subsequently interacts with a proton in the liquid hydrogen bubble chamber.[1]

The classes of Λ interactions we have seen are

$$\Lambda + p \rightarrow \Lambda + p \text{ (4 events)}, \quad (1)$$

$$\Lambda + p \rightarrow \Sigma^+ + n \text{ (2 events)}. \quad (2)$$

We have not yet seen any examples of the reaction

$$\Lambda + p \rightarrow \Sigma^0 + p. \quad (3)$$

[Charge independence predicts that Reaction (3) should be half as frequent as Reaction (2).]

The momentum spectrum of the Λ produced in our associated production experiment is shown in Fig. 1. The letters "Λ" and "Σ^+" in this figure indicate the Λ momentum that produced the above reactions. The threshold for the endothermic reaction (2) is 635 Mev/c. Table I contains the pertinent information concerning the reaction dynamics for each event.

Figure 2 shows one of the Λ elastic scattering events. The original Λ was produced in the direction indicated by arrow No. 2. (The associated K^0 did not decay in the chamber.) At Point A, the Λ scatters in the direction indicated by arrow No. 3. At point B, the Λ decays into a pion (Track 4) and a proton (Track 5). Track 6 is the recoil proton.

Figure 3 shows one of the $\Lambda + p \rightarrow \Sigma^+ + n$ interactions. Tracks 3 and 4 are the negative and positive decay pions of the K^0 (arrow No. 2) that was produced in the primary reaction $\pi^- + p \rightarrow K^0 + \Lambda$.

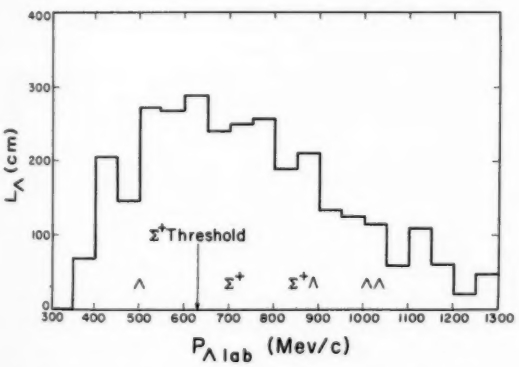

FIG. 1. This figure shows the Λ path length, L_Λ, as a function of the momentum of the Λ's prior to the interactions. The momenta of the Λ elastic scatterings are indicated by the "Λ" symbols, and the two $\Lambda + p \rightarrow \Sigma^+ + n$ reactions by the "Σ^+" symbols.

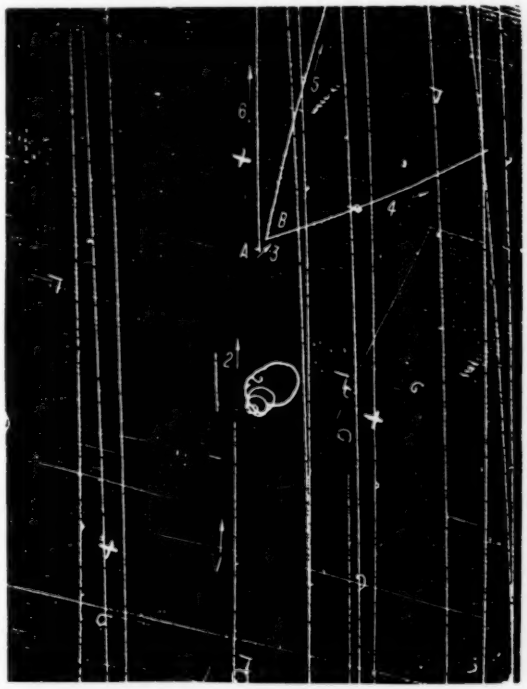

FIG. 2. The primary reaction is π^- (Track 1) $+ p \rightarrow \Lambda$ (arrow No. 2) $+ K^0$ (not seen). The Λ travels 3.7 cm and scatters elastically at point A in the direction indicated by arrow No. 3. Track 6 is the recoil proton. At point B the scattered Λ decays into a π^- (Track 4) and a proton (Track 5).

The Λ (arrow No. 5) interacts at point A to produce a Σ^+ (Track 6) and a neutron. The Σ^+ then decays at point B into a π^+ (Track 7) and a neutron.

The 655 Λ's that we have observed to decay in the chamber have traversed a total path length in liquid hydrogen of 2200 cm.

In addition to the observed Λ decays there were 195 cases in which only the K^0 decays. From the observed K^0 we can predict the direction in which the unseen Λ traverses the chamber. We then search along this direction for a recoil proton or a "recoil" Σ^+. We estimate that Λ's of this category traversed 700 cm of liquid hydrogen. From the combined path length in liquid hydrogen of 2900 cm, we obtain an elastic scattering cross section[2]

$$\sigma_{\Lambda\Lambda} = 40 \pm 20 \text{ mb}.$$

If the cross section is assumed to have the energy dependence of $\sigma = \epsilon \pi \lambda^2$(c.m.), with ϵ con-

FIG. 3. The primary reaction is π^- (Track 1)$+p\rightarrow\Lambda$ (arrow No. 5)$+K^0$ (arrow No. 2). The K^0 decays into a π^- (Track 3) and a π^+ (Track 4). The Λ subsequently interacts at point A to produce a Σ^+ (Track 6) plus a neutron. The Σ^+ decays at point B into a π^+ (Track 7) and a neutron.

stant, then by averaging over the Λ momentum spectrum we obtain

$$\epsilon_{\Lambda\Lambda}=\sigma_{\Lambda\Lambda}/\pi\langle\lambda\!\!\!^{-2}(\text{c.m.})\rangle=2.4\pm1.2.$$

Here $\lambda\!\!\!^{-}$(c.m.) is the de Broglie wavelength of the Λ in the c.m. system.

Of the total path length of 2900 cm, 2000 cm was traversed by Λ's of momentum higher than the threshold for the $\Lambda+p\rightarrow\Sigma^++n$ reaction. From the two observed reactions of type (2) we obtain

$$\sigma_{\Lambda\Sigma^+}=30\pm20\text{ mb}.$$

By averaging over Λ momenta above threshold, we find the corresponding value

$$\epsilon_{\Lambda\Sigma^+}=3\pm2.$$

Furthermore, by detailed balancing we can predict the cross section for the inverse reaction,[3] $\Sigma^++n\rightarrow\Lambda+p$, i.e.,

$$\sigma_{\Sigma^+n}=(p/p')^2\,\sigma_{\Lambda\Sigma^+}=120\pm80\text{ mb}.$$

The two events had momenta of 120 and 220 Mev/c in the Σ^++n c.m. system. If charge independence holds, we expect the $\Sigma^0+p\rightarrow\Lambda+p$ cross section to be 60 ± 40 mb. (We mention this because of the evidence for such an interaction in the K^-+d experiment of Horwitz et al.[4])

We are grateful to Professor Luis Alvarez for his stimulation and guidance during this experiment. We are indebted to Don Gow and the bubble chamber crew, and to Hugh Bradner and the scanners for their help. We thank George Kalbfleisch and Roger Douglass for their assistance with the data analysis.

---

*This work was done under the auspices of the U. S. Atomic Energy Commission.

[1]The two $\Lambda+p\rightarrow\Sigma^++n$ reactions have been discussed previously by Crawford, Cresti, Good, Gottstein, Solmitz, Stevenson, and Ticho, University of California Radiation Laboratory Report UCRL-3924, August, 1957 (unpublished).

[2]A Λ that scatters less than 10 degrees produces a recoil proton that would escape detection. Our elastic scattering cross section therefore corresponds to scatterings greater than 10 degrees.

[3]We assume that both the Λ and the Σ have the same

Table I. Reaction dynamics.

Event frame number	Initial momentum (lab) (Mev/c)	Hyperon angle (c.m.) (degrees)	Momentum in center of mass of "scattering" Incoming	Outgoing
A. $\Lambda+p\rightarrow\Lambda+p$				
318425	1000	65	420	420
321560	1000	120	430	430
389195	500	80	220	220
439748	880	170	380	380
B. $\Lambda+p\rightarrow\Sigma^++n$				
232018	700	40	310	120
309771	840	90	360	220

spin.

[4]Horwitz, Miller, Murray, Schwartz, and Taft, Bull. Am. Phys. Soc. Ser. II, 3, 363 (1958).

RADIATIVE DECAY OF THE MUON*

Toichiro Kinoshita
Laboratory of Nuclear Studies,
Cornell University, Ithaca, New York,

and

Alberto Sirlin
Physics Department,
Columbia University, New York, New York

(Received January 26, 1959)

The inner bremsstrahlung accompanying the muon decay ($\mu \to e + \nu + \bar{\nu} + \gamma$) has been studied previously, and its contribution to the radiative correction of the decay spectrum, the lifetime, and the asymmetry has been analyzed in detail.[1-3] Recently, some other aspects of this problem have been discussed by several authors.[4-6] The purposes of this note are to derive the spectrum of the photon emitted in the decay of muons in the framework of the two-component theory of the neutrino and to point out the possibility that this effect may be observed with present techniques.

The probability that a photon and an electron are emitted in muon decay with any given energies and momenta has been given by Eq. (17b) of reference 2. To find the photon spectrum in which we are now interested, we have only to integrate it with respect to the energy and angle of the electron, taking account of the conservation law of energy and momentum. The result is given by

$$\frac{dN}{N_0} = \frac{\alpha}{3\pi}(1-y)dy\left\{\left[2\ln\frac{m_\mu}{m_e} - \frac{17}{6} + \ln(1-y)\right] \times \left[\frac{3}{y} - 2(1-y)^2\right] - \frac{1}{12}(1-y)(22-13y)\right\}, \quad (1)$$

where N_0 is the total probability of muon decay without radiative corrections and $y = 2\omega/m_\mu$ is the photon energy in units of its maximum value. In deriving Eq. (1) the mass of the electron has been neglected in comparison with its energy whenever this approximation has not led to spurious divergences. This is certainly justified when the condition $(1-y)^2 \gg (2m_e/m_\mu)^2$ is fulfilled.

Integrating Eq. (1) further over the range of photon energy between $y = y_0 = 2\omega_0/m_\mu$ and $y = 1$, one finds the rate for muon decay accompanied by photons of energy greater than ω_0:

$$R(y_0) = \frac{\alpha}{3\pi}\left\{\left(\ln\frac{m_\mu}{m_e} - \frac{17}{12}\right)\left[6\ln\frac{1}{y_0} - 6(1-y_0) - (1-y_0)^4\right] + 3[L(1) - L(y_0)] - \tfrac{1}{2}[6 + (1-y_0)^3](1-y_0)\ln(1-y_0) + \frac{1}{48}(1-y_0)(125 + 45y_0 - 33y_0^2 + 7y_0^3)\right\}, \quad (2)$$

where

$$L(x) = \int_0^x \frac{dt}{t}\ln|1-t|. \quad (3)$$

For $y_0 \ll 1$, Eq. (2) coincides with the expression obtained by integrating Eq. (25b) of reference 2 over all electron energies.

Equation (2) shows that about 4.9% of muon decay is accompanied by photons of energy greater than $2m_e$, the threshold energy for the production of electron-positron pairs. Even for $\omega_0 \sim 20m_e$, the rate is still as large as 1.2%. Thus it seems likely that the inner bremsstrahlung accompanying the muon decay may be detected and investigated experimentally with techniques now available.

Equations (1) and (2) constitute a definite and clear-cut prediction of the two-component neutrino theory and of the usual laws of quantum electrodynamics as applied to the electron and muon fields. In particular, they are independent of the relative magnitudes of the V and A interactions in the order $(e\mu)(\nu\nu)$ or, what amounts to the same thing, of the S and V interactions in the order $(e\nu)(\nu\mu)$. Thus, if the predictions of Eqs. (1) and (2) were to be contradicted by experiments, the consequences would be far reaching indeed.

The question naturally arises as to whether measurements of the radiative decay rate can give us new information about the nature of the weak interaction in the more general framework of the four-component neutrino theory. This is now being studied.

One of us (A.S.) would like to thank Professor T. D. Lee for his comments and Dr. M. Bardon, Dr. D. Berley, and Dr. J. Lee for useful conversations.

*Supported in part by the joint program of the Office of Naval Research and the U. S. Atomic Energy Commission.

[1]A. Lenard, Phys. Rev. 90, 968 (1953).

[2]Behrends, Finkelstein, and Sirlin, Phys. Rev. 101, 866 (1956).

[3]T. Kinoshita and A. Sirlin, Phys. Rev. (to be published).

[4]R. H. Pratt, Phys. Rev. 111, 649 (1958).

[5]N. Tzoar and A. Klein, Nuovo cimento 8, 482 (1958). In this paper, it is asserted that the relative rate for inner bremsstrahlung is of order 10^{-5} per muon decay. If by the rate of $\mu \rightarrow e + \nu + \bar{\nu} + \gamma$ one understands the total rate of radiative decays with photons of energy greater than a certain energy ω_0, then their result is at variance with ours unless one arbitrarily chooses a relatively large value of ω_0.

[6]C. Fronsdal and H. Überall (to be published).

ABSTRACTS

In this section are printed the abstracts of Articles that have been forwarded to The American Institute of Physics for publication in THE PHYSICAL REVIEW. In quoting information obtained from this section before the appearance of the corresponding Article, reference should be made to "Physical Review (to be published)" rather than to this Journal.

EVAPORATION EFFECTS DURING SUPERFLOW OF LIQUID HELIUM II. K. R. Atkins, B. Rosenbaum, and H. Seki, Department of Physics, University of Pennsylvania, Philadelphia, Pennsylvania (Received October 6, 1958).

The rate of distillation of helium between two liquid surfaces at different temperatures has been measured and found to be in approximate agreement with simple kinetic theory. The influence of evaporation on the thermal effects accompanying film flow is discussed. It seems unlikely that the decrease in the rate of film flow at small level differences can be explained in terms of these thermal effects.

RELATIVISTIC HYDRODYNAMICS FOR A CHARGED NONVISCOUS FLUID. Chau-Chin Wei, Committee on Nuclear Power Development, Taiwan Power Company, Taipei, Taiwan, China (Received October 8, 1958).

The equations of relativistic hydrodynamics are derived from an alternative variation method and a generalized vorticity equation is obtained.

STATISTICAL MECHANICS OF STRINGS. Nandor L. Balazs, Enrico Fermi Institute for Nuclear Studies, University of Chicago, Chicago, Illinois (Received October 29, 1958).

In the usual statistical mechanical theory of strings the mean square potential energy of a string element is infinite. This result is in contradiction with the assumption that the potential energy of a string element is small; this assumption is used to linearize the equations of motion. In this note, we show that this defect can be remedied if we take into account the finite thickness of the string, introducing thereby additional terms to the energy connected with bending.

COULOMB SCATTERING IN A VERY STRONG MAGNETIC FIELD. L. M. Tannenwald, Research Laboratory, Missile Systems Division, Lockheed Aircraft Corporation, Palo Alto, California (Received May 26, 1958).

The spiralling of charged particles in an intense magnetic field is taken into account in the description of their collisions involving small fractional momentum transfer. The transition probability to the continuum of possible states is given. In addition, the transition probability is given for a particle's orbit center to be displaced from one magnetic line of force to another, with accompanying momentum change, as a result of scattering by a fixed charge. The equivalent results are derived for the scattering of two identical particles in their relative coordinate system.

As the result of scattering, the momentum change along the magnetic field in a uniform, collimated beam of spiralling particles is found to be very much smaller than the sum of the magnitudes of the individual momentum changes in that direction. In contrast to ordinary Coulomb scattering, one finds that there is a lower limit to the momentum transfer to individual particles and that there is an adiabatic cutoff distance associated with the interaction which, in some plasma situations, can be shorter than the value of the Debye distance.

The WKB approximation for generalized Laguerre polynomials is appended.

NUCLEAR SPIN-SATURATION BY ULTRASONICS IN SODIUM CHLORIDE. E. F. Taylor* and N. Bloembergen, Harvard University, Cambridge, Massachusetts (Received September 8, 1958).

An ultrasonic vibrational mode with rather well defined properties has been set up in a cylindrical single crystal of sodium chloride. The saturation of the spin levels of Na^{23} and Cl^{35} by acoustically induced quadrupole transitions, $\Delta m = \pm 2$, has been measured in the steady state by a standard nuclear magnetic resonance technique, for several orientations of the ultrasonic wave and external magnetic fields. The components of the fourth-order tensor connecting the electrical field gradient tensor at the nuclei with the strain deformation tensor have been determined. The components satisfy an isotropy condition rather

than the Cauchy relation. The results show the inadequacy of the ionic point-charge model coupled with an isotropic Sternheimer antishielding factor. The interpretation of the data requires a considerable amount of covalent character and configurational interaction on the Na^+ ion.

*Present address: Wesleyan University, Middletown, Connecticut.

OPTICAL TRANSMISSION OF HEAT-TREATED STRONTIUM TITANATE. H. W. Gandy, Electronics Laboratory, General Electric Company, Syracuse, New York (Received June 18, 1958).

The room temperature optical transmission spectra of pure and doped $SrTiO_3$ crystals have been studied after heating them in oxygen and vacuum; spectral measurements were made in the quantum energy range from 0.1 to 3.4 ev.

A blue color, with strong attendant absorption in the infrared, can be induced in the pure crystals by heating them in vacuum with absorption maxima occuring at 0.9 and 2.9 ev. This induced absorption can be removed by heating the crystals in oxygen. Prolonged heatings of the pure, stoichiometric crystals in oxygen have failed to induce any measurable change in the transmission spectra in the aforementioned energy range.

Optical absorption can be induced in iron- and cobalt-doped $SrTiO_3$ crystal samples by heating them in oxygen; this absorption can be removed by heating the crystals in vacuum. The induced absorption occurs primarily at high quantum energies in the spectra of these doped crystals, with maxima occurring at 2.75 and 2.2 ev in the iron-doped samples, and at 3.0 and 2.6 ev in the cobalt-doped samples. It is suggested that the induced absorption observed in the doped crystals involves a controlled change in the valence states of these impurities.

EFFECTIVE FERRIMAGNETIC RESONANCE PARAMETERS WITH GILBERT-TYPE RELAXATION TERMS. Roald K. Wangsness, United States Naval Ordnance Laboratory, White Oak, Maryland (Received October 10, 1958).

Steady-state effective parameters of the susceptibility tensor have been found for a two-sublattice system by using equations of motion with Gilbert-type relaxation terms. To the same order in the molecular field coefficient, these parameters differ from those previously found for Landau-Lifschitz type terms in that they have infinite discontinuities in the compensation region, there is no distinction between the effective gyromagnetic ratios characterizing the absorption and the Faraday effect, and there is no additional term appearing in the expression for the off-diagonal element.

THEORY OF ULTRASONIC ABSORPTION IN METALS: THE COLLISION-DRAG EFFECT. T. Holstein, Westinghouse Research Laboratories, Pittsburgh, Pennsylvania (Received June 23, 1958).

A basic assumption of the semiclassical treatments of ultrasonic absorption in metals is that of "collision-drag." This assumption states that, in the presence of an impressed ultrasonic wave, the velocity distribution towards which the conduction electrons relax is a Fermi distribution centered, not at the origin of velocity space, but at a point, $\vec{v}_i$, equal to the local, impressed lattice-displacement velocity. In the present paper, the explanation of this collision-drag effect in terms of basic electron-lattice theory is investigated for the case of collisions with thermal vibrations. The effect is found to originate from those higher-order terms in the electron-lattice interaction whose matrix elements are bilinear in the amplitudes of impressed and thermal lattice displacements. In the conventional perturbation-theory treatment, these matrix elements give rise to transitions in which both a thermal phonon and an impressed phonon are simultaneously either absorbed or emitted. However, in such a treatment, no collision-drag effects appear. In order to obtain them, it is necessary to alter the standard perturbation treatment so as to provide for space-time localization of collisions to within an interval small compared to the wavelength and period of the impressed sound wave. It is then found that the impressed ultrasonic wave produces a modification in the energy-conservation law of electron-lattice collisions, $\epsilon_{\vec{k}'} = \epsilon_{\vec{k}} \pm \hbar\omega_\lambda$, in which the effective electron energy, $\epsilon_{\vec{k}}$, is the Bloch energy, augmented by a term proportional to the impressed displacement velocity. When this modification is introduced into the collision term of the Boltzmann transport equation, the equilibrium distribution (defined as that for

which the collision term vanishes) is found to be a Fermi distribution centered about a point in $\vec{k}$ space equal to $m\vec{v}_i/\hbar$; for the free electron model, this result is in accord with the collision-drag assumption as stated above. An additional result of the treatment is that the crystal-momentum conservation law of electron-lattice collisions is altered by the inclusion of terms linearly proportional to the impressed strain; this modification, however, turns out to have no effect in ultrasonic absorption. The final section of the paper is devoted to an investigation of the effects on energy transfer arising from the bilinear matrix elements; these effects are shown to be describable, also, in terms of the collision-drag picture.

ANOMALOUS PHOTOVOLTAIC EFFECT IN ZnS SINGLE CRYSTALS. A. Lempicki, Research Laboratories, Sylvania Electric Products Incorporated, Bayside, New York (Received September 19, 1958).

Larger-than-band-gap photovoltages have been observed in both cubic and hexagonal crystals of ZnS with stacking faults. Under monochromatic excitation the photovoltage measured parallel to the c axis shows two sign reversals at about 3300 A and 3500 A and peaks at approximately 3250 A and 3400 A. The position of the 3400 A peak shifts by ~ 70 A depending on the crystal structure. In the direction perpendicular to the c axis the photovoltage does not change sign and remains smaller than the band gap. Hexagonal crystals free of stacking faults do not show anomalous photovoltages. Heat treatment causes appearance of both. A pyroelectric polarization is found to be correlated with the sign of photovoltage.

TRACER DIFFUSION IN A CHEMICAL CONCENTRATION GRADIENT IN SILVER-CADMIUM. John R. Manning,* Department of Physics, University of Illinois, Urbana, Illinois (Received July 22, 1958; revised manuscript received December 10, 1958).

Measurements have been made on seven Ag-αAgCd diffusion couples of the diffusion of a layer of radioactive tracer atoms (either Ag^{110} or Cd^{109}) located originally at the Ag-AgCd interface. It was found that the center of gravity of the layer of tracer atoms shifted from its original position, marked by tungsten wires. The shapes of the tracer profiles for Ag^{110} were quite different from those for Cd^{109}. However, for both silver and cadmium tracer, the center of gravity moved toward the cadmium-rich region.

A theoretically predicted shift in center of gravity is obtained, taking into consideration the fact that the diffusion coefficient, correlation factor, and chemical potential are functions of chemical composition. The predicted shift in center of gravity arising from the flow of imperfections and the lattice distortion associated with the Kirkendall shift also are considered. Good agreement is found between theory and experiment.

Chemical interdiffusion and Kirkendall shift measurements were consistent, within errors, with those predicted by Darken.

*Present address: Metal Physics Section, National Bureau of Standards, Washington, D. C.

PENETRATION DEPTH IN IMPURE SUPERCONDUCTORS. Peter B. Miller, Department of Physics, University of Illinois, Urbana, Illinois (Received October 17, 1958).

The equation giving the current density as a functional of the vector potential for an impurity superconductor derived by Mattis and Bardeen is used to compute the temperature dependence of the penetration depth of impure superconductors. Results of calculations for different values of the ratio of the coherence distance to the mean free path and also for different values of the ratio of the coherence distance to the London penetration depth are given. The results are applied to tin as an example, and appreciable deviations from the $(1-t^4)^{-1/2}$ temperature dependence of the penetration depth are found for all values of the mean free path.

EXCITATION OF SPIN WAVES IN AN ANTIFERROMAGNET BY A UNIFORM rf FIELD. R. Orbach and P. Pincus, Department of Physics, University of California, Berkeley, California (Received October 27, 1958).

It is possible to excite exchange and magnetostatic spin waves in an antiferromagnet by a uniform rf field, provided that spins on the surface of the specimen experience anisotropy interactions different from those acting on the

spins in the interior. Modes with an odd number of half-wavelengths should be excited in a flat plate. The condition for different anisotropy interactions is worked out and proves to be a lenient condition. Experiments which would determine the exchange energy constant and the anisotropy field should be possible using sufficiently thin platelets of single crystals having parallel faces.

OPTICAL CONSTANTS OF GERMANIUM IN THE REGION 1 TO 10 ev. H. R. Philipp and E. A. Taft, General Electric Research Laboratory, Schenectady, New York (Received October 20, 1958).

The reflectance, $|r(\lambda)|^2$, of single-crystal germanium was measured in the range 0.6 to 11.3 ev. The phase, $\theta(\lambda)$, was computed from these data using the Kramers-Kronig relation between the real and imaginary parts of the complex function $\ln r = \ln|r| + i\theta$. The optical constants, n and k, were then determined from the Fresnel reflectivity equation. The real part of the refractive index, n, has maxima of 5.5 at 2.07 ev and 4.2 at 3.2 ev. Above 6 ev, the index is very nearly 1. The extinction coefficient, k, shows maxima of 2.0 at 2.5 ev and 4.2 at 4.4 ev. Below 3.5 ev, the results are in good agreement with the recent measurements of Archer. Beyond this point, they depart from his extrapolated curve.

ELECTRICAL CONDUCTION IN CRYSTALS AND CERAMICS OF WO_3. S. Sawada and G. C. Danielson, Department of Physics and Institute for Atomic Research, Iowa State College, Ames, Iowa (Received October 13, 1958).

The specific resistivities of crystals and ceramics of WO_3 have been measured from room temperature to 1000°C, and the sign and order of magnitude of the Hall coefficient have been examined near room temperature. From the results for single crystals, it was found that WO_3 behaves like an impurity semiconductor having a saturation region below 740°C and becoming intrinsic above 910°C. The specific resistivity versus temperature curve had a distinct anomaly at 740°C, suggesting an alteration in the electronic structure at this temperature. Below 740°C, the specific resistivity of ceramic samples showed a remarkable hysteresis phenomenon, probably arising from a cracking of crystallites on heating. The sign of the Hall coefficient was positive at room temperature and its magnitude gave reasonable values for the number and mobility of the carriers. Nonohmic and rectifying characteristics were observed by means of an oscilloscope.

DOMAIN STRUCTURE OF WO_3 SINGLE CRYSTALS. S. Sawada and G. C. Danielson, Department of Physics and Institute for Atomic Research, Iowa State College, Ames, Iowa (Received October 17, 1958).

Transparent single crystals of WO_3, in the form of plates as large as 10 mm×10 mm, have been prepared by a sublimation method. The domain structure of these crystals was investigated from room temperature to 1350°C, and a new and peculiar domain structure was found between 740°C and 810°C. This domain structure is probably associated with the change in crystal structure from orthorhombic to tetragonal. Lattice parameters determined optically from measurements of the angle between extinction positions of two neighboring domains agreed well with those obtained by x-ray analysis. The shift in the absorption edge to the infrared at 740°C was observed to take place for light polarized in a direction perpendicular to the c axis, but not for light polarized parallel to the c axis.

OPTICAL INDICES OF REFRACTION OF WO_3. S. Sawada and G. C. Danielson, Department of Physics and Institute for Atomic Research, Iowa State College, Ames, Iowa (Received October 17, 1958).

A modified Chaulnes' method using polarized light has been developed to measure the indices of refraction of WO_3. By this method, the three principal indices of refraction of a crystal were obtained by observations in the direction of only one optic principal axis. For WO_3, the mean value of the indices of refraction and the maximum value of birefringence at room temperature were found to be 2.5 and 0.42, respectively. The crystals were positive below 740°C and negative above this temperature. Distinct anomalies in the indices of refraction were observed at 330°C and 740°C. The results are compared with those

for some other perovskite-type ferroelectrics and antiferroelectrics.

FUNDAMENTAL OPTICAL ABSORPTION IN THE IIA-VIB COMPOUNDS. George A. Saum* and Eugene B. Hensley, Department of Physics, University of Missouri, Columbia, Missouri (Received October 21, 1958).

The fundamental optical absorption in the range of $h\nu$ from 2.5 to 5.8 ev has been measured on well-annealed thin films of the following compounds: BaO, SrO, BaS, SrS, CaS, BaSe, SrSe, CaSe, MgSe, BaTe, SrTe, CaTe, and MgTe. The absorption peaks are ascribed to excitons and are observed to shift to lower energies for increasing atomic numbers of either the IIA or VIB elements. A doublet splitting is observed which is close to the values for the spin-orbit splitting of the free negative VIB ions for the selenides and tellurides but which is somewhat larger for the heavier oxides and sulfides.

*Now at General Electric Research Laboratory, Schenectady, New York.

EXCITATION OF LUMINESCENT MATERIALS BY IONIZING RADIATION. H. Kallmann and J. Dresner,* Department of Physics, New York University, Washington Square, New York, New York (Received October 2, 1958).

The buildup of light emission under irradiation by x-rays and fast electrons was determined for several inorganic phosphors at room temperature and at -70°C. Measurements were performed under excitation by x-rays of 35 kv and 3.5 kv and by Sr^{90} β-rays. From a knowledge of these rise curves of light emission, the effective volume of phosphor excited by a single ionizing event can be calculated. For the three types of irradiation used, it was found that the effective volumes of these channels of excitation are proportional to the amount of energy transferred to the phosphor by each ionizing particle and that the ratio between the initial and final values of the light emission is almost independent of the mode of excitation. This implies that the excited electrons diffuse out from the path of the ionizing particle until they are stopped by traps. Evaluation of this diffusion process indicates that only a small percentage of all available deep traps are filled within the effective channel volume by one single event and that a non-bimolecular process participates in the initial light emission. In the above cases, the electrostatic field produced by the positively charged core of the channels is too small to interfere with the diffusion of the excited electrons. In the case of irradiation by high-energy α particles, this field is large enough to inhibit the diffusion process completely. Only a small part of the energy dissipated by the α particle is expended in filling all the traps in a narrow channel, the rest being available for radiative processes. This channel model thus accounts for the almost instantaneous rise of light emission which is observed under irradiation by α particles.

*Now at R.C.A. Laboratories, Princeton, New Jersey.

EFFECT OF MINORITY IMPURITIES ON IMPURITY CONDUCTION IN p-TYPE GERMANIUM. H. Fritzsche* and K. Lark-Horovitz, Department of Physics, Purdue University, Lafayette, Indiana (Received October 10, 1958).

Hall coefficient R and resistivity ρ of various p-type germanium samples which contained the same concentration of acceptors N_A but different amounts of compensating donors N_D have been measured between 300°K and 1.3°K. The process of impurity conduction at low impurity concentrations differs from that at high concentrations in that it requires the presence of empty majority centers. As in the case of n-type Ge, the two different impurity conduction processes could be distinguished by observing the change of ρ resulting from a change in the degree of compensation in the temperature range of impurity conduction. At large impurity concentrations ($N_A = 2.4\times10^{17}$/cc) the resistivity is independent of temperature only if the concentration of mobile carriers is sufficiently large. The resistivity increases with a finite activation energy in strongly compensated samples.

*Present address: Institute for the Study of Metals, University of Chicago, Chicago, Illinois.

NUCLEAR SPIN RELAXATION IN NORMAL AND SUPERCONDUCTING ALUMINUM. L. C. Hebel* and C. P. Slichter, University of Illinois, Urbana, Illinois (Received October 22, 1958).

Nuclear spin-lattice relaxation times have been measured in normal and superconducting

Al from 0.94°K to 4.2°K, and as a function of static field in the normal state. In the normal state the relaxation rate is proportional to temperature as predicted by Redfield and others. The field dependence is somewhat greater than predicted. Relaxation in the superconductor was studied by a field-cycling method which allowed the measurements to be made in the normal state but relaxation to occur in the superconductor. The results disagree with a simple two-fluid model, but are explained by the theory of Bardeen, Cooper, and Schrieffer. The contrast between the temperature dependence of nuclear relaxation and ultrasonic absorption confirms the central feature of the Bardeen-Cooper-Schrieffer theory that electrons of opposite spin and momentum are correlated.

*Now at the Bell Telephone Laboratories, Murray Hill, New Jersey.

MILLIMETER-WAVE PARAMAGNETIC RESONANCE SPECTRUM OF ^6S STATE IMPURITY (Fe^{+++}) in $MgWO_4$. Martin Peter, Bell Telephone Laboratories, Murray Hill, New Jersey (Received October 1, 1958).

A broad-band millimeter-wave paramagnetic resonance spectrometer has been assembled. At room temperature, with a linewidth of one oersted and a time constant of one second, the least number of spins that can be detected is 2×10^{14}, in reasonable agreement with theoretical prediction.

The spectrum discovered by Bowers in slightly Ni-doped $MgWO_4$ has been investigated and ascribed to an impurity in the ^6S state (Fe^{+++}). It is described by the spin Hamiltonian

$$H = D[S_z^2 - \tfrac{1}{3}S(S+1)] + E(S_x^2 - S_y^2) + g\beta \vec{H}\cdot\vec{S},$$

with $S=5/2$, $D=-20.6$ kMc/sec, $E=+5.22$ kMc/sec, and $g=2.0$ ($T=78$°K). The y axis is parallel to the b axis; the z axis is turned away from the $+a$ axis towards the $+c$ axis by 40 degrees.

ORIENTATION DEPENDENCE OF ELASTIC WAVES IN SINGLE CRYSTALS. P. C. Waterman,* Metals Research Laboratory, Department of Applied Mathematics, Brown University, Providence, Rhode Island (Received July 16, 1958).

A description of the properties of plane elastic waves in single crystals is of interest both from a theoretical point of view and in the interpretation of high-frequency pulsed ultrasound experiments. The perturbed eigenvalue problem that arises when nearly pure transverse or compressional modes are propagated is considered, and the resulting phase velocities and displacement vectors tabulated for a number of cases of physical interest. A unified approach to the properties of pure modes is provided through a consideration of individual rotational symmetries of the crystals, and the energy flux associated with both pure and nearly pure modes is discussed.

*Now at Linde Company, Tonawanda, New York.

STOPPING OF LOW-ENERGY H^+ AND He^+ IONS IN PLASTICS. Donald C. Lorents* and Edward J. Zimmerman, University of Nebraska, Lincoln, Nebraska (Received October 27, 1958).

The stopping cross sections of polystyrene, polyethylene and Gr-S rubber for 40- to 340-kev H^+ and He^+ ions have been measured. A nearly monoenergetic analyzed beam of ions of known energy was deflected 90° in the field of a magnetic spectrometer. A thin film of the stopping material was placed in the beam path at the spectrometer entrance. The energy loss of the beam was determined by measuring the decrease in magnetic field necessary to restore the beam to the 90° deflection angle. The film thickness was obtained by weighing a known area of film. The probable errors in the measurements are 2.3 -2.8% for H^+ and 3-4% for He^+. Proton stopping cross-section measurements on gold with this equipment agree with the results obtained by Bader et al. at the California Institute of Technology. Above 75 kev the He^+ cross sections vary linearly with the ion velocity.

*Now at Westinghouse Research Laboratories, Pittsburgh, Pa.

HOT ELECTRON BEHAVIOR IN GERMANIUM UNDER THE INFLUENCE OF A MAGNETIC FIELD. Louis Gold,* Lincoln Laboratory, Massachusetts Institute of Technology, Lexington, Massachusetts (Received June 26, 1958; revised manuscript received December 12, 1958).

The theory of the hot electron problem in many-valley semiconductors based upon the individual ellipsoidal energy surface model is extended for

germanium to the circumstance of a superposed magnetic field $\vec{B}$. A first approach, ignoring collisional effects, allows ready delineation of the electron orbits; directional energy gain is evaluated for $\vec{E}_{100}$ and $\vec{E}_{110}$ with $\vec{B}$ rotated in longitudinal and transverse orientations. The anisotropy is found to be quite marked (decidedly stronger than for $\vec{B}=0$) with the longitudinal arrangement more effective than the transverse one. The introduction of scattering considerably complicates the analysis and here consideration is given to the effective ratio b of Larmor to scattering frequency. In the limit $b \to \infty$ and the scattering decidedly anisotropic, transverse energy gain vanishes, whereas in the longitudinal alignment the energy gain becomes extremely anisotropic. The shift in the optimal energy gain direction(s) is noted for selected combinations of $\vec{E}$ and $\vec{B}$ and comparisons made with the case $\vec{B}=0$. As $b \to 0$, the anisotropy diminishes; detailed calculations have been performed for $b=1$, $0.1, \infty$ for the limiting cases of isotropic and strong anisotropic scattering.

*Present address: Edgerton, Germeshausen and Grier, Inc. Boston, Massachusetts.

SOME PROPERTIES OF GREEN AND RED-GREEN LUMINESCING CdS. Y. T. Sihvonen, D. R. Boyd, and C. D. Woelke, Research Staff, General Motors Corporation, Detroit, Michigan (Received August 18, 1958).

A series of electro-optical experiments at room temperature have been made with two types of high-purity single crystals of CdS. Those of Type *A*, believed to have near-perfect stoichiometry, luminesce green (5145A) under 3650A ultraviolet irradiation, have low dark conductivity (2.5×10^{-11} mho cm^{-1} at 300°K), exhibit no photopeak, and have a relatively short carrier lifetime (about 4 microseconds or less). Those of Type *B*, believed to have a sulfur deficiency, luminesce first strongly red (≅7200A), then strongly green (>5145A) as the exciting radiation is increased in intensity. Simultaneously both emissions shift toward longer wavelengths. Also, as the red emission intensity begins to saturate, the intensity-rate change of conductivity abruptly changes. It is suggested that red luminescence is the result of a free hole capture by one of the electrons residing in a sulfur vacancy. This trapping sensitizes the crystal but at the expense of increasing carrier lifetime to millisecond magnitudes. Furthermore, some of these vacancies (~0.4 ev below the conduction band) act as donors to increase dark conductivity (about 10^{-9} mho cm^{-1} at 300°K).

EFFECTS OF CHEMICAL BINDING ON THE NEUTRON CROSS SECTION OF HYDROGEN. W. L. Whittemore* and A. W. McReynolds, John Jay Hopkins Laboratory for Pure and Applied Science, General Atomic Division of General Dynamics Corporation, San Diego, California (Received September 8, 1958).

Fermi derived the energy dependence of the neutron scattering cross section of hydrogen chemically bound such that it acts as a harmonic oscillator. For comparison with this theory, the total cross section was measured with a high-resolution crystal spectrometer for hydrogen bound in four materials. In zirconium and yttrium hydrides, in which chemical bonding is relatively isotropic, the predicted structure with discrete energy levels is observed. In the less isotropic magnesium hydride, there is some evidence of energy levels, although not clearly resolved. For water the variation in the cross section is smooth, with no evidence of energy levels.

*Guest physicist at Brookhaven National Laboratory, Upton, New York.

CHARGE TRANSFER FOR PROTONS IN H_2. R. Curran, T. M. Donahue, and W. H. Kasner,* University of Pittsburgh, Pittsburgh, Pennsylvania (Received October 27, 1958).

A precise measurement of the electron capture cross section for protons in H_2 is reported for proton energies between 2.4 and 60 kev. The method involves collection of the residual ions by a sequence of identical condensers. The same scattering chamber is also used for the measurement of σ_{01} and $(\sigma_{01}+\sigma_{10})$. The recent measurements of Stier and Barnett are in close agreement with our results.

*Present address: Department of Physics, The University of Maryland, College Park, Maryland.

ELECTRON RECOMBINATION IN ATOMIC HYDROGEN. R. G. Fowler and W. R. Atkinson, Department of Physics, University of Oklahoma, Norman, Oklahoma (Received October 28, 1958).

The absolute intensity of radiation of the continuum associated with the Balmer lines has

been measured in a region of zero electric field by observing the expanding plasma in a shock tube. It is shown that the corresponding continuum energy can be explained by assuming that it is composed of the recombination and affinity spectrum of atomic hydrogen at a certain electron temperature. Values of the electron recombination coefficients can be derived which agree with those calculated by Cillie and disagree with those obtained from microwave and other measurements.

K-SERIES FLUORESCENCE YIELDS OF VANADIUM, MANGANESE, AND NEON. W. F. Frey, R. E. Johnston, and J. I. Hopkins,* Vanderbilt University, Nashville, Tennessee (Received July 14, 1958).

K-series fluorescence yield (w_K) measurements have been made for vanadium, manganese, and neon using the proportional counter method. The values obtained are the following: vanadium, 0.304 ± 0.013; manganese, 0.308 ± 0.015; and neon, 0.043 ± 0.004. A discussion of method and errors is given and a comparison of these values with other computed and experimental values is made.

*Now at Davidson College, Davidson, North Carolina.

ATTACHMENT OF LOW-ENERGY ELECTRONS IN MIXTURES CONTAINING OXYGEN. G. S. Hurst and T. E. Bortner, Health Physics Division, Oak Ridge National Laboratory, Oak Ridge, Tennessee (Received October 27, 1958).

Electron attachment to O_2 has been studied for O_2-N_2 and O_2-C_2H_4 mixtures over a wide range of pressures and electric fields. It was found that α, the probability of capture per cm and per mm Hg of O_2, depends on the partial pressures of both gases in the O_2-N_2 mixture but only on the C_2H_4 pressure in the O_2-C_2H_4 mixture. The data have been interpreted in terms of an extension of the mechanism postulated by Bloch and Bradbury, and by Bates and Massey, which involves first the formation of O_2^{-*} (excited O_2^-) with subsequent collisional stablization. On this basis, estimates were made of the cross section for stabilization of O_2^{-*} by collisions with various kinds of molecules.

CHEMICAL REACTIONS OF POSITRONIUM IN AQUEOUS SOLUTIONS. J. McGervey and S. DeBenedetti, Carnegie Institute of Technology, Pittsburgh, Pennsylvania (Received October 31, 1958).

An attempt to a preliminary but systematic study of the chemical properties of the element positronium is described. It is verified (in agreement with Green and Bell) that positrons react with nitrates; it is believed that this reaction is an oxidation process. It is found that positronium is not so readily attacked by the ions Cl^- and SO_4^{--}. In chloride and sulfate solutions positronium more effectively replaces the metals which are lowest in the electrochemical series; this result opens the possibility of determining the position of positronium in the electrochemical scale.

NONELASTIC SCATTERING CROSS SECTION FOR 8-20 Mev NEUTRONS. T. W. Bonner and J. C. Slattery, The Rice Institute, Houston, Texas (Received May 8, 1958).

Measurements of the nonelastic scattering cross section for neutrons with energies of 8.2, 9.8, 15.5, 17.0, 18.5 and 20.0 Mev have been made in Cu, Ag, Sn, Pb, and Bi. Cross sections were determined from transmissions through spherical shells. Neutrons of 8.2 and 9.8 Mev were obtained from the reaction $Be^9(\alpha, n)C^{12}$ and the higher energy neutrons from the reaction $T^3(d,n)He^4$. Biased scintillation detectors were used so that lower energy neutrons were not counted. The results show that the nonelastic cross sections decrease slowly with increasing neutron energy, in contrast to the cross sections for elastic scattering which show broad maxima at 7, 13, 13, 18, and 18 Mev, respectively, for Cu, Ag, Sn, Pb, and Bi. The ratio of the nonelastic cross sections to the elastic cross sections vary from a maximum value of 1.05 ± 0.05 to a minimum value of 0.71 ± 0.05 in the energy range which was covered.

OPTICAL MODEL EVIDENCE FOR SURFACE ABSORPTION OF NEUTRONS. Harvey J. Amster, Bettis Atomic Power Division, Westinghouse Electric Corporation, Pittsburgh, Pennsylvania (Received September 15, 1958).

Data-matching with the complex square well model for neutron scattering suggests that the

imaginary part of the potential should be largest at the nuclear surface; such an effect is also in accord with present physical pictures of the interaction. However, when a diffuse edge is attached to the model and the other parameters are changed to provide experimental agreement, the need for surface absorption appears diminished. To investigate further, cross sections resulting from a surface-absorbing and a uniformly absorbing potential, both with a diffuse edge, are calculated and compared. The results differ considerably less from each other than from the data, but the strength of absorption is more nearly independent of mass number when it is concentrated at the surface.

SCATTERING OF NEUTRONS BY NONSPHERICAL NUCLEI. H. M. Schey, Radiation Laboratory, University of California, Livermore, California (Received October 2, 1958).

A discrepancy between experiment and the optical model calculations of Bjorklund and Fernbach exists in the scattering of 7-Mev neutrons by tantalum. The possibility is investigated that this discrepancy is due to the quadrupole deformation in tantalum. The deformation is represented by a term proportional to $P_2(\cos\gamma)$ added to the spin-dependent potential of Bjorklund and Fernbach (γ is the angle between the assumed nuclear symmetry axis and the radius vector to the scattered particle). The added term is treated as a perturbation and the calculation is carried to second order. The Schrödinger equation is solved numerically on an IBM-704 computer to obtain the differential cross section for the elastic scattering of neutrons and the results are applied to the scattering of 7-Mev neutrons by tantalum. Parameters are determined which bring the theoretical results into adequate agreement with experiment.

DISINTEGRATION SCHEME OF LONG-LIVED ALUMINUM-26. Robert A. Rightmire,* James R. Simanton,† and Truman P. Kohman, Department of Chemistry, Carnegie Institute of Technology, Pittsburgh, Pennsylvania (Received September 11, 1958).

The disintegration scheme of the long-lived ground-state isomer of Al^{26} has been determined, based on the following observations.

The maximum positron energy as determined by absorption measurements is 1.16 ± 0.05 Mev; this agrees with the expected 1.17 Mev. The spectrum appears to be simple.

The scintillation gamma-ray spectrum shows intense positron annihilation radiation, a strong peak at 1.83 ± 0.03 Mev, and weak peaks at 1.12 ± 0.03 Mev and 2.96 ± 0.05 Mev, corresponding to transitions from the known Mg^{26} states at 1.82 and 2.97 Mev. A peak at 0.68 Mev is from the addition of two annihilation photons, one being backscattered from the source and surroundings; the gamma ray of ~0.7-Mev energy reported by others is not present. The peak at 2.97 Mev is shown to result from 2.97-Mev photons as well as from addition of 1.82- and 1.15-Mev photons.

The relative intensities of the annihilation and gamma radiations indicates that Al^{26} undergoes (84.6 ± 1.8)% positron emission to the 1.82-Mev state of Mg^{26}; (11.4 ± 1.9)% electron capture to the same state; (3.7±0.3)% electron capture to the 2.97-Mev state followed by emission of 1.15- and 1.82-Mev gamma-rays; and (0.30 ± 0.03)% electron capture to the same state followed by 2.97-Mev radiation. Other energetically possible transitions are apparently negligible in intensity.

Auger electrons and x-rays were observed in a proportional counter spectrometer. Analysis of the spectra yielded K-shell fluorescence yields of 0.008 ± 0.003 for magnesium and 0.008 ± 0.003 for aluminum.

*Present address: Chemical and Physical Research Division, Standard Oil Company of Ohio, Cleveland, Ohio.

†Present address: Particle Accelerator Division, Argonne National Laboratory, Lemont, Illinois.

FURTHER POLARIZATION MEASUREMENTS NEAR 17 Mev. William A. Blanpied, Palmer Physical Laboratory, Princeton University, Princeton, New Jersey (Received October 21, 1958).

Experimental angular distributions of the polarization of protons elastically scattered from magnesium, calcium, copper, silver, and gold near 17 Mev are presented, and comparison with certain theoretical calculations made. Data are also given on the polarization of inelastic protons scattered from magnesium with $Q = -1.37$ Mev. The familiar double-scattering method was used, with carbon serving as second scatterer. It is concluded that appreciable elastic polariza-

tion may be universally expected at this energy, and that therefore some form of spin-orbit interaction is important.

DECAY OF 13-HOUR Re^{182}. C. J. Gallagher, Jr., J. O. Newton, and Virginia S. Shirley, Radiation Laboratory and Department of Chemistry, University of California, Berkeley, California (Received October 23, 1958).

An electron- and gamma-spectroscopic study of the levels of W^{182} populated by the 13-hour electron-capturing isomer Re^{182} has been made. The levels observed support previous studies on the W^{182} levels as observed in Ta^{182} decay. Evidence for weakly populated levels around 2 Mev is reported, which indicates that the decay energy of the isomer is greater than 2 Mev. On the basis of the spins and parities of the levels populated, the isomer is assigned spin 3, negative parity.

$Si^{28}(d,\alpha)Al^{26}$ REACTION. Cornelius P. Browne,* Physics Department and Laboratory for Nuclear Science, Massachusetts Institute of Technology, Cambridge, Massachusetts (Received October 31, 1958).

Earlier work on the $Si^{28}(d,\alpha)Al^{26}$ reaction was extended and improved. The ground state Q-value of the reaction was remeasured and found to be 1.428 ± 0.004 Mev. Levels were found with excitation energies of (in Mev) 0.229 ± 0.003, 0.418 ± 0.002, 1.060 ± 0.002, 1.762 ± 0.003, 1.853 ± 0.003, 2.073 ± 0.003, 2.368 ± 0.003, 2.548 ± 0.004, 2.663 ± 0.004, 2.741 ± 0.005, 2.916 ± 0.006, 3.075 ± 0.006, 3.160 ± 0.006, 3.407 ± 0.006, 3.510 ± 0.010, and 3.596 ± 0.010. Seven of these have not been reported previously. The yields of the reaction leading to the ground state, the first excited state, and the second excited state were measured as a function of bombarding energy in the range 5.5 Mev to 7.5 Mev. There is strong resonance structure. The angular distributions for the reaction leading to these three states were obtained at 7.03 Mev bombarding energy. At this energy the total yield of the isotopic-spin forbidden reaction leading to the first excited state is 10% of the yield to the ground state. This violation of the selection rule can be explained by Coulomb force effects. The second $T = 1$ level could not be observed and the previous suggestion that the level at 3.16 Mev is the third $T = 1$ level seems to be incorrect. A comparison of the data with the results of other experiments is made. Energy levels of Al^{27} seen in the $Si^{29}(d,\alpha)Al^{27}$ reaction are listed and compared with results from $Al^{27}(p,p')Al^{27*}$. A new level at 5.745 ± 0.012 Mev was found plus several levels above the range of excitation previously covered.

*Much of the track counting and data analysis was done at the author's present address, The University of Notre Dame, Notre Dame, Indiana.

NEUTRON FISSION CROSS SECTIONS OF Pu^{236} AND Pu^{237}. J. E. Gindler, J. Gray, Jr., and J. R. Huizenga, Argonne National Laboratory, Lemont, Illinois (Received October 23, 1958).

The thermal-neutron fission cross sections of plutonium isotopes 236 and 237 were determined by counting samples placed in the thermal column of the Argonne heterogeneous heavy-water reactor, *CP*-5. Comparison of the fission counting rate of the Pu^{236} and Pu^{237} samples with that of a Pu^{239} standard gave cross sections of 170 ± 35 barns and 2500 ± 500 barns, respectively, for the two nuclides. The K-to-total electron capture branching ratio for Pu^{237} was found to be 0.38 ± 0.06.

PHASE SHIFT ANALYSIS OF PROTON-PROTON SCATTERING EXPERIMENTS BELOW 40 Mev. Malcolm H. MacGregor, Radiation Laboratory, University of California, Livermore, California (Received October 27, 1958).

A phase shift analysis has been made of p-p angular distribution measurements at 1.855, 4.203, 9.68, 9.73, 18.2, 19.8, 31.8, and 39.4 Mev. At 1.855 Mev, Coulomb effects plus the nuclear S-wave phase shift are sufficient to give agreement within experimental errors. At 10 Mev, S-, P-, and D- wave effects are apparent. At 40 Mev, F-wave components are also necessary. With the aid of the Clementel-Villi parametrization method, it has been possible to determine all of the least-squares fits to the angular distribution data in the S, P, D approximation. Polarization measurements and potential model calculations can be used to restrict further the allowable phase shifts sets. It is shown that angular distribution measurements with an accuracy of 0.1% would not lead to a unique set of

phase shifts. Both double and triple scattering experiments are necessary in order to remove the ambiguity.

DETERMINATION OF THE ABSOLUTE VALUE OF THE FISSION CROSS SECTION OF U^{235} BY THE MEASUREMENT OF α. George J. Safford and Edward Melkonian, Columbia University, New York, New York (Received July 9, 1958).

The absolute fission cross section of U^{235} at 0.0253 ev has been determined by measuring (σ_t/σ_f) at 5.3 A and combining this with scattering, absorption, and relative fission cross section measurements. Two multiplate ionization chambers, one containing B^{10} and the other U^{235}, were constructed. The flux is determined by making the two chambers as nearly alike as possible and comparing counting rates in the same neutron beam. The amounts of U^{235} and B^{10} in the beam are determined by transmission measurements. After small corrections for chamber efficiencies, residual differences between chambers, and incoherent scattering, a value for $(1+\alpha)=1.885\pm0.7\%$ at 5.3 A was obtained. This leads to a value of 571.3 ± 6 barns as the absolute fission cross section at 0.0253 ev.

PROTON-GAMMA ANGULAR CORRELATION STUDIES OF Be^9 AND $Ca^{40}(d,p\gamma)$ STRIPPING REACTIONS. R. T. Taylor,* University of Michigan, Ann Arbor, Michigan (Received October 23, 1958).

To investigate the applicability of the Butler stripping theory, the angular correlations have been measured between the protons and γ-rays from the reactions $Be^9(d,p\gamma)Be^{10*}$ (3.37 Mev) and $Ca^{40}(d,p\gamma)Ca^{41*}$ (1.95 Mev), using 7.78-Mev deuterons. Both correlations in the (d,p) plane are of the form $1+A_2P_2(\cos\theta)$, where θ is the angle between the γ-ray and the recoil nucleus, as predicted by theory. For Be^9 the coefficient $A_2=-0.33\pm0.04$, in reasonable agreement with the previously reported value of -0.40 ± 0.05 for a deuteron energy of 4 Mev, and hence confirming the theoretically expected energy independence. This value of A_2 is close to that of -0.40 predicted on the assumption of L-S coupling with the assignment of a $^3P_2$ state for the first excited level of Be^{10}. For Ca^{40}, $A_2=+0.17\pm0.04$ in satisfactory agreement with the predicted value of +0.143 using the reasonable assumption of j-j coupling with less than $10^{-3}\%$ $M3$ in the predominantly $E2$ γ-transition. Both transitions show less than 6% effect in the correlation in the plane perpendicular to the recoil axis, in agreement with the isotropy expected from the simplified stripping theory.

*Now at the Nuclear Physics Research Laboratory, University of Liverpool, Liverpool, England.

PHOTONUCLEAR REACTIONS OF GALLIUM AND ARSENIC WITH 70-Mev BREMSSTRAHLUNG. Fritz D. Schupp, Clifford B. Colvin, and Don S. Martin, Jr., Institute for Atomic Research and Department of Chemistry, Iowa State College, Ames, Iowa (Received October 20, 1958).

Radiochemical techniques were utilized in the measurement of yields of photonuclear reactions induced by 70-Mev bremsstrahlung in gallium and arsenic targets. For As targets the yields of As^{74}, Ga^{73}, Ga^{72}, Ga^{68}, Zn^{69}, and Zn^{69m} were determined. In the gallium targets the yields of Zn^{69}, Zn^{69m}, Ni^{65}, and Co^{61} were measured. The integrated cross sections for the indicated photonuclear reactions were estimated from the yields. The integrated cross sections of five $(\gamma,3p3n)$ processes were compared. The relative yields of the Zn^{69} isomeric pair depended upon the process of formation.

HIGH-ENERGY ELECTRON SCATTERING AND THE CHARGE DISTRIBUTION OF CARBON-12 AND OXYGEN-16. Hans F. Ehrenberg,* Robert Hofstadter, Ulrich Meyer-Berkhout, D. G. Ravenhall,† and Stanley E. Sobottka, Department of Physics and W. W. Hansen Laboratories of Physics, Stanford University, Stanford, California (Received August 20, 1958).

The scattering of high-energy electrons from C^{12}, reported previously, has been extended to 420 Mev. The elastic and inelastic scattering from the first excited level at 4.43 Mev has been studied between 33 and 70°. The new data are in good agreement with what one would expect from the earlier measurements on C^{12} performed at 187 Mev. Additional measurements of the elastic O^{16} scattering cross sections of 240-, 360-, and 420-Mev electrons as functions of the scattering angle furnish information on the size and shape of the O^{16} nucleus. Pronounced diffraction minima in the angular distributions were observed for C^{12} and O^{16}. The experimental re-

sults are compared with the predictions of a theoretical phase-shift analysis derived for the harmonic-well independent-particle model of the nucleus. Preliminary best fits confirm the shell-model predictions for the charge density distribution of these p-shell nuclei. The preliminary analysis of the data shows that the length parameter of the well is 1.66×10^{-13} cm for C^{12}, and 1.76×10^{-13} cm for O^{16}, thus indicating a slight variation of the curvature of the harmonic well as the p shell is filled in.

*Now at University of Bonn, Bonn, Germany.
† Now at University of Illinois, Urbana, Illinois.

COSMIC-RAY INCREASES ASSOCIATED WITH SOLAR FLARES. L. C. Towle and J. A. Lockwood, University of New Hampshire, Durham, New Hampshire (Received June 27, 1958).

Data from a standard IGY neutron monitor located on Mt. Washington, New Hampshire, have been examined for possible increases associated with solar flares. The 0400 and 0900 impact zones have been located for both the standard centered dipole and the westward rotated centered dipole approximations. No increases $\geq 0.25\%$ have been found for the years 1956 and 1957. An additional maximum in the mean daily cycle at the time of impact zone passage has not been observed during this period. Possible explanations for this result are presented.

NEUTRAL K MESON AS A PARTICLE MIXTURE. William B. Fowler, Richard L. Lander, and Wilson M. Powell, Radiation Laboratory, University of California, Berkeley, California (Received July 23, 1958).

This experiment was designed to demonstrate the recently predicted particle-mixture property of the neutral K meson. The prediction asserts that the neutral K meson contains a short-lived component, θ_1^0, and a longer-lived component, θ_2^0. The θ_2^0 should have the property that it regenerates the short-lived component and also produces hyperons upon traversing matter. Under proper conditions the observation of such mesons or hyperons demonstrates the predicted mixture property. The neutral K mesons in this experiment were produced by 1.25-Bev/c π^- mesons striking a $4 \times 4 \times 12$-inch aluminum target. Neutral particles emitted from the aluminum at an angle of 5° with respect to the π^- beam traveled 9.3 ft to a propane bubble chamber operated in a 12-kilogauss magnetic field. A sweeping magnet removed charged particles from this beam. θ_2^0 mesons could interact in the walls of the chamber or in the liquid propane, yielding θ_1^0 meson and Λ^0 hyperon decays in the sensitive region of the chamber. Twenty thousand pictures, corresponding to about 3×10^8 pions incident on the aluminum, were scanned for V^0 events. About 14 Λ^0 decays and about 12 θ_1^0 decays were observed. Spurious sources of these decays have been estimated to be negligible.

p-n ASYMMETRIES AT 143 Mev. Stuart G. Carpenter* and Richard Wilson, Cyclotron Laboratory, Harvard University, Cambridge, Massachusetts (Received August 11, 1958).

The asymmetry of neutrons produced by bombardment of C, Al, Cu, and Pb by 143-Mev polarized protons, at angles 20° to 70°, has been measured. The asymmetry is almost independent of target element but is inconsistent with that from a free p-n collision. The mechanism for the process is discussed.

*Now at Atomics International, Canoga Park, California.

HIGH-SENSITIVITY MASS-SPECTROMETRIC MEASUREMENT OF STABLE HELIUM AND ARGON ISOTOPES PRODUCED BY HIGH-ENERGY PROTONS IN IRON. Oliver A. Schaeffer and Josef Zähringer,* Chemistry Department, Brookhaven National Laboratory, Upton, New York (Received September 18, 1958).

A high-sensitivity mass spectrometer has been used to measure the helium, argon, and neon produced in iron by 0.16-, 0.43-, and 3.0-Bev protons. The spectrometer has a sensitivity of 1.4×10^{-10} standard cc per millivolt for helium. The He^4 cross sections are 120 mb, 450 mb, and 1300 mb at 0.16, 0.43, and 3.0 Bev, respectively, while the He^3/He^4 cross-section ratios are respectively 0.09, 0.10, and 0.18. At 0.43 Bev, cross sections of 1.0 mb, 3.3 mb, 8 mb, and 4.1 mb were found for the argon isotopes 36, 37, 38, and 39, respectively. The cross section for neon-21 is 0.1 mb at 0.43 Bev. The results are discussed in relation to evaporation theory and the rare gas content of iron meteorites. The He^3 yields are all higher than previously meas-

ured tritium values. At 3 Bev the He^3/T ratio is 2.4. It is suggested that in the case of iron in evaporation theory the Coulomb barrier is not as important relatively as previously thought. Alternatively, a large fraction of the He^3 and tritium may be produced during the nuclear cascade which precedes the evaporation from the excited nuclei. The cross sections measured bear directly on the cosmic-ray-produced rare gases in meteorites. From the cross section of directly produced He^3 relative to T, previous measurements of He^3-T exposure ages of meteorites must be reduced by a factor of about 3. From the argon isotope cross sections it is seen that 80% of the A^{36} in meteorites is the result of β decay of cosmic-ray-produced Cl^{36} and thus A^{36}-Cl^{36} should be a reliable method for measuring exposure ages of meteorites.

*Present address: Max Planck Institut für Kernphysik, Heidelberg, Germany.

NUCLEON FORM FACTORS FROM ELECTROPRODUCTION OF PIONS. S. Gartenhaus* and C. N. Lindner, Stanford University, Stanford, California (Received September 12, 1958).

The dispersion-relation analysis of Fubini, Nambu, and Wataghin for pion production by electrons has been applied to the experiments of Panofsky and Allton as an independent means for studying nucleon structure. The results are in qualitative agreement with those from elastic scattering experiments. Some of the limitations inherent in the form factor measurements by this process are also discussed.

*Now at Purdue University, Lafayette, Indiana.

LITHIUM, BERYLLIUM, AND BORON IN THE PRIMARY COSMIC RADIATION. P. S. Freier, E. P. Ney, and C. J. Waddington, University of Minnesota, Minneapolis, Minnesota (Received October 1, 1958).

In order to resolve the controversy concerning the abundance of the light elements ($3 \leq Z \leq 5$) in the primary cosmic radiation, a further experiment has been performed. The charge spectrum of the cosmic radiation has been determined on October 19, 1957, in a stack of nuclear emulsions exposed nearer the top of the atmosphere than before. The results of the experiment prove that these light elements make up an appreciable fraction of all those nuclei with $Z \geq 3$ present in primary cosmic radiation. The flux values found after correction to the top of the atmosphere are, in particles/m^2 sec sterad:

Li, Be, B (L-nuclei)	1.9 ± 0.3
CNOF (M-nuclei)	5.1 ± 0.5
$Z \geq 10$ (H-nuclei)	1.7 ± 0.3

These values appear to be lower than observed previously, in agreement with the decrease in α-particle flux associated with the sun's increased activity.

NUCLEON CORRELATION EFFECTS IN HIGH-ENERGY ELECTRON SCATTERING. W. E. Drummond, Department of Physics, Stanford University, Stanford, California (Received June 18, 1958).

Using Schiff's high-energy approximation, a sum rule is developed which relates the scattering of high-energy electrons from heavy nuclei to the two-particle correlation function for the nucleus. It is shown that correlations due to the Pauli principle give a large effect in the region of momentum transfer from 100 to 300 Mev/c, and that correlations with a range of less than 10^{-13} cm do not make an appreciable contribution.

MULTIPLE MESON PRODUCTION BY PHOTONS IN HYDROGEN. J. M. Sellen,* G. Cocconi, V. T. Cocconi, and E. L. Hart, Laboratory of Nuclear Studies, Cornell University, Ithaca, New York (Received October 22, 1958).

Pictures of a H_2 diffusion cloud chamber with magnetic field taken at the 1.1-Bev Cornell synchrotron have been analyzed to study multiple meson production by photons on protons. They have yielded 108 cases of double charged meson production ($\gamma + p \rightarrow p + \pi^+ + \pi^-$) and 4 cases of triple meson production.

For each event of double meson production, the energy of the incoming photon and the angles and momenta of the emitted particles could be determined. The most significant results are the following.

The cross section for double charged meson production rises rapidly around 500 Mev to approximately 70 microbarns, a value of the same order as the total cross section for single meson

production.

In the reaction leading to a charged meson pair, π^+ and π^- play dissimilar roles, as evidenced by the marked dissimilarities in their c.m. angular and momentum distributions. The Q-distributions suggest the interpretation that the predominant mode of pair production in the energy range from 500 to 700 Mev is $N^* + \pi^-$, $N^* \to p + \pi^+$, where N^* likely is the resonant 3/2, 3/2 excited state of the proton. The fact that the angular distributions for the protons and the π^--mesons are asymmetric about 90° indicates that the reaction does not derive from a single state, but from a mixture of at least two interfering states.

*Now at Ramo-Wooldridge Corporation, Los Angeles, California.

REMARKS ON THE SCATTERING AND ANNIHILATION OF ANTIHYPERONS BY NUCLEONS. D. B. Lichtenberg, Michigan State University, East Lansing, Michigan (Received October 31, 1958).

A number of assumptions about the nature of antihyperon-nucleon forces are made which, if valid, allow the antihyperon-nucleon scattering and annihilation cross sections to be given as simple linear combinations of the antiproton-proton and antineutron-proton cross sections.

STUDY OF NEUTRAL PION PRODUCTION IN PROTON-PROTON COLLISIONS. C. York, R. March, W. Kernan, and J. Fischer, The Enrico Fermi Institute for Nuclear Studies, The University of Chicago, Chicago, Illinois (Received October 23, 1958).

A large lead glass Cerenkov counter has been used to measure the energy spectrum of gamma rays resulting from neutral pions produced in proton-proton collisions. A liquid hydrogen target was bombarded with protons of 447 Mev, 415 Mev and 397 Mev. Gamma rays emitted at 90° to the incident proton beam were detected by a counter telescope comprised of an anticoincidence counter, a $\frac{1}{8}$-in. lead converter, two coincidence counters, and the lead glass counter. Pulses from the lead glass counter were fed through a gating circuit into a 100-channel pulse height analyzer. The three pulse height spectra obtained have been compared with those predicted from the phenomenological theory, to estimate the contributions of the various possible final angular momentum states. It is found that the spectra are consistent with isotropic emission of the π^0's in the center-of-mass system. The differential cross sections for π^0 production are 12.6±2.0, 9.0±1.9, and 7.4±1.7 microbarns/sterad at 445, 415, and 397 Mev respectively.

DIRECT-INTERACTION CALCULATION OF HIGH-ENERGY PROTON-CARBON SCATTERING. Alan H. Cromer, Laboratory of Nuclear Studies, Cornell University, Ithaca, New York (Received October 31, 1958).

An optical potential has been derived which includes, to first order in q^2, the effect of the nucleon-nucleon angular dependence. Nucleon-nucleon scattered amplitudes calculated from the 310-Mev nucleon-nucleon phase shifts have been put into the potential, and the proton-carbon scattered amplitudes calculated from it by WKB approximation. Good agreement was obtained with the scattered amplitudes as derived directly from the 313-Mev proton-carbon data using an extension of the analysis employed previously by Bethe. The inclusion of the nucleon-nucleon angular dependence in the potential was found to be important in order to obtain the correct value of the imaginary part of the forward scattered amplitude and the correct proton-carbon angular dependence at moderately small angles. Phase shift solutions 1 and 6 of Stapp et al. were investigated and found to give essentially the same agreement with the differential cross section at small angles. Solution 6 was found to give a better fit to the polarization data than solution 1, but the significance of this is not clear.

POSITRON SPECTRUM FROM THE DECAY OF THE μ MESON. Walter F. Dudziak, Ryokichi Sagane, and James Vedder, Radiation Laboratory, University of California, Berkeley, California (Received October 20, 1958).

A magnetic spiral-orbit spectrometer was used to study the positron spectrum from an isotropic μ^+ decay. The detected positrons were identified by an electronic technique designed to measure the lifetime of the muon. Our measured weighted mean value of the μ^+ mean life is $\tau_\mu = 2.21 \pm 0.02$ μsec.

The data have been analyzed according to the

simplified one-parameter theory of Michel, as modified by Behrends, Finkelstein, and Sirlin and corrected by Berman to include radiative corrections to the muon decay theory. We obtained $\rho_M = 0.741 \pm 0.027$ for the Michel parameter as the weighted mean value from four experiments. In these experiments the measurements in the low-energy positron region were not of sufficient accuracy to yield an estimate of the second Michel parameter.

Included is a measurement of the maximum positron energy. The weighted mean value of this measurement is $W = 52.87 \pm 0.07$ Mev. From this value and its simple algebraic relation to the masses of the decay particles one obtains a value of the μ^+ mass $\mu = (206.94 \pm 0.27) m_e$.

Tables of the radiative correction to muon decay are given as well as the total corrections that must be added to the Michel parameter that is derived from experimental data by using the simple Michel theory without radiative corrections. For the energy region of the majority of experiments from which the ρ_M value is determined, this total correction in $\Delta\rho$ is approximately 0.040.

From our measured value of the maximum positron energy, an estimate is made of the possible upper limit on the mass of the neutral particle in muon decay. This upper limit is reported as 8 electron-mass units.

PHOTOPRODUCTION OF POSITIVE PIONS IN HYDROGEN IN THE ANGULAR RANGE $7° < \theta_{c.m.} < 27°$ AND PHOTON ENERGY RANGE 220 Mev $< k < 390$ Mev. Alan J. Lazarus,* W. K. H. Panofsky, and F. R. Tangherlini,† Department of Physics and High-Energy Physics Laboratory, Stanford University, Stanford, California (Received October 20, 1958).

Relative measurements of the cross sections for the production of positive pions by photons on protons have been carried out in the range of c.m. angles $7° < \theta_{c.m.} < 27°$ for four photon energies from 220 to 390 Mev. Positive pions were detected via the decay positron from the π-μ-e chain which was observed in a series of gates following a pulse of photons and electrons from the Mark III linear accelerator. The results have been compared with new dispersion theory calculations using a range of values of the coupling constant and resonance energy. The experimental data at these small angles are in good agreement with the calculations; however, the fit of the calculations with available data at larger angles is not satisfactory. It is shown that the fit in either case in substantially poorer if the so-called "retardation term," i.e., the diagram in which the photon is absorbed by a virtual meson, in omitted.

*Now at RAND Corporation, Santa Monica, California.
†Now at the Institute for Theoretical Physics, Copenhagen, Denmark.

PHOTOPRODUCTION OF CHARGED PIONS FROM DEUTERIUM. Robert H. Land,* Physics Department and Laboratory for Nuclear Science, Massachusetts Institute of Technology, Cambridge, Massachusetts (Received September 15, 1958).

The photoproduction of charged pions from deuterium has been studied using a "monochromatic" gamma-ray beam of 292 ± 8 Mev. The energy spectra of both positive and negative pions at the laboratory angle of 120° were determined and both agreed within experimental error with that predicted by the theory of Lax and Feshbach. The negative-to-positive ratio at 120° was 1.07 ± 0.16 and, within experimental error, was independent of meson energy. At an angle of 73° the ratio was 0.90 ± 0.23 for 98.7-Mev mesons. The measured negative-to-positive ration disagrees both with the simple classical picture of Brueckner and the phenomenological theory of Watson. Some results on the ratio using a bremsstrahlung beam are given.

*Now at the Argonne National Laboratory, Lemont, Illinois.

STUDY OF THALLIUM, LEAD, AND BISMUTH NUCLEI PRODUCED IN THE BOMBARDMENT OF GOLD WITH 380-Mev PROTONS. Albert E. Metzger and J. M. Miller, Department of Chemistry, Columbia University, New York, New York (Received October 30, 1958).

Gold has been bombarded by the 380-Mev proton beam of the Nevis cyclotron in a study of secondary reactions. Secondary reactions produce nuclei with charges greater than that of a target nucleus by means of an intermediate fragment emitted from one target nucleus and absorbed in a second. The increase in atomic number permits isolation of the effect by chemical separation.

Thallium, lead, and bismuth fractions were

separated from irradiated gold bars and carefully purified. The radioactive decay of these samples was followed with a NaI(Tl) crystal scintillation counter. Nuclei produced by secondary reactions were detected for all three elements, the yields decreasing rapidly with increasing atomic number. From the secondary reaction yields of thallium and lead isotopes, it has been possible to calculate the upper portion of the energy distribution of the respective intermediate alpha and lithium fragments. This provides a comprehensive picture of a secondary reaction and demonstrates (1) that the yield of secondary particles is a rapidly increasing function of the bombardment energy for a given target nucleus, (2) that the energy distribution of the secondary fragment possesses an appreciable high-energy tail, and (3) that secondary reactions can be treated in terms of conventional nuclear reaction theory.

EQUATIONS OF MOTION OF POINT PARTICLES IN FIELDS OF NONZERO REST MASS AND SPIN. Peter Havas, Department of Physics, Lehigh University, Bethlehem, Pennsylvania (Received September 22, 1958).

A classical theory of free fields corresponding to quanta of arbitrary integral spin has been formulated by Dirac and Fierz. Sources of such neutral fields were considered by Harish-Chandra, who also obtained the equations of motion for arbitrary multipole singularities. It is noted that for fields of nonzero rest mass and spin, the conditions imposed on the sources by Harish-Chandra are more stringent than is required by the invariance properties of the fields, and a more general set of equations is proposed. The corresponding equations of motion are obtained for arbitrary multipole singularities. The theory is extended to charged and charge-symmetric fields.

INDICATION FOR K, Λ, Σ RELATIVE PARITIES FROM EFFECTIVE-RANGE ANALYSIS OF K^+p SCATTERING. D. Amati, Istituto di Fisica, Università di Roma, Istituto Nazionale di Fisica Nucleare, Sezione di Roma, Italy (Received October 30, 1958).

From dispersion relations an effective range formula is derived for K^+p scattering. In the expression for the effective range, the integrals over the cross sections are certainly convergent and weighted against the contributions from the unphysical region. This expression is then analyzed under the experimentally suggested hypothesis of rather constant K^+p cross sections up to ~110 Mev; it is observed that the effective range is rather energy independent and the integrals contributing to it are estimated to be all of the same sign. The expression for the effective range is then quantitatively evaluated, and it is shown that the comparison with the low-energy dependence of σ^+ indicates equal Λ and Σ parities with opposite K parity (K pseudoscalar). The possibility of evaluating the coupling constants from the low-energy behavior of the K^+p cross section is then briefly stated.

CONSTRUCTION OF UNITARY IRREDUCIBLE REPRESENTATIONS OF THE LORENTZ GROUP, AND THEIR USE IN SYNTHESIZING THE COVARIANT THEORIES OF FREE FIELDS. Christian Fronsdal, CERN, Geneva, Switzerland (Received September 9, 1958).

The unitary irreducible representations of the inhomogeneous, proper Lorentz group are determined, using a prescription given by Wigner, with special emphasis on the case of zero rest mass. The principal results are (a) the construction of one-component representations for the case of zero mass and discrete spin; (b) the existence of a Foldy-Wouthuysen transformation for zero mass and spin 1/2; (c) the construction of "position operators" for zero mass and spins 1/2, 1; (d) the complete synthesis of the Dirac, Majorana, and Maxwell one-particle theories.

FORMATION OF DISCONTINUITIES IN CLASSICAL NONLINEAR ELECTRODYNAMICS. Morton Lutzky and John S. Toll, Department of Physics, University of Maryland, College Park, Maryland (Received September 22, 1958).

It is shown that discontinuities can develop in the propagation of initially smooth waves governed by a classical nonlinear theory of electrodynamics. The type of theory considered includes as a special case that of Heisenberg and Euler, which describes the modifications that must be made in the Maxwell equations to include the classical limit of the nonlinear vacuum effects of quantum electrodynamics. A particular solution of the equations is constructed

by the method of characteristics; this example illustrates how, with the appropriate well-behaved initial conditions, the characteristics can be made to intersect at later times, thus forming discontinuities. The classical approximation fails when the gradient of the field strength becomes large, so that no definite conclusion can be drawn as to the actual physical creation of singularities.

SYMMETRY LAWS AND STRONG INTERACTIONS. J. J. Sakurai,* Radiation Laboratory, University of California, Berkeley, California (Received October 16, 1958).

An attempt is made to explore the possible connection between symmetry laws in internal space (e.g., isospin space) and symmetry laws in Lorentz space with special attention to the question: Why are the strong interactions parity-conserving? For direct (nonderivative-type) pion-nucleon interactions, CP invariance and charge independence are sufficient to guarantee the separate conservation of P and C, as previously pointed out. For derivative-type pion-nucleon interactions, charge independence and G invariance (rotational and inversion invariance in three-dimensional isospin space) require that parity (and CP) be conserved: in addition we can also show that the charge-triplet pion must be pseudoscalar, provided that the virtual Yukawa process $\pi^0 \rightleftarrows p + \bar{p}$ is allowed or, equivalently, the π^0 can be regarded as a bound state of a proton and an antiproton as far as symmetry laws are concerned. For the K couplings, analogous conditions cannot be obtained from the usual assumption of charge independence alone. However, if the K couplings (rather than the π couplings) exhibit a higher internal symmetry in the sense that the K couplings are universal, the high K symmetry plus charge independence in the usual sense imply parity conservation both in the case of CP-invariant nonderivative-type K interactions and in case of G-invariant derivative-type K interactions. The high K symmetry also implies that the relative $N\Xi$ parity as well as the relative $\Lambda\Sigma$ parity is even. It is conjectured that, if the K couplings must be of a derivative type, only ps-pv coupling is allowed, which means that the K particle is pseudoscalar. The global symmetry model which cannot be reconciled with our assumption of the high K symmetry is re-examined. The high K symmetry is destroyed in a specific and definite manner by the π couplings, and relations among the various coupling constants are inferred from the baryon mass spectrum. Some empirical implications of our model are discussed. Whereas G invariance requires the symmetric appearance of the two chiral spinors $\frac{1}{2}(1+\gamma_5)\psi$ and $\frac{1}{2}(1-\gamma_5)\psi$ for strangeness-conserving processes, for strangeness-nonconserving processes G conjugation carries charge-conserving interactions into inadmissible interactions that do not conserve electric charge. Hence if we take the point of view that parity-conserving interactions are generated by G conjugation, we have some understanding of the puzzling fact that strangeness conservation and parity conservation have the same domain of validity. Further theoretical speculations are made.

*On leave of absence from the University of Chicago.

ALTERNATIVE METHOD FOR COMPARING PION-PROTON SCATTERING DATA WITH DISPERSION EQUATIONS. Howard J. Schnitzer and George Salzman,* Department of Physics and Astronomy, University of Rochester, Rochester, New York (Received October 20, 1958).

A method for comparing pion-proton scattering experiments with the predictions of the forward angle scattering dispersion equations is proposed, which allows the usual statistical measure (χ^2) of the agreement. A slight discrepancy is found between negative pion-proton data and the theory; however, the over-all agreement is considered satisfactory. Values of the coupling constant and S-wave zero-energy scattering lengths are determined. They are $f^2 = 0.08 \pm 0.01$, $a_1 = 0.193 \pm 0.050$, and $a_3 = -0.089 \pm 0.048$.

*Now at CERN on leave of absence from the University of Colorado.

UNPHYSICAL REGION IN HEAVY-MESON—NUCLEON DISPERSION RELATIONS. San Fu Tuan,* Radiation Laboratory, University of California, Berkeley, California (Received October 23, 1958).

The contribution to K-meson–nucleon dispersion relations from the unphysical region due to absorption is examined in perturbation theory; it is found that the contribution need not be negligible for scalar K-mesons or the case where Λ has opposite relative parity from (K, Σ). The

influence this has on a dispersion-theoretic analysis of K-meson scattering is noted. In the Appendix the mass relationships for a rigorous derivation of the dispersion relations are discussed.

*Present address: c/o Imperial College, London, England.

RADIATIVE CORRECTIONS TO FERMI INTERACTIONS. Toichiro Kinoshita, Laboratory of Nuclear Studies, Cornell University, Ithaca, New York, and Alberto Sirlin, Physics Department, Columbia University, New York, New York (Received October 23, 1958).

The radiative correction to the decay spectrum of polarized muons is recalculated taking into account a mistake in our previous work which was recently pointed out by Berman. The revised values for the radiative correction to δ, ξ, and integrated asymmetries for the high- as well as low-energy decay electrons have turned out to be practically identical with the old values. The ρ value determined from experiments, on the other hand, has to be increased by about 1% because of the new correction. Thus the over-all effect of the radiative correction to the ρ value is now an increase of the order of 5.6% when the experimental and theoretical spectral distributions are compared in the region $0 \leq p/p_{max} \leq 0.95$. The radiative corrections to the spectrum and lifetime of the neutron decay arising from the charge interactions of the electron and proton are also studied. Use of this expression gives a correction of -1.7% for the lifetime of O^{14}. The corrected Feynman–Gell-Mann coupling constant is $G = (1.40 \pm 0.01) \times 10^{-49}$ erg/cm^3. In the universal V-A theory of weak interactions, the calculated muon mean life becomes $\tau_\mu = (2.31 \pm 0.05) \times 10^{-6}$ sec. (These three values depend logarithmically on ultraviolet cutoff λ and the corrections to τ_μ increase for increasing values of λ.) It is found that the corrections to the spectral shape of β decay are rather large in the case in which the end-point energy $E_m \gg m_e c^2$. The radiative corrections to the lifetime and the total asymmetry for muon decay are found to be well defined and finite for $m_e \to 0$ in spite of the fact that the differential spectrum itself diverges logarithmically in the same limit. The same situation is encountered in the case of radiative corrections to the neutron β decay. A physical explanation for such behavior of the radiative corrections is attemped. In an Appendix a simplified expression is given for the determination of the Michel parameter.